A STUDY OF THE MARINE PHYTOFLAGELLATE *Pyramimonas pseudoparkeae* PIENAAR *et* AKEN (PRASINOPHYCEAE)

by

Mark Ernest Aken

Submitted in partial fulfilment of the
requirements for the degree of Doctor of Philosophy
in the Department of Botany, University of Natal,
Pietermaritzburg, 1985.

VOLUME TWO

PLATES

and

PLATE - ANNOTATIONS

LIST OF ABBREVIATIONS

B_1	=	proximal body scale
B_2	=	intermediate body scale
B_3	=	distal body scale
B	=	bacterium
Bcb	=	basal connecting band
C	=	chloroplast
Csm	=	cytoskeletal microtubules
D	=	dictyosome (ff = forming face; mf = mature face)
Du	=	duct of scale reservoir
E	=	eyespot
Er	=	endoplasmic reticulum
F_1	=	proximal pentagonal flagellar scale
F_2	=	proximal square flagellar scale
F_3	=	limuloid scale
F_4	=	hairscale
F	=	flagellum
Fb	=	flagellar basal body
Fba	=	flagellar basal body apparatus
Fp	=	flagellar pit
Frb	=	fibrillar band
K	=	kinetochore
L	=	lipid
LC	=	l-cell
LV	=	lysosomal vesicle
M	=	mitochondrion
Mb	=	microbody
Mp	=	metaphase plate
N	=	nucleus
No	=	nucleolus
P	=	pyrenoid
Pcf	=	proximal connecting fibre
Pf	=	pericentriolar fibre
R	=	root (microtubular)
Rh	=	rhizoplast
S	=	starch granule

Sb = scale boundary

Sc = scales

Sr = scale reservoir

Sy = synistosome

T = trichocyst

TC = t-cell

U = underlayer scales

V = vacuole

VLP = virus-like particle

W = cell wall of cyst

W_1 = outer cell wall of cyst

W_2 = inner cell wall of cyst

PLATE 2.1

Structure - light microscopy

Scale bar on all figures = 5 μm.

Figs. 1 and 2. Two lateral views of the same cell (Nomarski optics).

Fig. 1. The cell is pyriform in shape and has an anterior flagellar pit from which the flagella emerge. The parietal chloroplast (C) contains a posterior pyrenoid (P). Trichocysts (arrowheads) are present around the flagellar pit and between the chloroplast lobes.

Fig. 2. Focussing at a different level the eyespot (E) is evident in one of the chloroplast lobes. A field of trichocysts (arrowhead) is seen at the anterior end of the cell.

Figs. 3, 4 and 5. Cells seen in apical view.

Fig. 3 The four flagella arise from the flagellar pit in a cruciate pattern (Nomarski optics).

Fig. 4 Focussing into the cell the four flagella can be seen within the flagellar pit and between the lobes of the cell on the outside. A ring of trichocysts (arrows) surround the flagellar pit. (Nomarski optics).

Fig. 5 Many cells settled out on their recurved flagella. When one cell settles this seems to elicit a settling response in other cells (bright field).

Fig. 6. The nucleus (N) is clearly visible in Feulgen stained preparations (phase contrast).

Fig. 7. An osmotically lysed cell showing the four-lobed chloroplast (C) containing a pyrenoid (P) and eyespot (E). Many extended trichocysts (arrowheads) are seen emanating from the cell (phase contrast).

Fig. 8. The laminated pyrenoid (P) is evident in Feulgen stained cells. Two cup-shaped starch grains surround the pyrenoid (phase contrast).

Figs. 9 and 10. Cells fixed in glutaraldehyde and OsO_4. In Fig. 9 the basal body apparatus (arrowhead) stains densely. In Fig. 10, the rhizoplast (arrowhead) is seen extending from the basal body apparatus toward the pyrenoid (phase contrast).

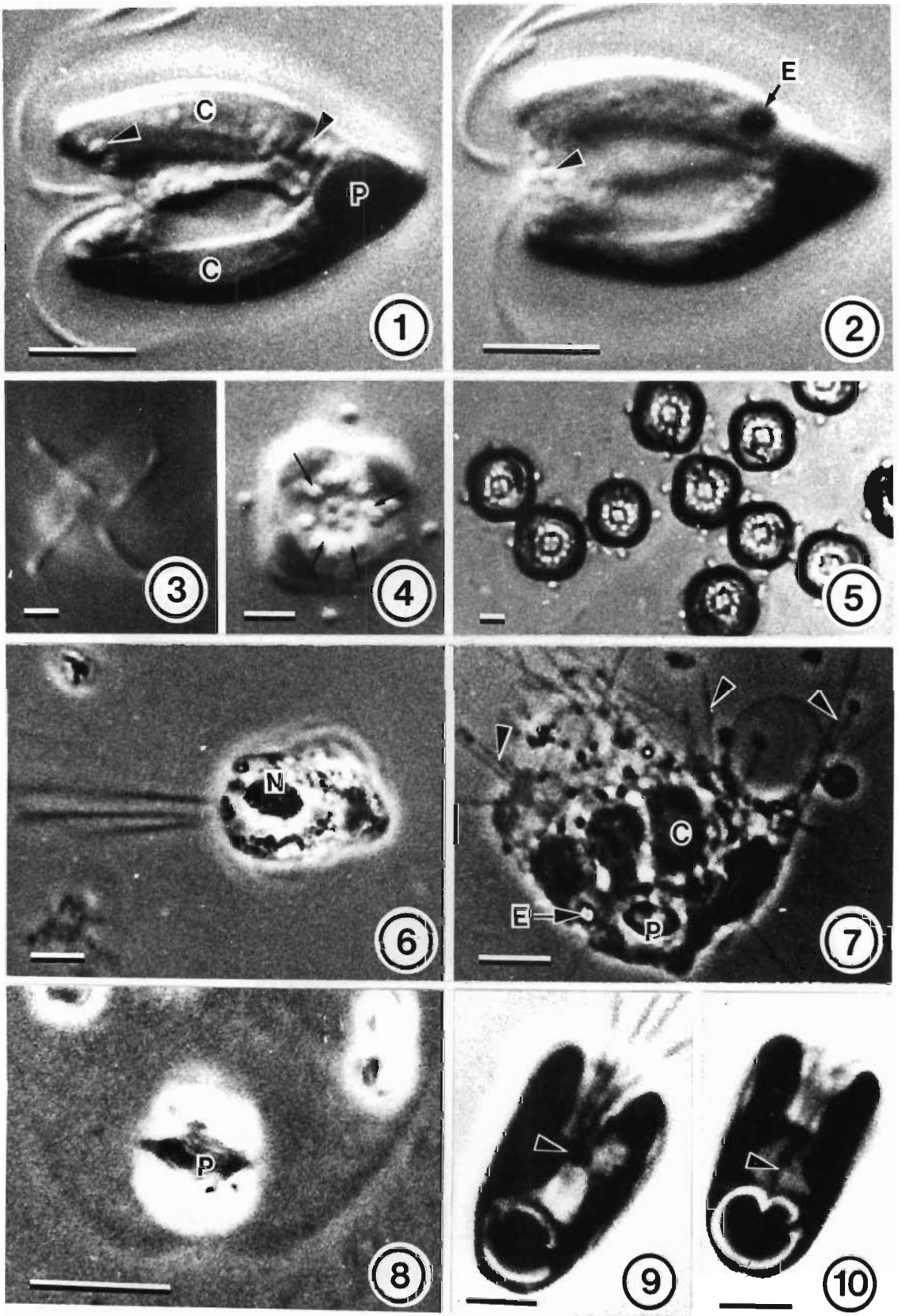
C
P
C
1
E
2
3
4
5
N
6
C
E
P
7
P
8
9
10

PLATE 2.2

Micromorphology as seen with the scanning electron microscope

Fig. 1. A lateral view of the cell showing its pyramidal shape. The promiment anterior lobes (L) are separated by longitudinal furrows. Four isokont flagella (F) emerge from the anterior end of the cell.

Fig. 2. A view of the anterior end of the cell showing the four flagella (F) emerging from a deep flagellar pit (Fp).

Fig. 3. A magnified portion of the surface of the cell showing the outer body scales (B_3).


L
L
L
F
3 µm
1

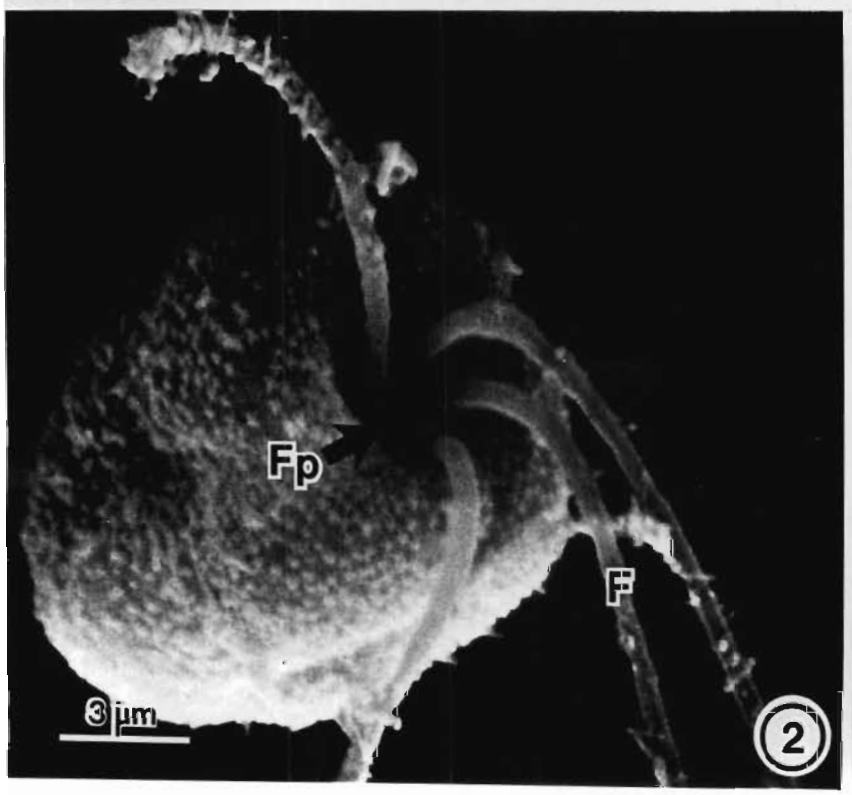
Fp
F
3 µm
2


B3
500nm
3

PLATE 2.3

Micromorphology

Fig. 1. A heavy metal shadowed cell showing the scale-boundary (Sb) on the four flagella (F) and on the cell body.

Fig. 2. A magnified view of the distal portion of the flagellum (F) in a Au/Pd shadowed preparation. The flagellum has a bluntly rounded tip. Five different scale types are seen in this micrograph.

B_1 = inner body scale
B_2 = intermediate body scale
B_3 = outer body scale

F_3 = outer flagellar scale
F_4 = hairscale

Underlayer scales (F_1 and F_2) are not seen here.

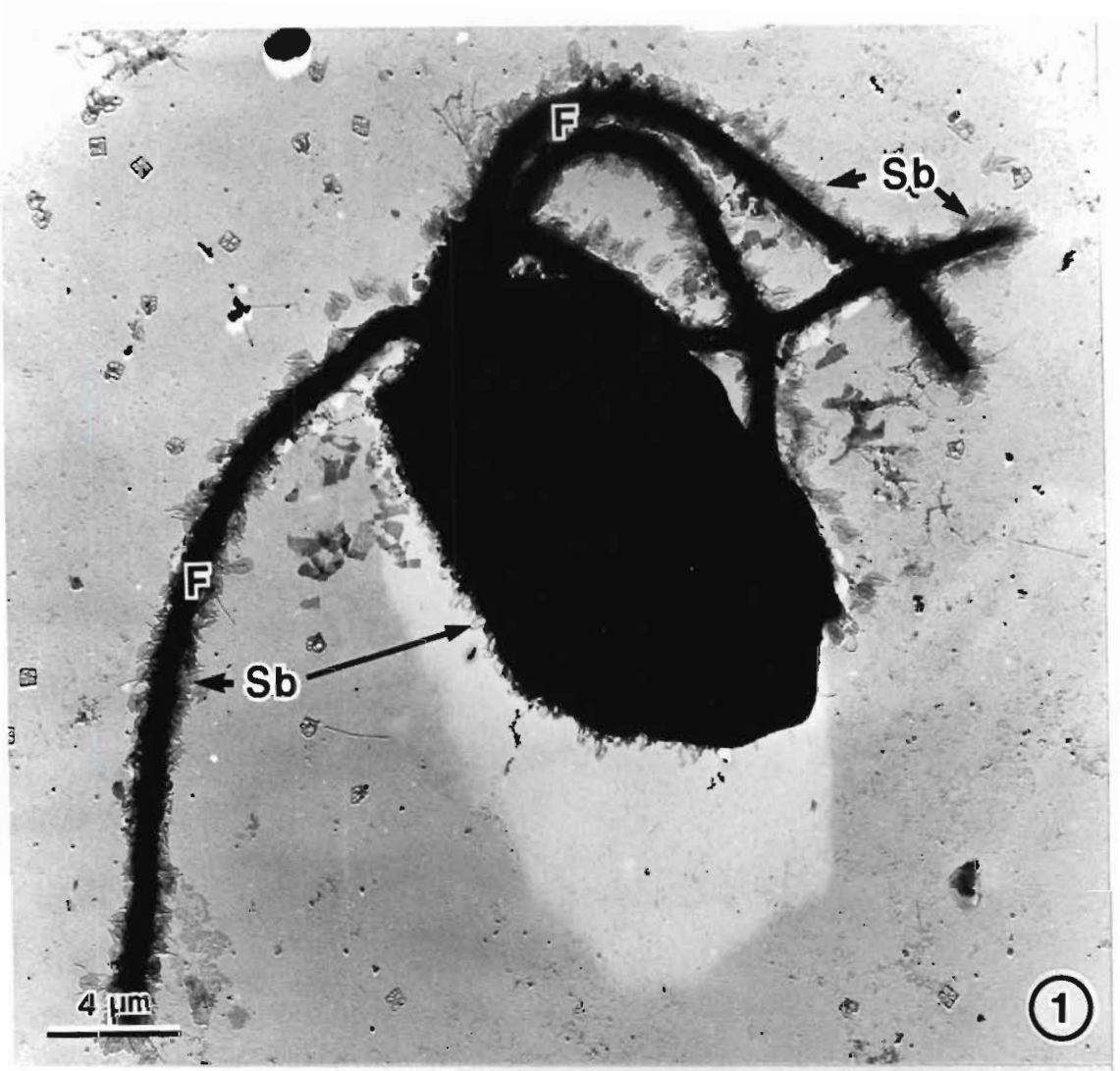
F
Sb
F
Sb
4 µm
1

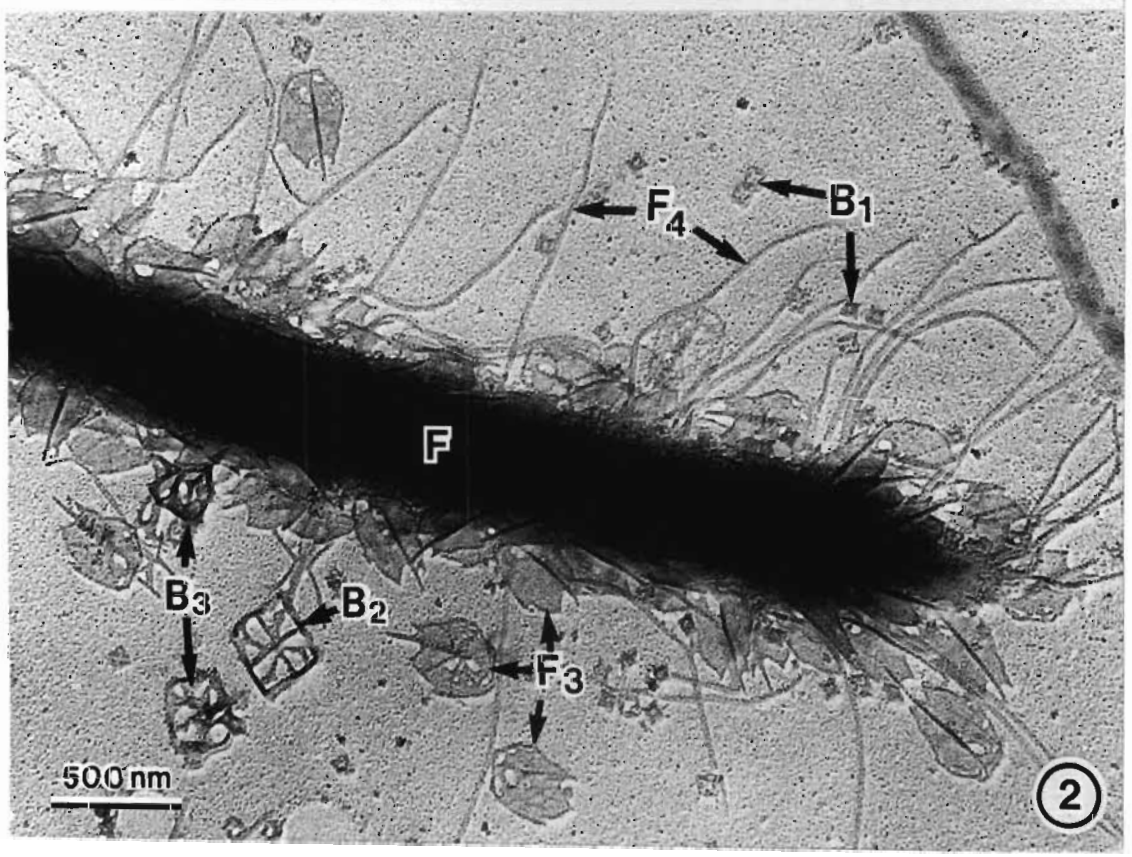
F4
B1
F
B3
B2
F3
500 nm
2

PLATE 2.4

The scale-boundary

Fig. 1. A section through the cell showing the positions of the three body scales.

B_1 = inner body scale
B_2 = intermediate body scale
B_3 = outer body scale

Fig. 2. A longitudinal section through a flagellum showing the proximal F_1 scale layer and the overlying F_3 scale layer. The F_3 scales are arranged in an imbricate manner.

Figs. 3 and 4. Two glancing sections of the flagellum showing the F_3 scales (Fig. 3) and the F_1 scales (Fig. 4). The F_3 scales are arranged in longitudinal rows with the dorsal spines aligned to form a ridge. The F_1 scales characteristically form a spiral-pattern on the flagellum.

Figs. 5 and 6. Two glancing sections of the scale-boundary. Each B_2 scale usually covers sixteen B_1 scales (Fig. 5). This is not apparent when the scale-boundary is distorted during some fixation procedures. B_3 scales are positioned so that the centre of the scale lies over the point where four adjacent B_2 scales abut (Fig. 6).

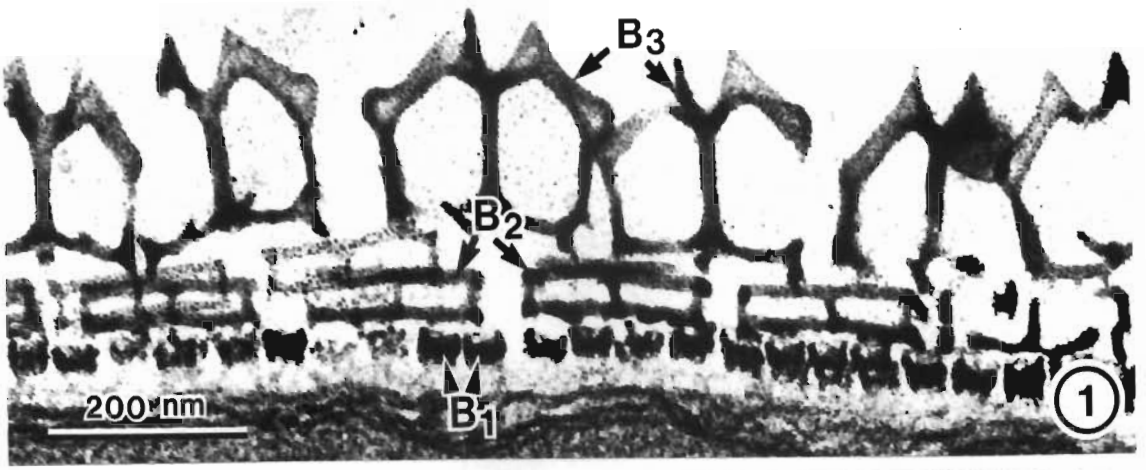
B3
B2
B1
200 nm
1


F3
F1
200 nm
2

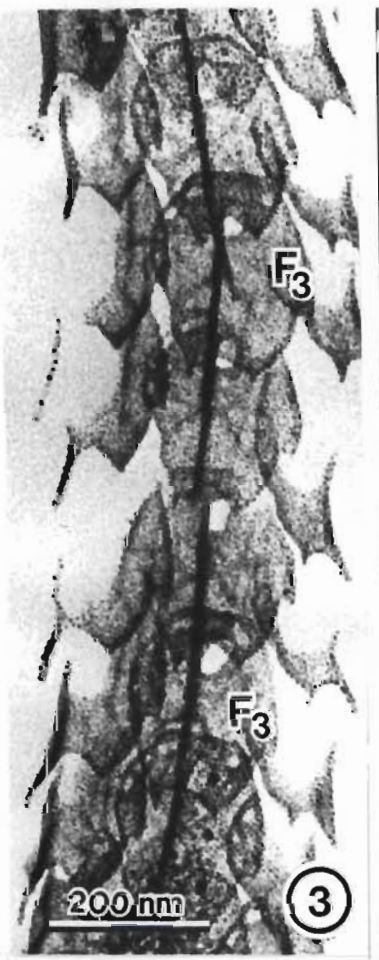
F3
F3
200 nm
3


F1
200 nm
4

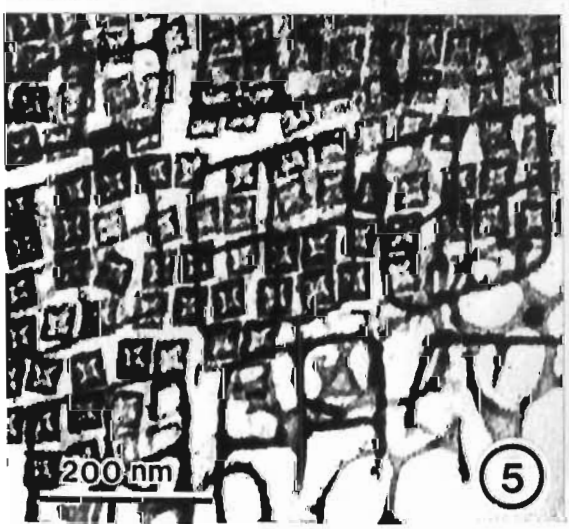
200 nm
5

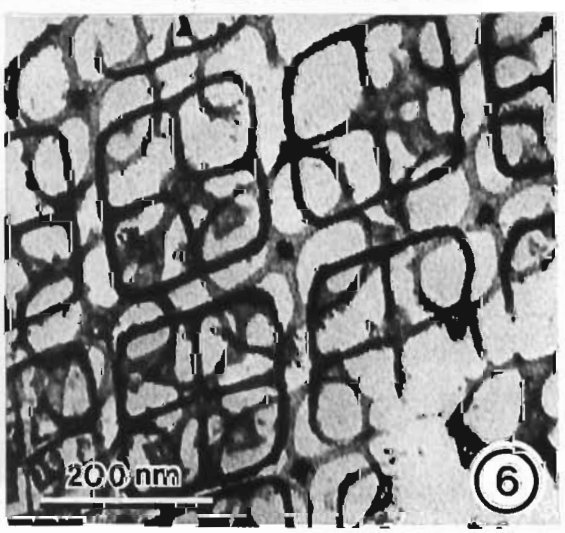
200 nm
6

PLATE 2.5

The scale-boundary

Fig. 1. During fixation the scale-boundary is often lost so that the cells appear naked. It is interesting that the dislodged scales (Sc) shown in this micrograph are lost as a unit. It appears that there may be some cohesion between scales in the scale-boundary.

Fig. 2. A glancing section of the flagellum showing the longitudinal row of paired F_2 scales (arrowheads).

Fig. 3. A longitudinal section of the flagellum showing three F_4 scales arranged in a row. The F_4 scales are attached by their tapered heads. The shaft of the scale projects perpendicularly from the surface of the flagellum. Though not shown here the F_4 scales are distichously arranged along the length of the flagella.

Fig. 4. A transverse section of the flagellum showing the attachment of the hairscale (F_4) between a pair of F_2 scales.

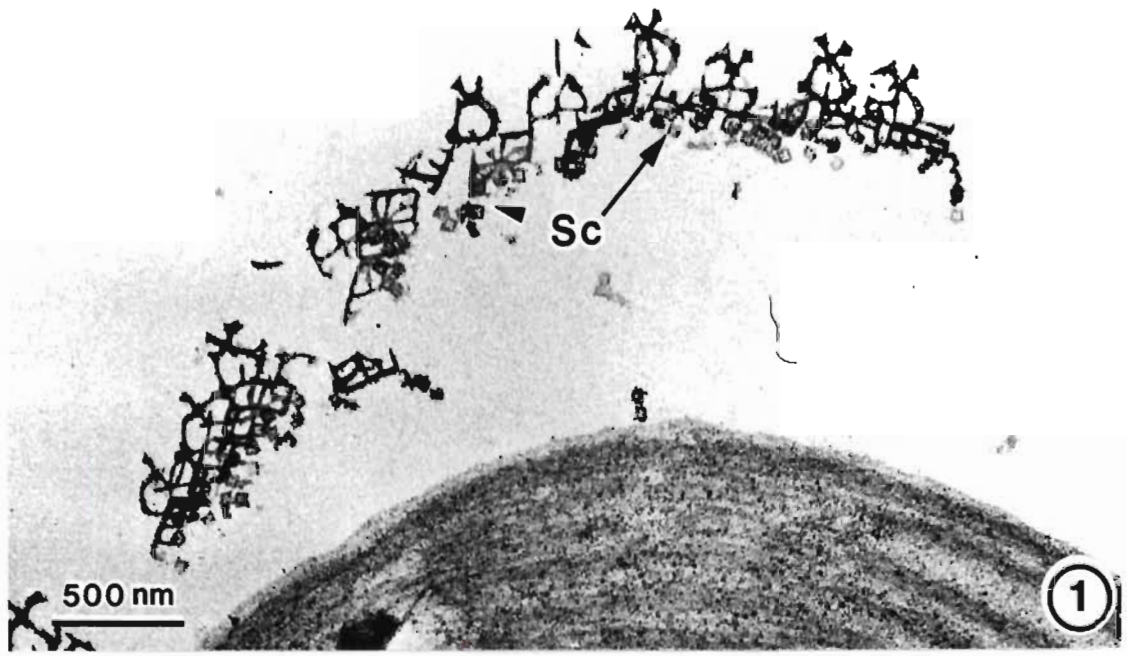
Sc
500 nm
1

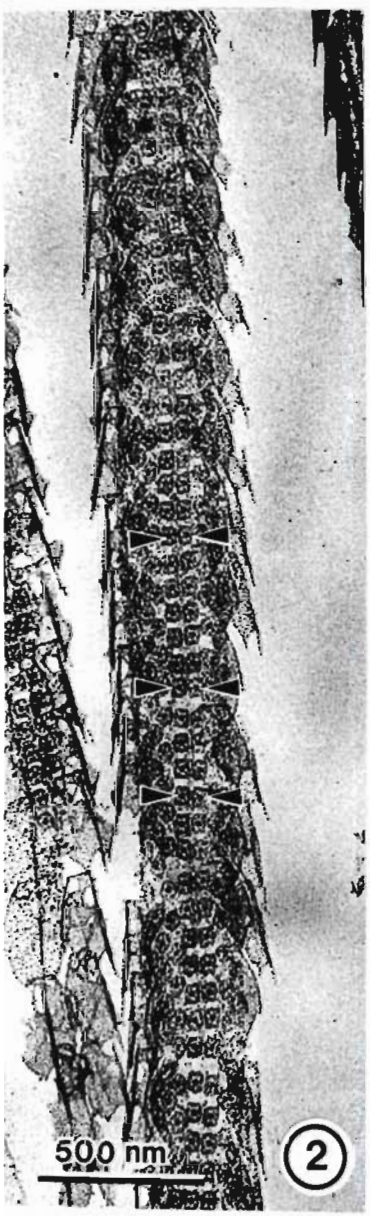
500 nm
2

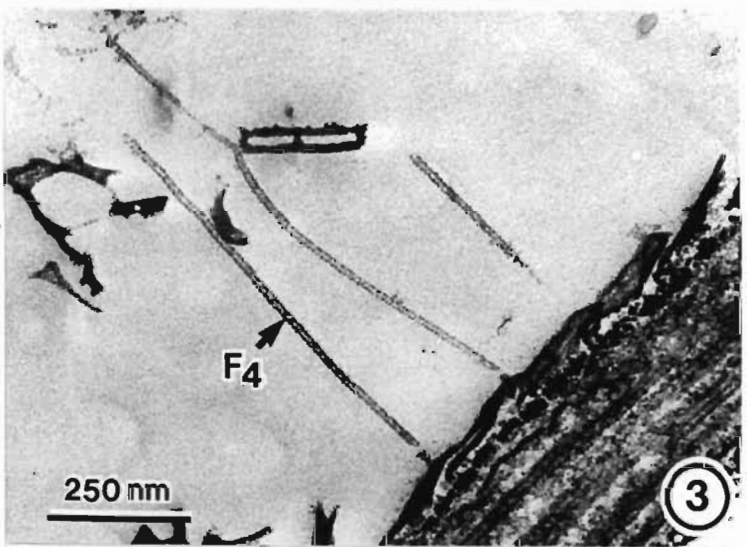
F4
250 nm
3

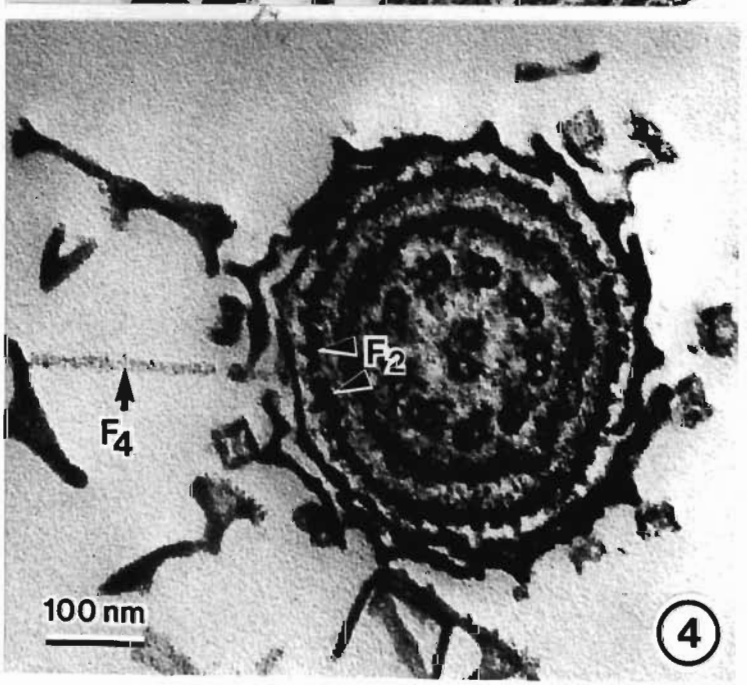
F2
F4
100 nm
4

PLATE 2.6

Internal Organization

Figs. 1. and 2. Longitudinal sections through two cells showing a deep anterior flagellar pit (Fp) from which the flagella (F) emerge. The cells have a large parietal chloroplast (C) containing a posterior pyrenoid (P) and a lateral eyespot (E). Starch grains (S) surround the pyrenoid but often occupy other positions within the chloroplast.

The two cells depicted here were cut in two planes at right angles to one another. Thus Fig. 1 shows the anterior position of the two dictyosomes (D) in the dorsal and ventral lobes of the cell. This cell has a complete covering of scales forming the scale-boundary (Sb). In Fig. 2 the laterally positioned nucleus (N) is seen in the right side (RS) of the cell. The scale reservoir (Sr) and vacuole (V) are opposite the nucleus in the left side (LS) of the cell. This cell appears naked because the scales were lost during fixation.

The median longitudinal section of the cell (Fig. 2) shows the position of the flagellar basal bodies (Fb) at the base of the flagellar pit. A striated rootlet (Rh) extends from the basal bodies toward the posterior end of the cell. Trichocysts (T) surround the mouth of the flagellar pit. Numerous mitochondrial profiles (M) are obvious on the centripetal surface of the chloroplast. A nucleolus (No) is present in the nucleus.

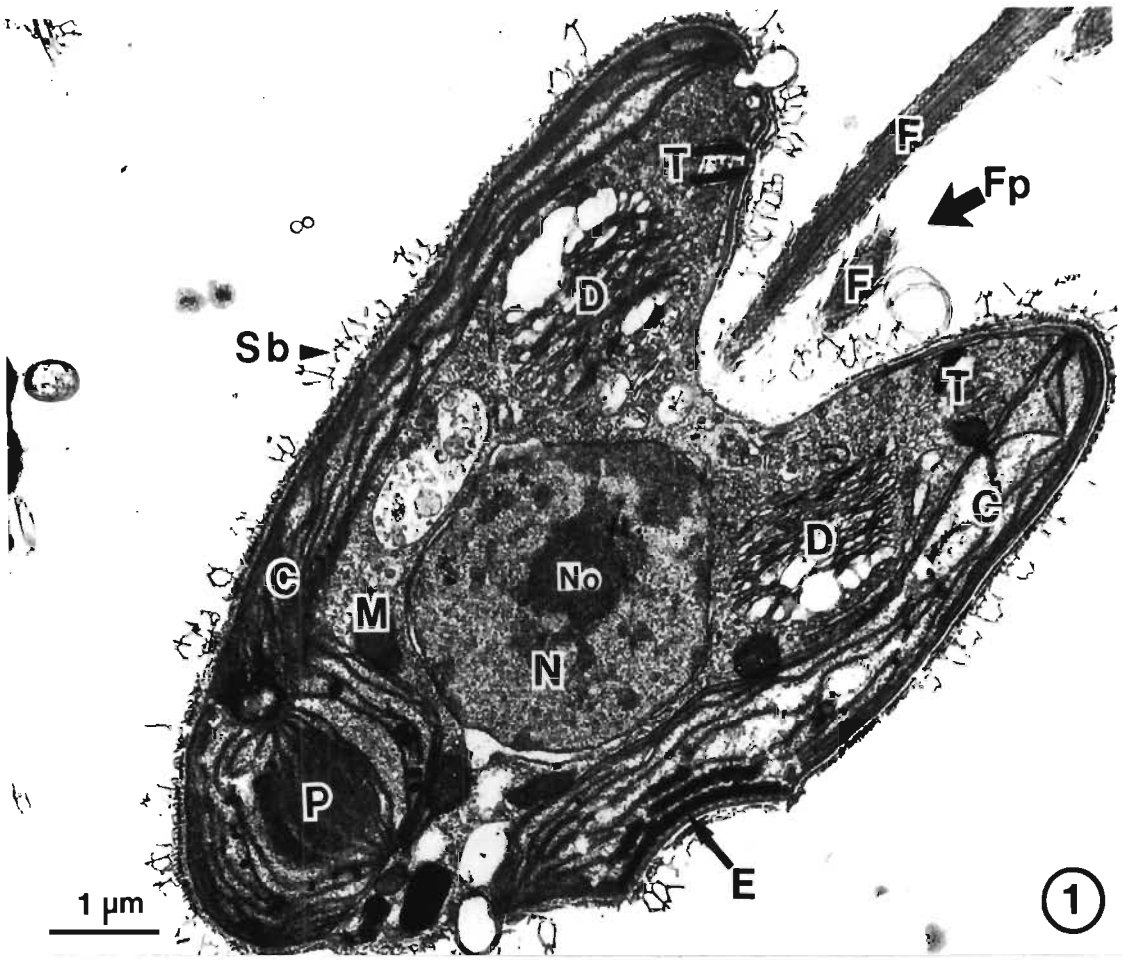
T
F
Fp
F
D
Sb
T
C
D
No
C
M
N
P
E
1 µm
1

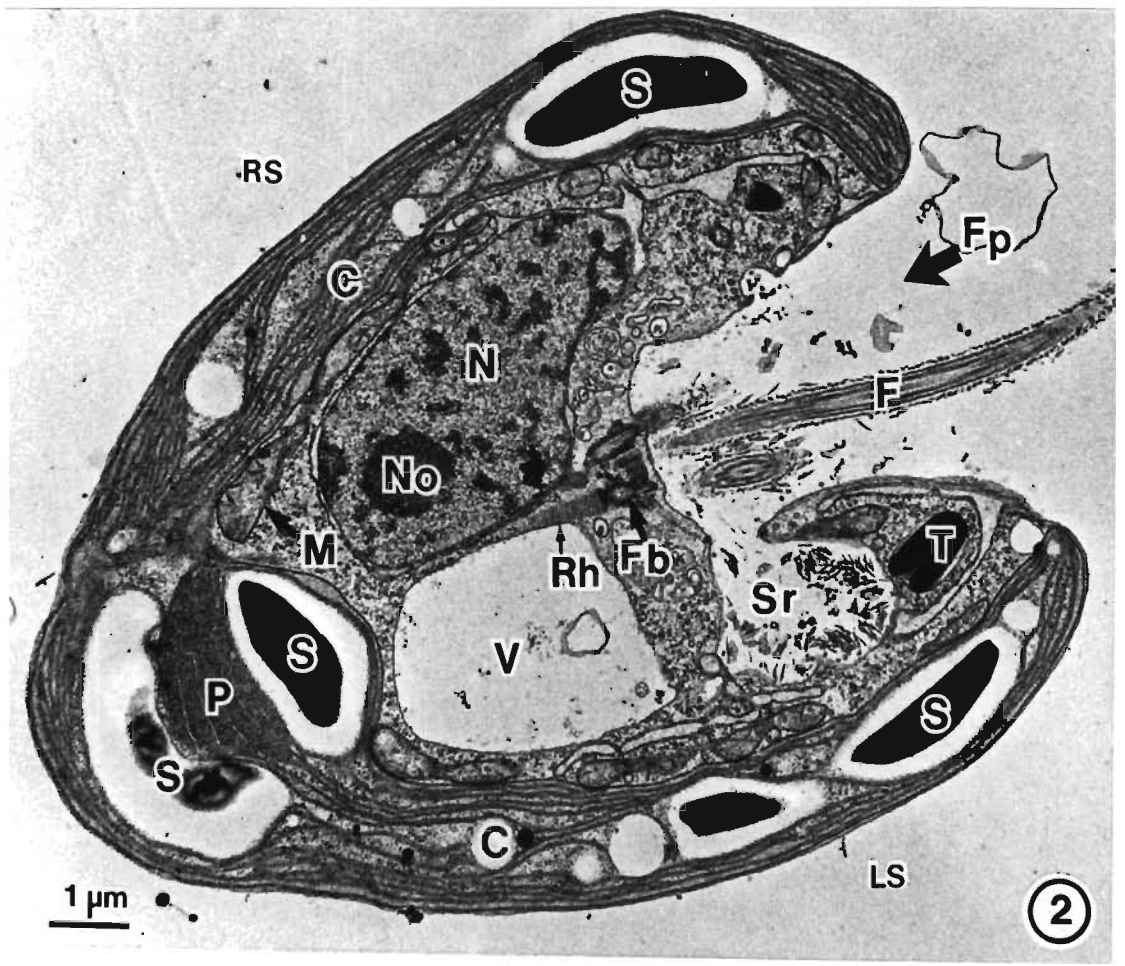
S
RS
Fp
C
N
F
No
M
Rh
Fb
T
Sr
V
S
P
S
S
C
LS
1 µm
2

PLATE 2.7

Internal organization

Figs. 1 and 2. Transverse sections through the anterior region of two cells. The section in Fig. 2 was taken just posterior to that in Fig. 1.

The anterior lobes of the chloroplast (C) contains starch grains (S) and occupy the lobes of the cell body. Trichocysts (T) often occur in the longitudinal grooves of the cell between adjacent chloroplast lobes (Fig. 2). A circular flagellar pit (Fp) is centrally positioned and contains the profiles of four flagella (F). A scale reservoir (Sr) is connected with the flagellar pit via a duct (Du). This duct enters the flagellar pit asymmetrically as it passes around a cytoplasmic spur (dark arrow in Fig. 1). This spur points towards the ventral side (VS) of the cell (see direction of dark arrow). The opposite side is the dorsal side (DS). The nucleus occupies the right side (RS) of the cell and the scale reservoir the left side (LS) of the cell. The two dictyosomes (D) occupy the dorsal and ventral lobes of the cell.

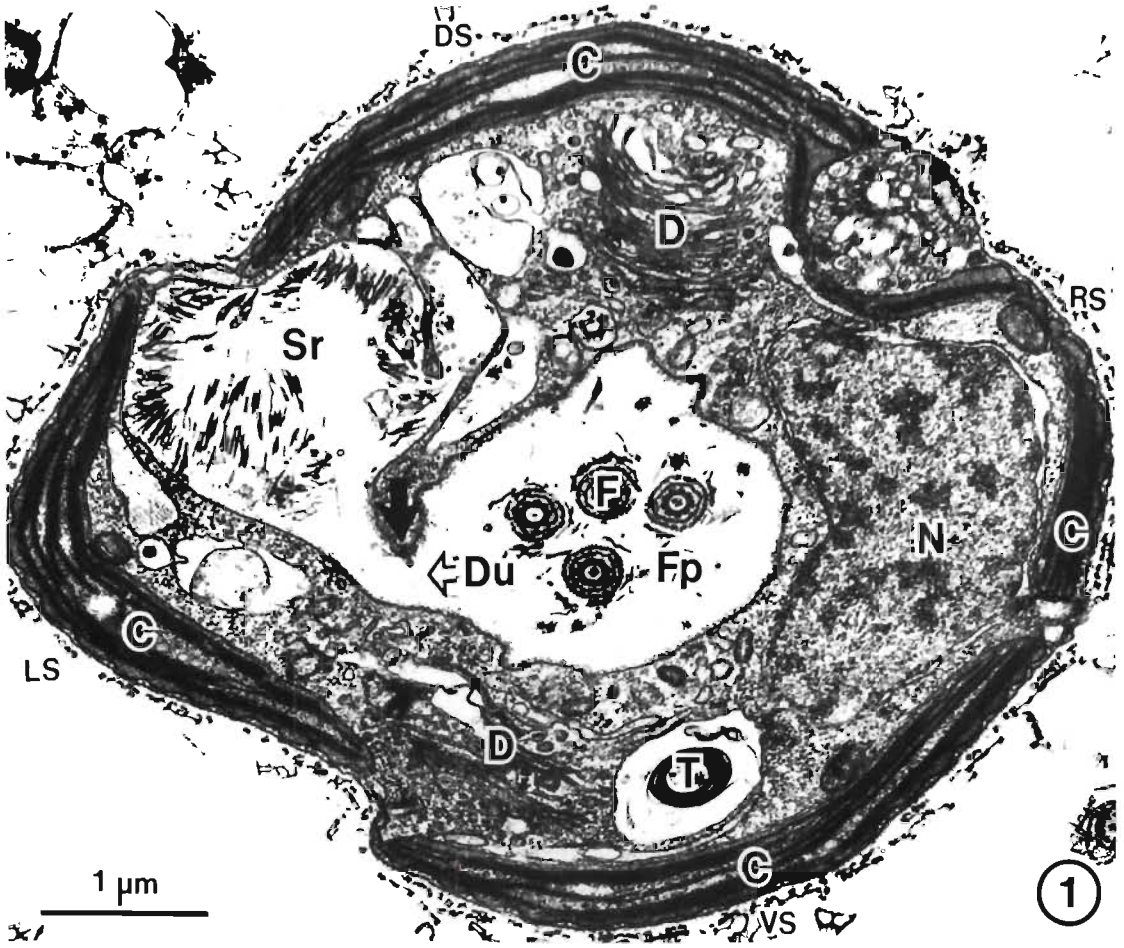
DS
C
D
RS
Sr
F
N
C
Du
Fp
C
LS
D
T
C
VS
1 µm
1

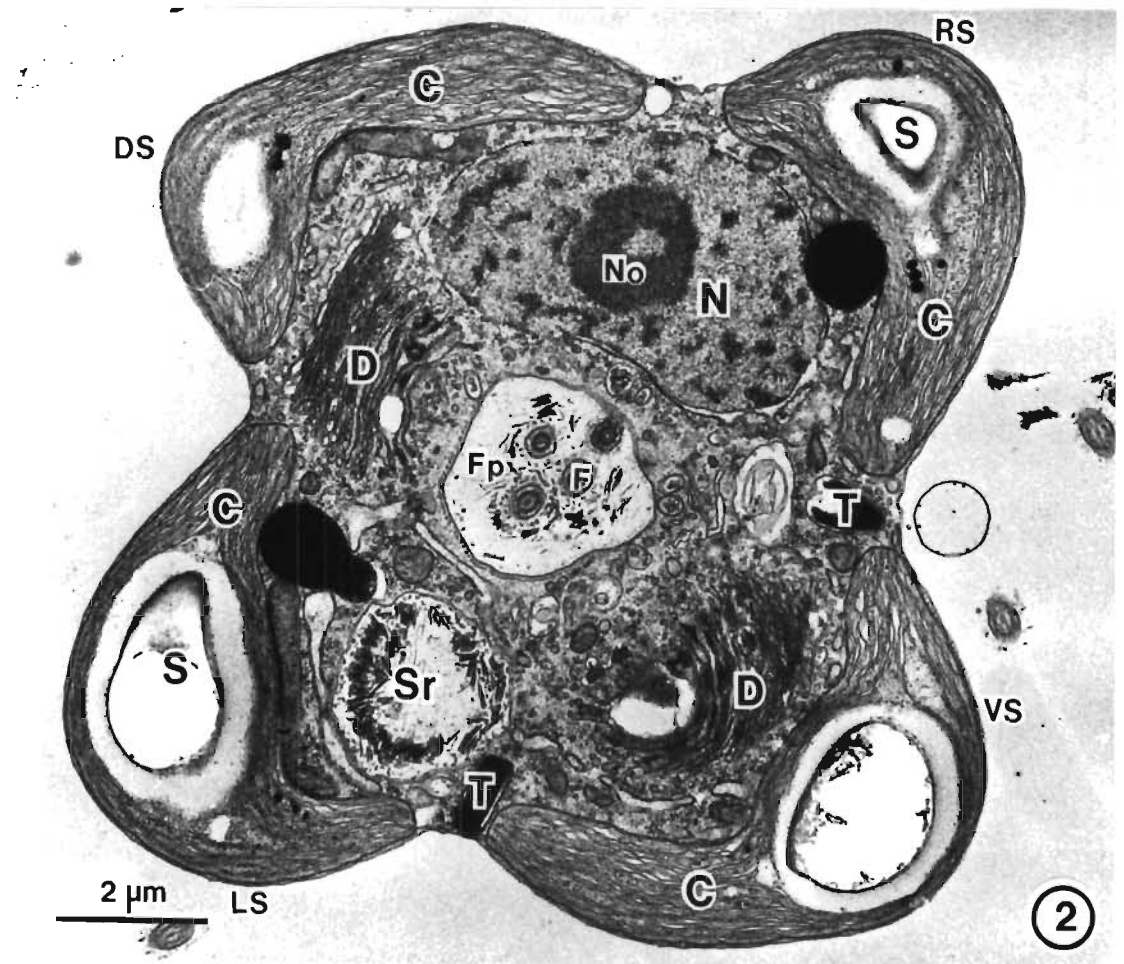
RS
C
S
DS
No
N
C
D
Fp
F
C
T
S
Sr
D
VS
T
C
2 µm
LS
2

PLATE 2.8

The flagellar apparatus.

Fig. 1. A longitudinal section through the flagellum showing the flagellar axoneme, transition region and basal body. The position of the synistosome (Sy), proximal connecting fibre (Pcf) and basal connecting band (white arrowhead) are shown. Letters A-F correspond with the transverse sections shown in Figs. 2 - 7.

Figs. 2 - 7. Transverse sections showing the structure of the flagellum in different regions shown in Fig. 1.

Fig. 2 - 9+2 microtubular structure of the axoneme
Fig. 3 - showing transitional helix-like structure
Fig. 4 - showing absence of central microtubules
Fig. 5 - showing stellate pattern of fibrils
Fig. 6 - inclined triplet microtubules with connecting fibrils
Fig. 7 - incline triplet microtubules.

Fig. 8. A longitudinal section through the flagellar apparatus showing that the basal bodies (Fb) are angled so that they are closer proximally.

Fig. 9. A transverse section of the flagellar basal bodies showing the four microtubular rootlets (R) arising from between the basal bodies in a cruciate pattern.

Fig. 10. A transverse section through the flagellar basal body apparatus. The basal bodies (1 - 4) are connected to each other and the synistosome (Sy) by pericentriolar fibres (Pf). A fibrillar band (Frb) connects basal bodies 1, 3 (and 4).

Fig. 11. A transverse section of the synistosome (Sy) lying between basal bodies 2 and 3. Note the fibrils (arrowhead) connecting the central band with the peripheral band on the concave surface.

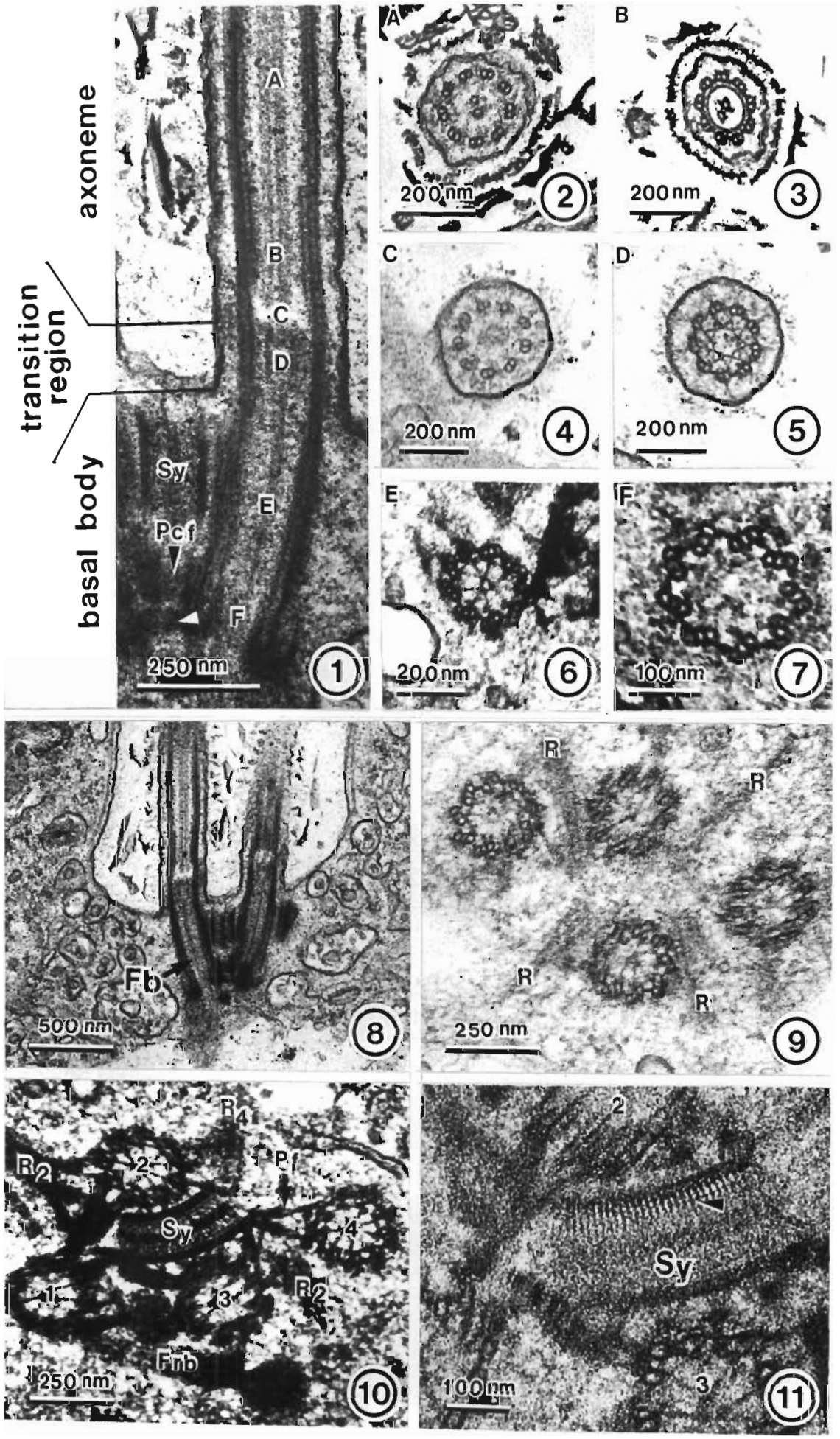
axoneme
transition region
basal body
A
B
C
D
Sy
E
Pcf
F
250 nm
1
200 nm
2
200 nm
3
200 nm
4
200 nm
5
200 nm
6
100 nm
7
Fb
500 nm
8
R
R
R
R
250 nm
9
R4
R2
2
Pf
Sy
4
1
3
R2
Fnb
250 nm
10
2
Sy
3
100 nm
11

PLATE 2.9

Microtubular roots and the basal body apparatus

Figs. 1 and 2. Transverse sections of the microtubular roots in the region of the flagellar pit. The R_4 root with four microtubules has the latter arranged in a 3 over 1 pattern (arrowheads - Fig. 1). The R_2 root has two microtubules lying side by side (arrowheads-Fig. 2).

Fig. 3. A transverse section through the proximal part of the basal bodies (1 - 4) showing the curved microbody (Mb) situated between basal bodies 2 and 4. The basal body closest to the nucleus (N) is called basal body 4.

Fig. 4 - 6. Sections through the basal body apparatus showing characteristics of the compound R_2 root (R_2c). The R_2c root arises from between basal bodies 1 and 2 (Figs. 4 and 6) and extends toward the scale reservoir where it bifurcates (open arrow in Fig. 4) and surrounds the duct (Du) of the scale reservoir (Figs. 5 and 6). The R_2C root gains approximately four additional microtubules shortly after leaving the basal bodies (Fig. 6). The opposite R_2 root has only two microtubules (Figs. 5 and 6). Fig. 6 also shows the position of the basal bodies (1 - 4) and connecting fibres; Frb = fibrillar band, Pf = pericentriolar fibres, Sy = synistosome.

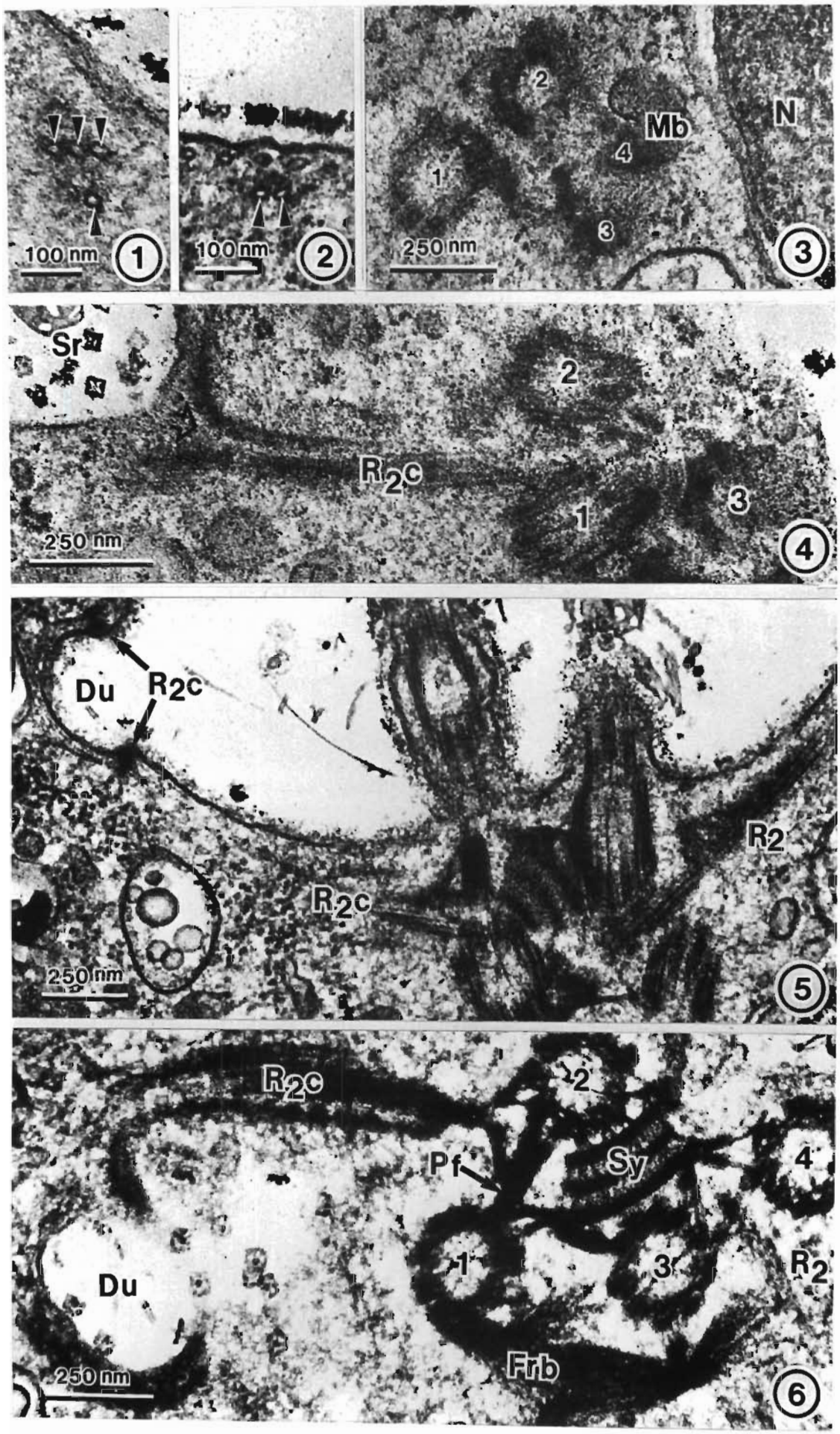
100 nm
1
100 nm
2
2
Mb
N
4
1
3
250 nm
3
Sr
2
R2c
1
3
250 nm
4
Du
R2c
R2
R2c
250 nm
5
R2c
2
Pf
Sy
4
1
3
R2
Du
Frb
250 nm
6

PLATE 2.10

Microtubular roots, cytoskeletal microtubules and the rhizoplast-microbody-nucleus complex

Figs. 1 - 3. Median longitudinal sections through cells.

Fig. 1. The rhizoplast (Rh) and microbody (Mb) lie adjacent to one another and are attached to the proximal part of the basal bodies (Fb). The nucleus (N) has many nuclear pores (arrowheads).

Fig. 2. The R_4 microtubular root arising near the flagellar basal bodies (Fb) extends anteriorly and terminates soon after it overlaps with the cytoskeletal microtubules (Csm).

Fig. 3. The rhizoplast (Rh) bifurcates near the basal bodies (Fb). The two trunks of the rhizoplast attach to basal bodies 2 and 3.

Fig. 4. A transverse section of a cell showing the rhizoplast-microbody-nucleus complex. The microbody (Mb) is usually "sandwiched" between the rhizoplast (Rh) and nucleus (N).

Fig. 5. A median longitudinal section of a cell showing the rhizoplast-microbody-nucleus complex. The microbody (Mb) lies adjacent to the nucleus (N) for much of its length. The rhizoplast (Rh) extends further into the cell where it bifurcates to lie over the chloroplast in the region of the pyrenoid (P).

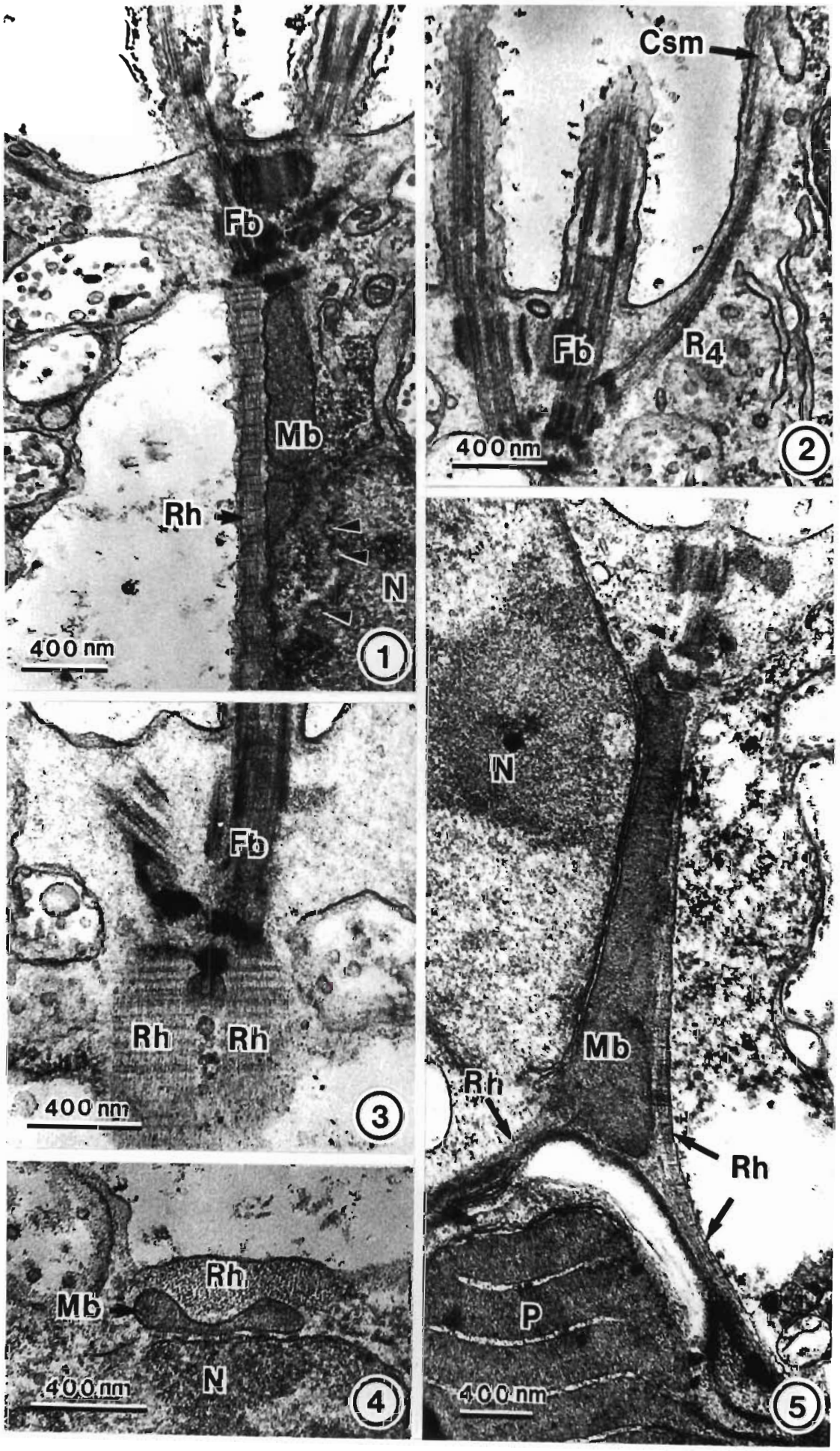
Fb
Mb
Rh
N
400 nm
1
Csm
Fb
R4
400 nm
2
Fb
Rh
Rh
400 nm
3
Rh
Mb
N
400 nm
4
N
Mb
Rh
Rh
P
400 nm
5

PLATE 2.11

Cytoskeletal microtubules

Fig. 1. A transverse section through the flagellar pit (Fp) showing a ring of cytoskeletal microtubules (Csm) lying just beneath the plasmalemma. Endoplasmic reticulum (ER) always surrounds the flagellar pit in this region.

Figs. 2 and 3. Glancing sections of cells showing the cytoskeletal microtubules (Csm). These are more widely spaced than in the flagellar pit. Most often they occur singly (fig. 2). but sometimes they occur in pairs (fig. 3).

Figs. 4 and 5. Transverse sections of cells showing single (fig. 4) or paired (fig. 5) cytoskeletal microtubules (Csm). These lie between the plasmalemma and chloroplast and are accommodated in furrows of the chloroplast. Microtubules are concentrated in the longitudinal grooves of the cell (open arrow - fig. 5).

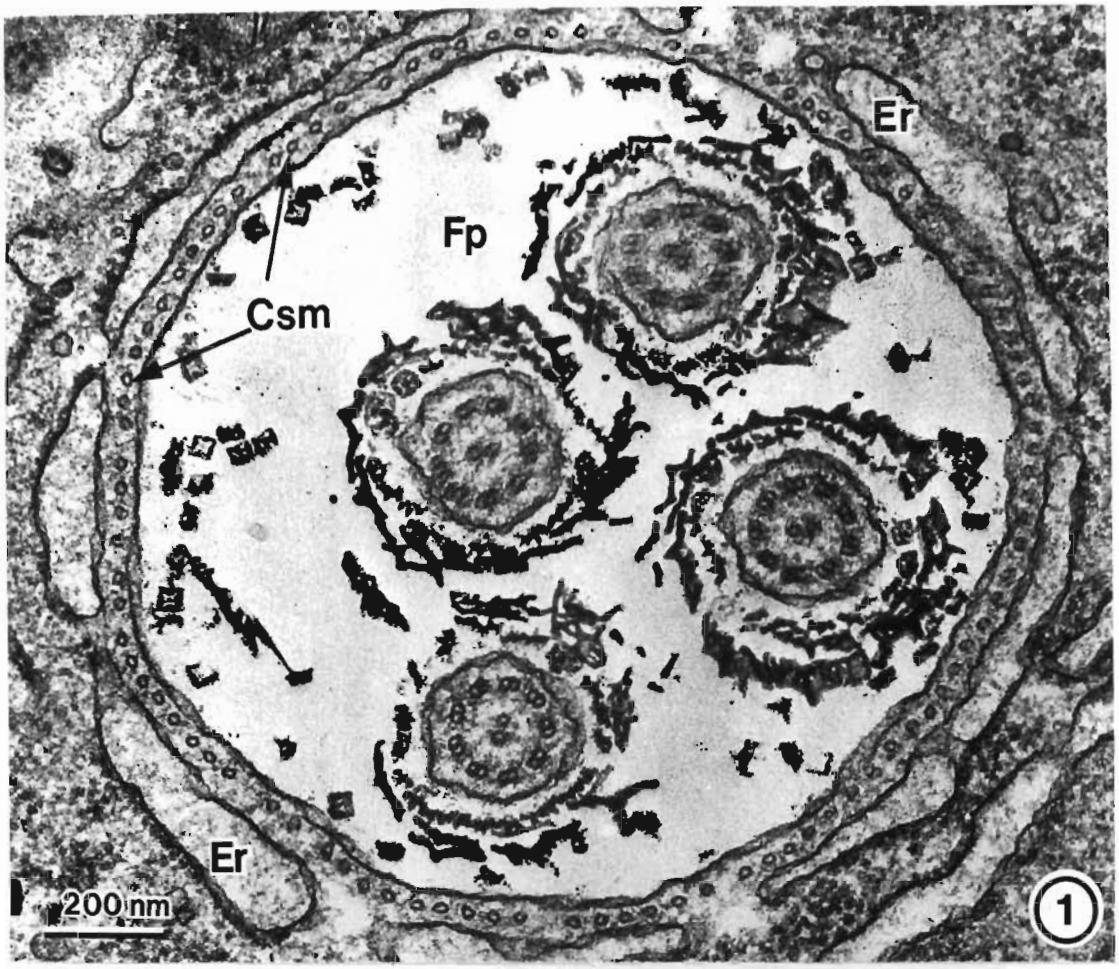
Er
Fp
Csm
Er
200nm
1

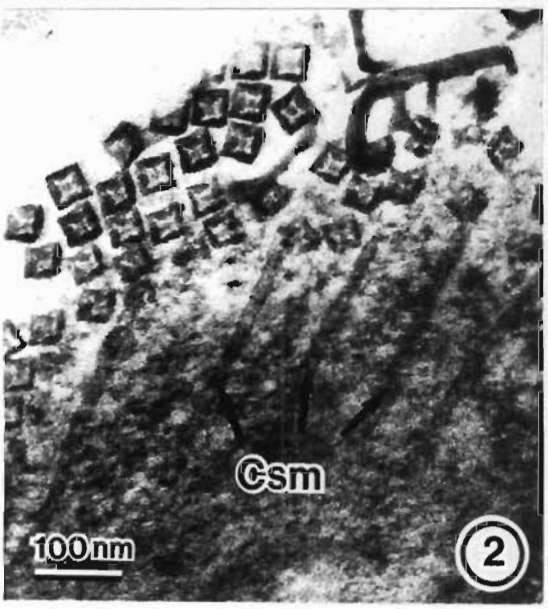
Csm
100nm
2

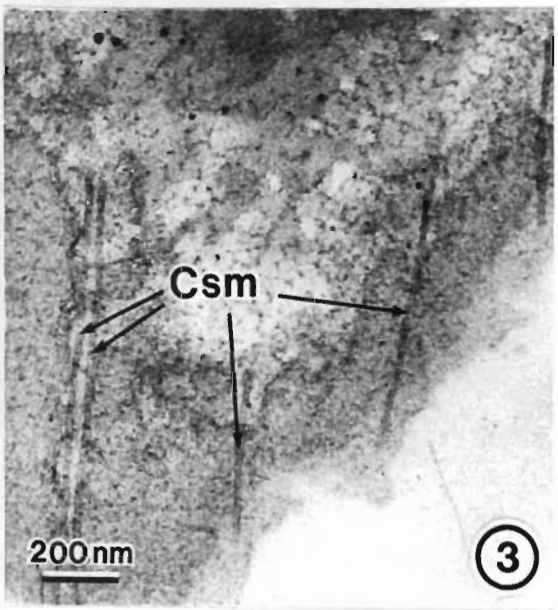
Csm
200nm
3

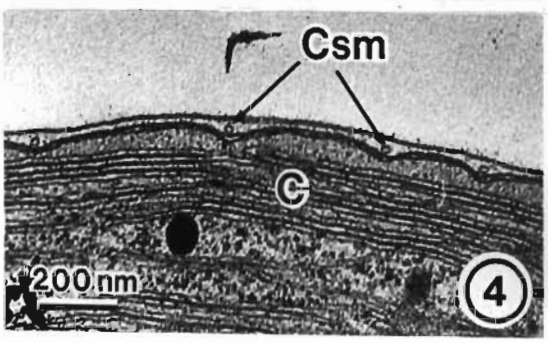
Csm
C
200nm
4

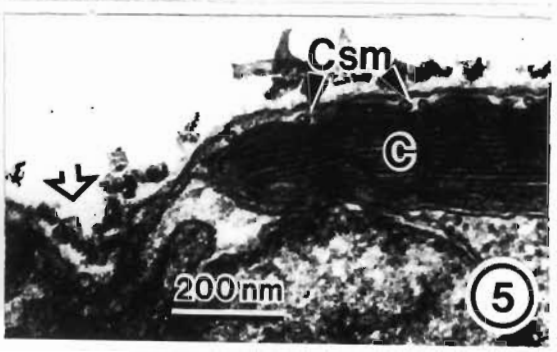
Csm
C
200nm
5

PLATE 2.12

The chloroplast, eyespot, pyrenoid and mitochondrion

Figs. 1 and 2. Sections through the chloroplast (C) showing the thylakoids arranged in stacks of two (fig. 1) or more (fig. 2). The thylakoids end abruptly at the radial boundary of the chloroplast (fig. 1). Thylakoids do not pass through the eyespot (E).

Figs. 3 and 4. Sections through the eyespot (E). This organelle is usually comprised of three layers of carotenoid globules and is situated within the chloroplast (C) beneath a depression in the cell surface (fig. 3). A glancing section of an eyespot (fig. 4) shows the tight packing of these globules giving a hexagonal pattern.

Figs. 5 and 6. A longitudinal (fig. 5) and transverse section (fig. 6) of the pyrenoid (P). The pyrenoid is traversed by parallel thylakoids which enter it laterally (fig. 5). Two cup-shaped starch grains (S) usually surround the pyrenoid (fig. 5). Because the parallel thylakoids are often curved, a transverse section sometimes reveals the concentric pyrenoid lamellae (fig. 6).

Figs. 7 and 8. Two serial sections showing mitochondrial profiles (M) adjacent to the chloroplast (C). What appear to be isolated mitochondria in fig. 7 are in fact profiles of the same mitochondrion (fig. 8).

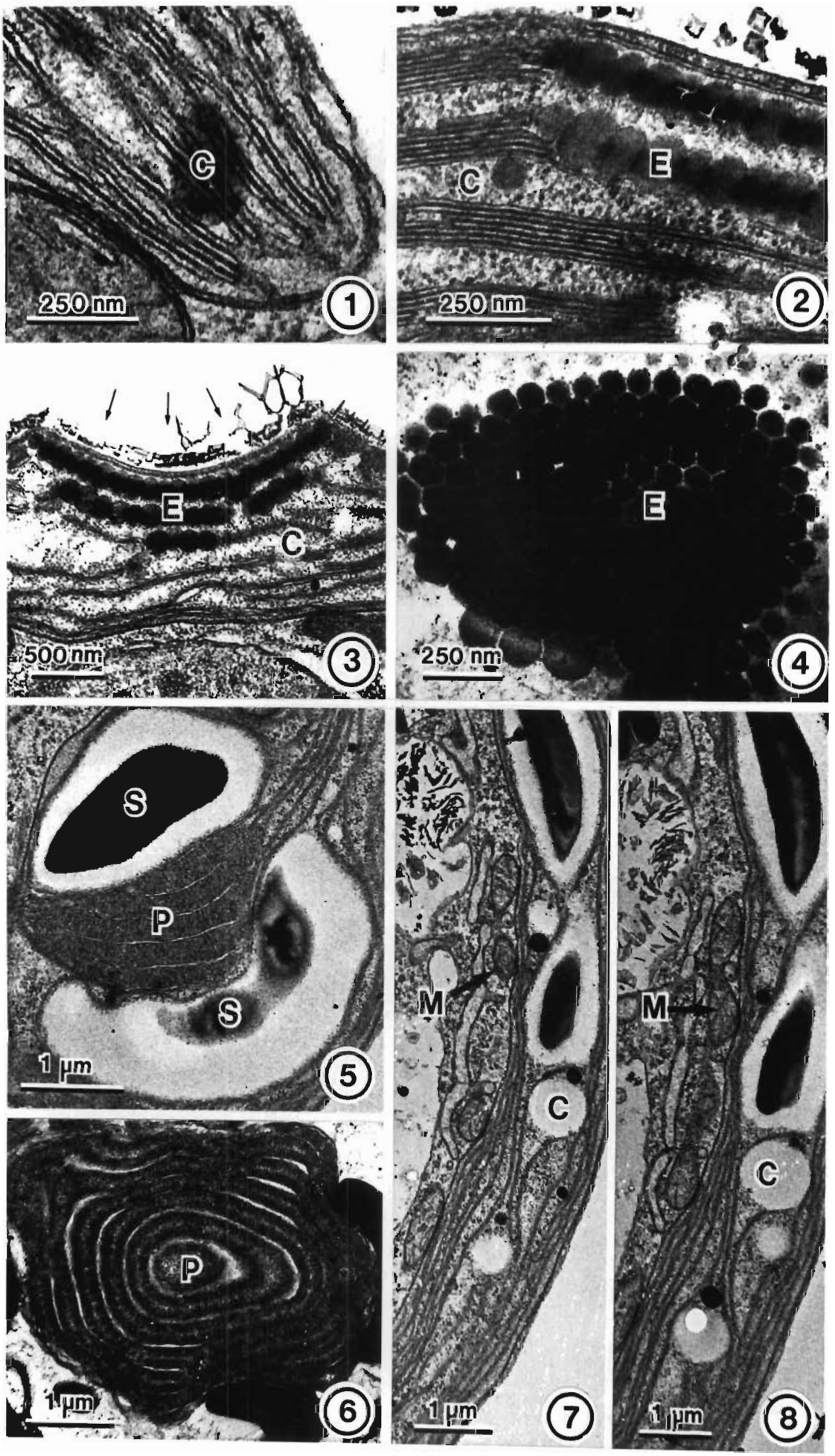
C
250 nm
1
C
E
250 nm
2
E
C
500 nm
3
E
250 nm
4
S
P
S
1 µm
5
P
1 µm
6
M
C
1 µm
7
M
C
1 µm
8

PLATE 2.13

The mitochondrion and trichocyst

Figs. 1 and 2. Sections showing the detailed structure of the mitochondrion (M). This organelle is always closely appressed to the chloroplast (C). It is bounded by a double unit membrane. The inner membrane is convoluted to form flattened cristae (arrowheads in fig. 1). In actively growing cells the mitochondrion sometimes has very long cristae which lie parallel to the chloroplast thylakoids. (Fig. 2).

Fig. 3. A longitudinal section through a trichocyst (T) showing numerous vesicles in the trichocyst lumen. The trichocyst is contained in a membrane bound chamber which has a cytoplasmic papillae (arrow) at the proximal end.

Figs. 4 and 5. Transverse sections through the trichocysts (T). The trichocyst is ribbon-like having a coiled appearance in section (fig. 5). In the lumen of the trichocyst many small vesicles fuse with the ribbon (fig. 4). The material they deposit increases the length of the ribbon.

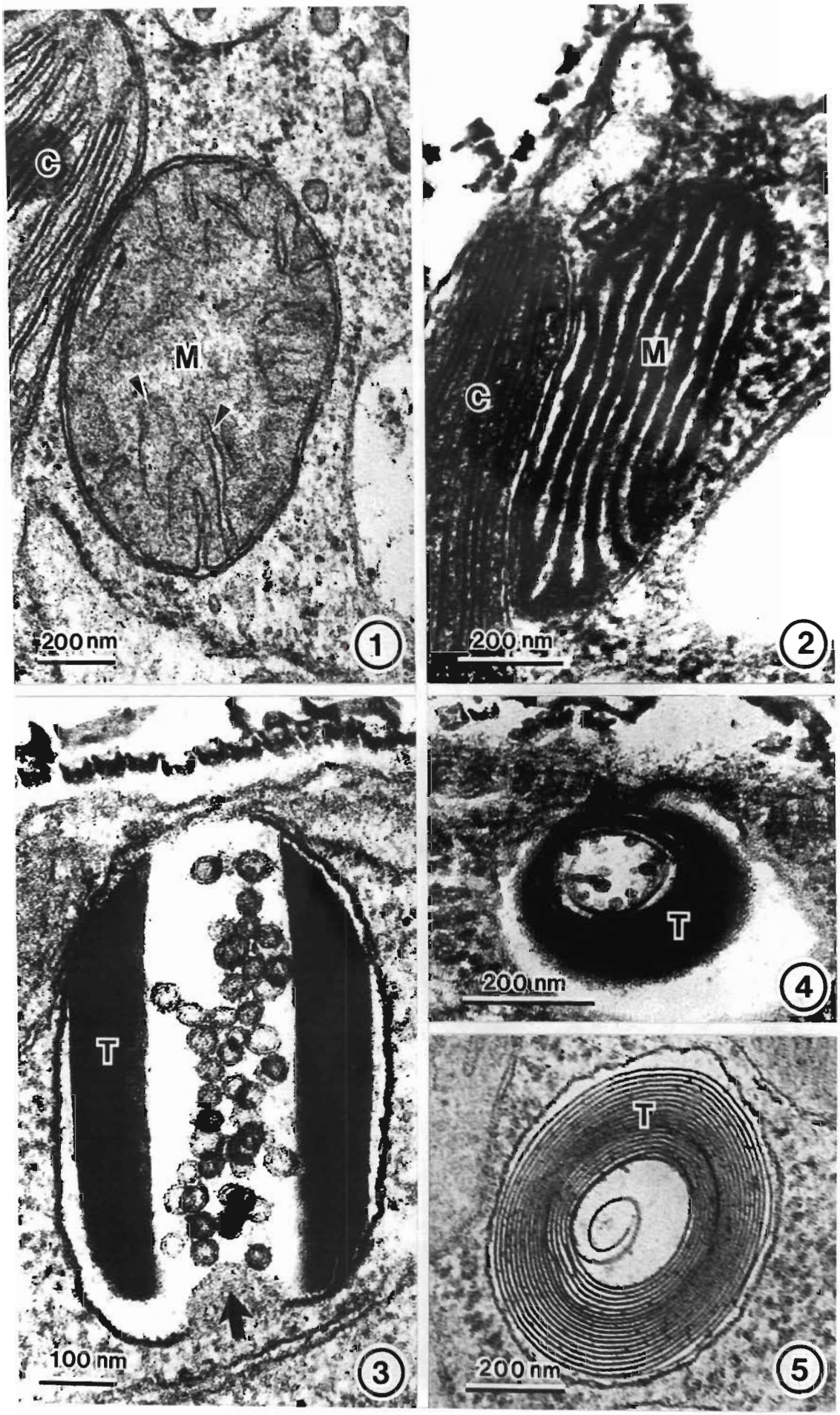
C
M
200 nm
1
C
M
200 nm
2
T
100 nm
3
T
200 nm
4
T
200 nm
5

PLATE 2.14

The trichocyst

Fig. 1. An oblique section through an almost mature trichocyst (T) showing the large vesicle produced by the cytoplasmic papilla.

Fig. 2. A longitudinal section through a mature trichocyst (T) showing the position of the large vesicle (arrowhead) at the distal end of the trichocyst lumen. Many smaller vesicles are distributed throughout the rest of the lumen.

Figs. 3 and 4. Longitudinal sections through ejecting trichocysts (T). When the trichocyst is first released (fig. 3) the plasmalemma forms a collar (arrows) that apparently isolates the trichocyst chamber from the external medium. When the trichocyst is ejected the inner coils extend in a telescoping action (fig. 4).

Fig. 5. A heavy metal shadowed preparation of an ejected trichocyst (T) showing the telescoped ribbon with overlapping coils.

Figs. 6 and 7. The ejected trichocyst (T) is tubular in transverse section (fig. 7). The coils of the trichocyst ribbon overlap so that the ejected organelle maintains its tubular structure. (Fig. 6).

Fig. 8. Empty trichocyst chambers (arrows). The membrane of the trichocyst chamber fuses with and is incorporated into the plasmalemma.

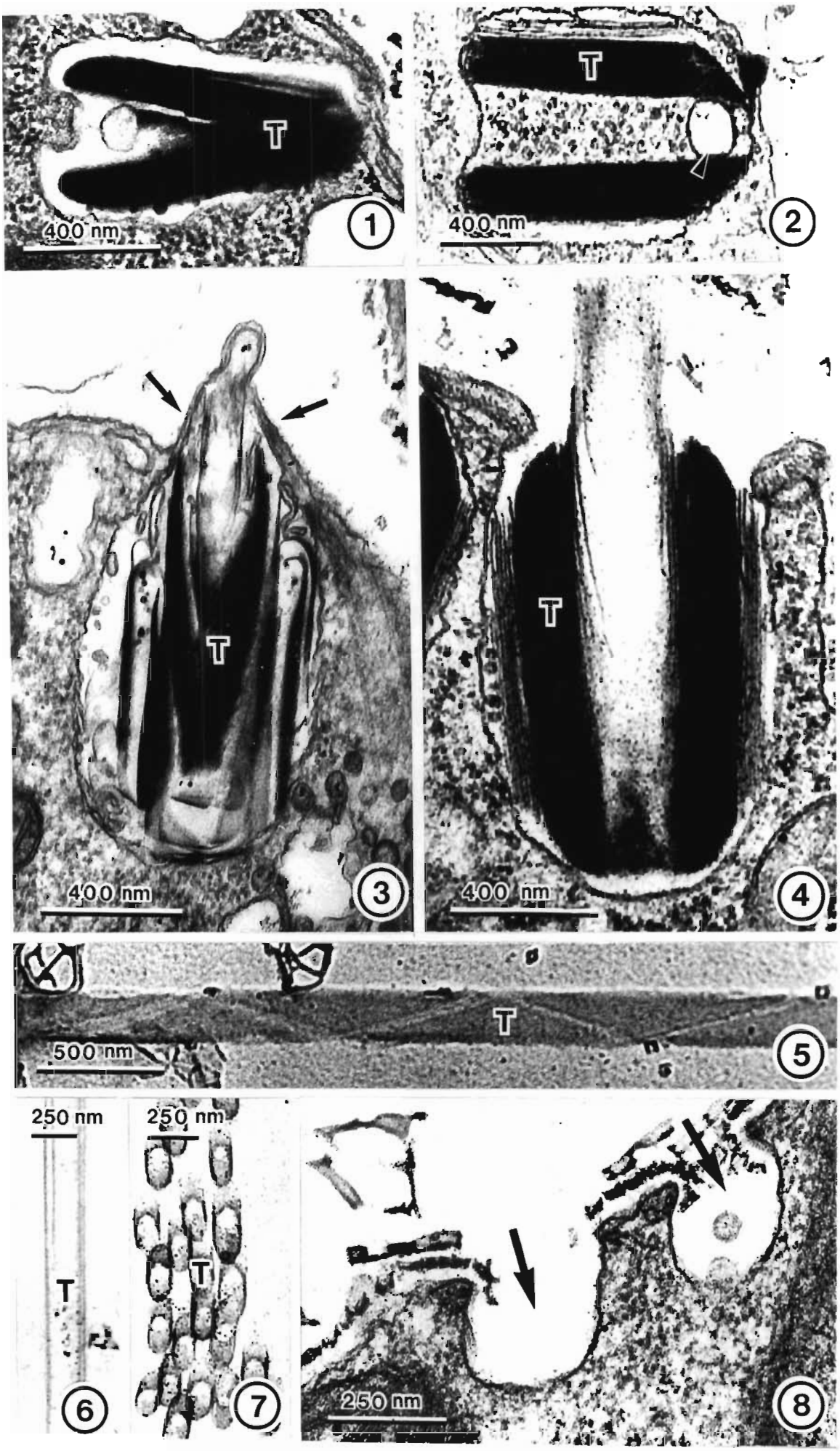
T
400 nm
1
T
400 nm
2
T
400 nm
3
T
400 nm
4
T
500 nm
5
250 nm
T
6
250 nm
T
7
250 nm
8

PLATE 2.15

The endoplasmic reticulum and dictyosome

Fig. 1. A transverse section through a cell showing the two "horns" of endoplasmic reticulum (ER) arising from the nucleus (N). This peripheral ER extends to the forming faces of the dictyosomes (D) where it becomes more reticulate. The flagellar pit ER is confluent with the nuclear envelope.

Fig. 2. A longitudinal section of the anterior part of a cell showing the dictyosomes (D) on opposite sides of the flagellar pit. The peripheral ER lies close to the chloroplast and extends anteriorly past the dictyosomes to the flagellar pit. The ER lining the flagellar pit is referred to as the flagellar pit ER. The peripheral ER appears to hold the mitochondrion (M) against the chloroplast (C).

Fig. 3. A section through a dictyosome (D) showing the endoplasmic reticulum (arrowheads) near the forming face (ff) of the dictyosome. At the mature face (mf) scale profiles can be seen in the cisternae.

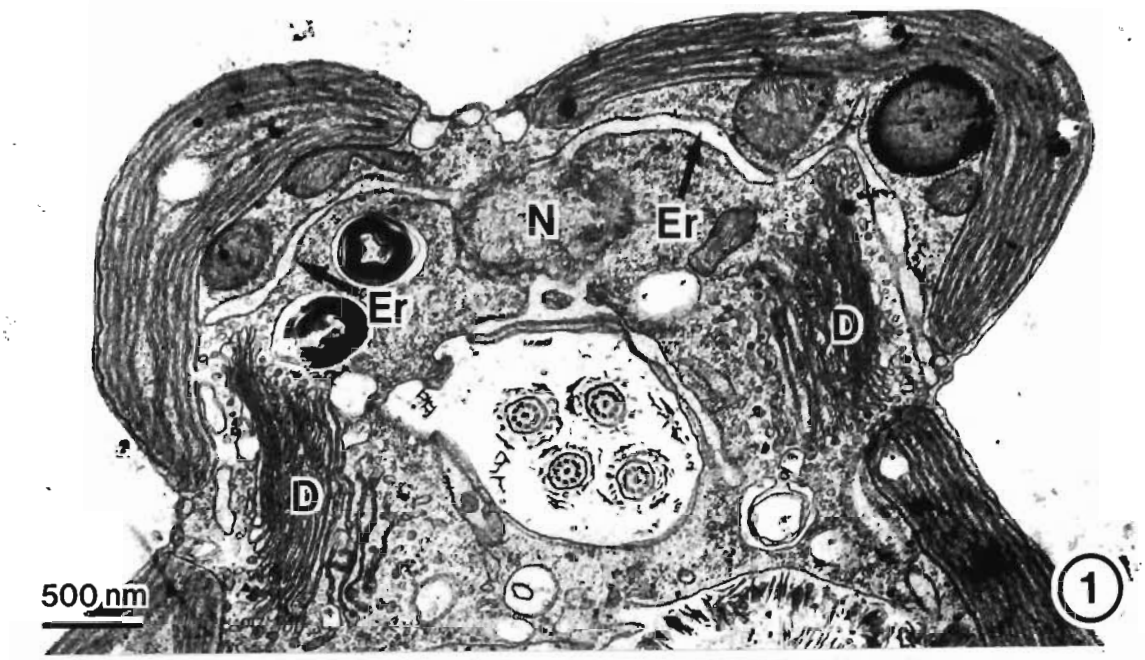
N
Er
Er
D
D
500 nm
1

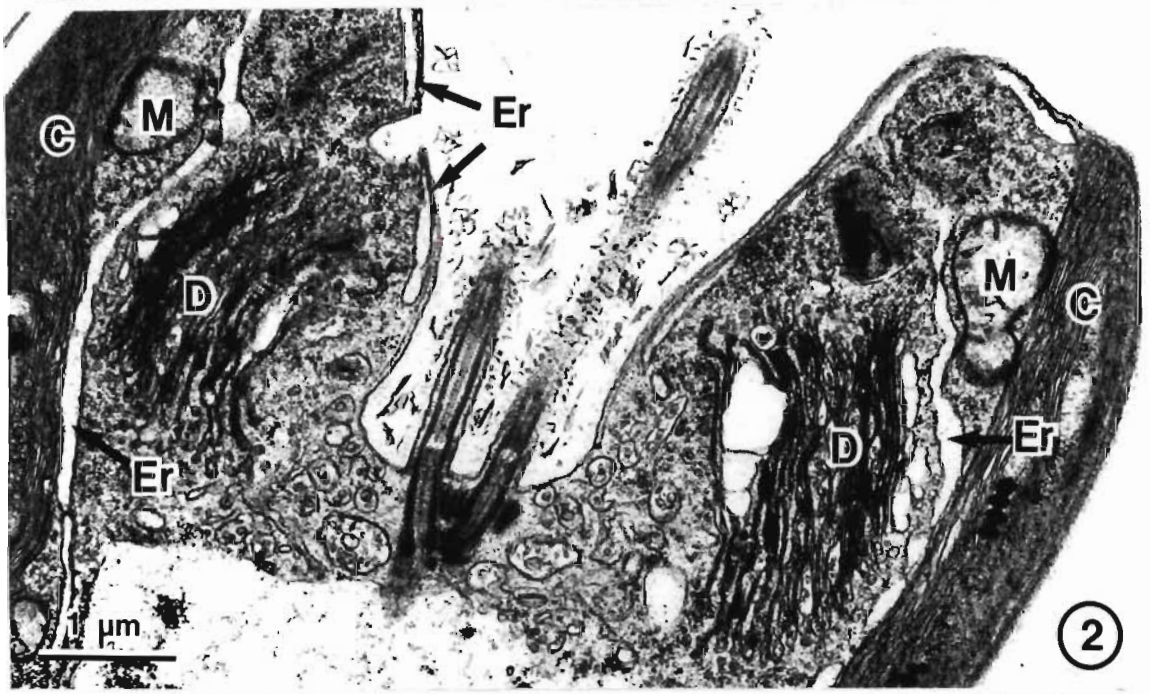
C
M
Er
D
Er
M
C
D
Er
1 µm
2

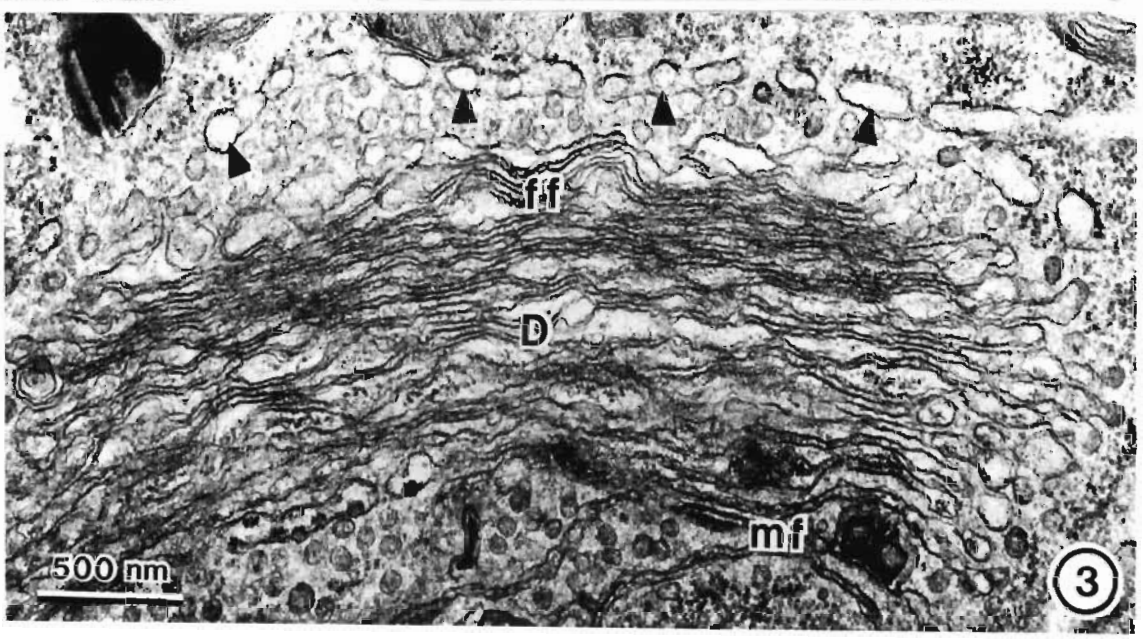
ff
D
mf
500 nm
3

PLATE 2.16

The scale reservoir and nucleus

Fig. 1. A transverse section showing the flagellar pit (Fp) and scale reservoir (Sr). The scale reservoir is connected with the flagellar pit via a duct (Du) which passes around a cytoplasmic spur (arrow). Note flagellar scales in the scale reservoir.

Fig. 2. A longitudinal section of a cell showing the scale reservoir (Sr) and extensive duct system (open arrows) containing small underlayer scales. There appears to be some organization of flagellar scales in the reservoir.

Fig. 3. A section of a nucleus (N) with two nucleoli (No). The nuclear envelope is a double unit membrane which is confluent with the endoplasmic reticulum (see arrowheads). The nucleoplasm and cytoplasm are continuous at the nuclear pores (arrows).

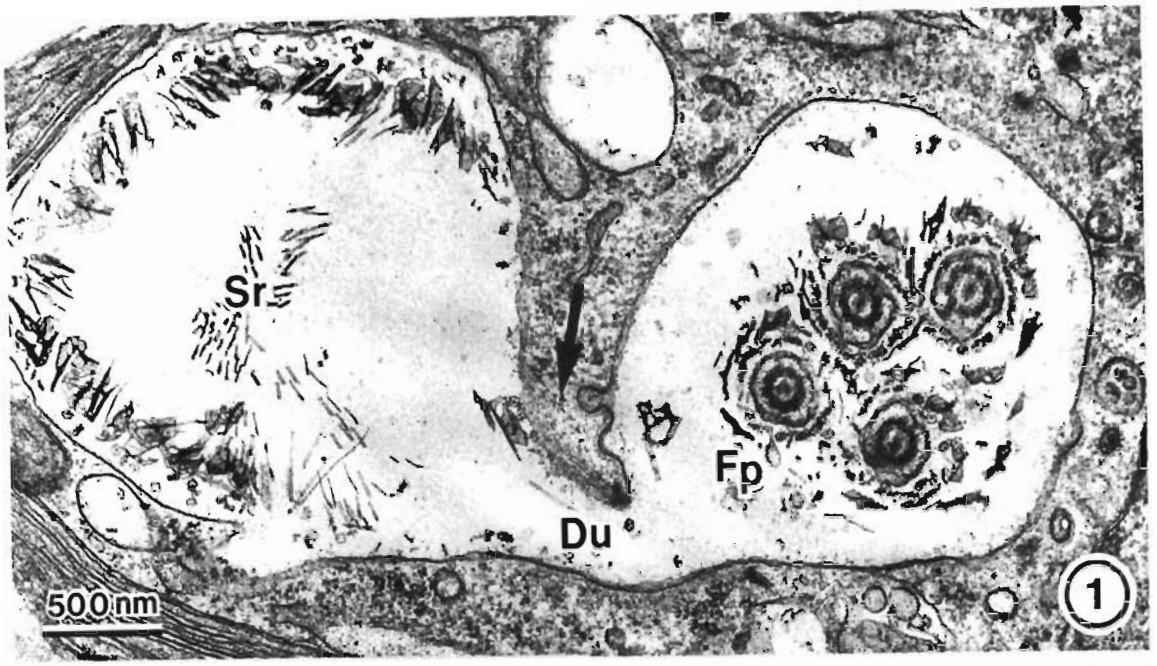
Sr
Fp
Du
500 nm
1

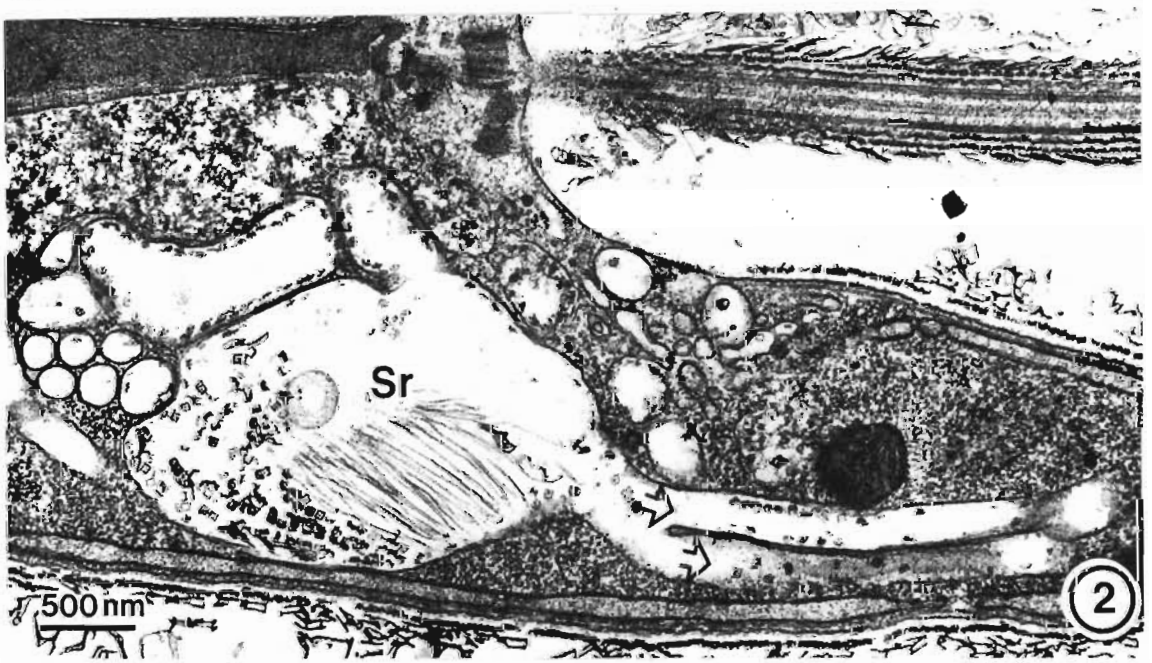
Sr
500 nm
2

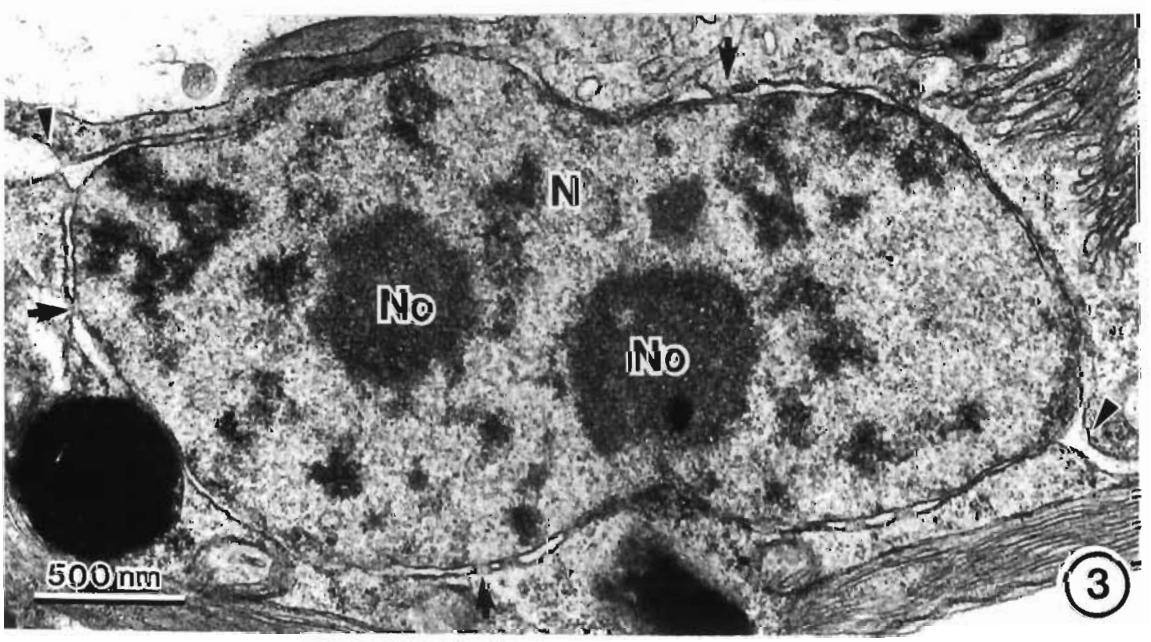
N
No
No
500 nm
3

PLATE 5.1

CELL DIVISION

Light microscopy

Figs. 1 - 7. Cell division in *P. pseudoparkeae* as seen with the light microsope (phase contrast; scale bars = 10 µm).

Fig. 1 The first sign of cell division is marked by the elongation of an axial strand (the microbody - arrowhead). This extends into the chloroplast and cleaves the anterior starch grain capping the pyrenoid (P).

Fig. 2. Further elongation of the microbody causes the chloroplast to divide in the region of the pyrenoid.

Fig. 3. The flagellar basal bodies replicate and four new flagella (arrowheads) emerge from the flagellar pit. The base of the flagellar pit broadens at this stage.

Fig. 4. Two sets of basal bodies move apart and the nucleus (N) takes up a position between these. A posterior cleavage furrow (arrowhead) is evident.

Fig. 5. The nucleus enters anaphase and two chromatin masses (arrowheads) begin to separate.

Fig. 6. An anterior cleavage furrow (arrowhead) develops as the nuclei (N) enter telophase.

Fig. 7. Rapid cleavage of the anterior furrow produces two daughter lobes which are attached just above the pyrenoids. These lobes undergo torsion to give the "back-to-back" stage represented here.

Electron microscopy - chloroplast division

Fig. 8. A longitudinal section of the posterior region of a cell showing the microbody (Mb) entering the chloroplast (C) in the region of the pyrenoid (P). The pyrenoid starch grains (S) are cleaved by an anterior and posterior invagination of the chloroplast envelope.

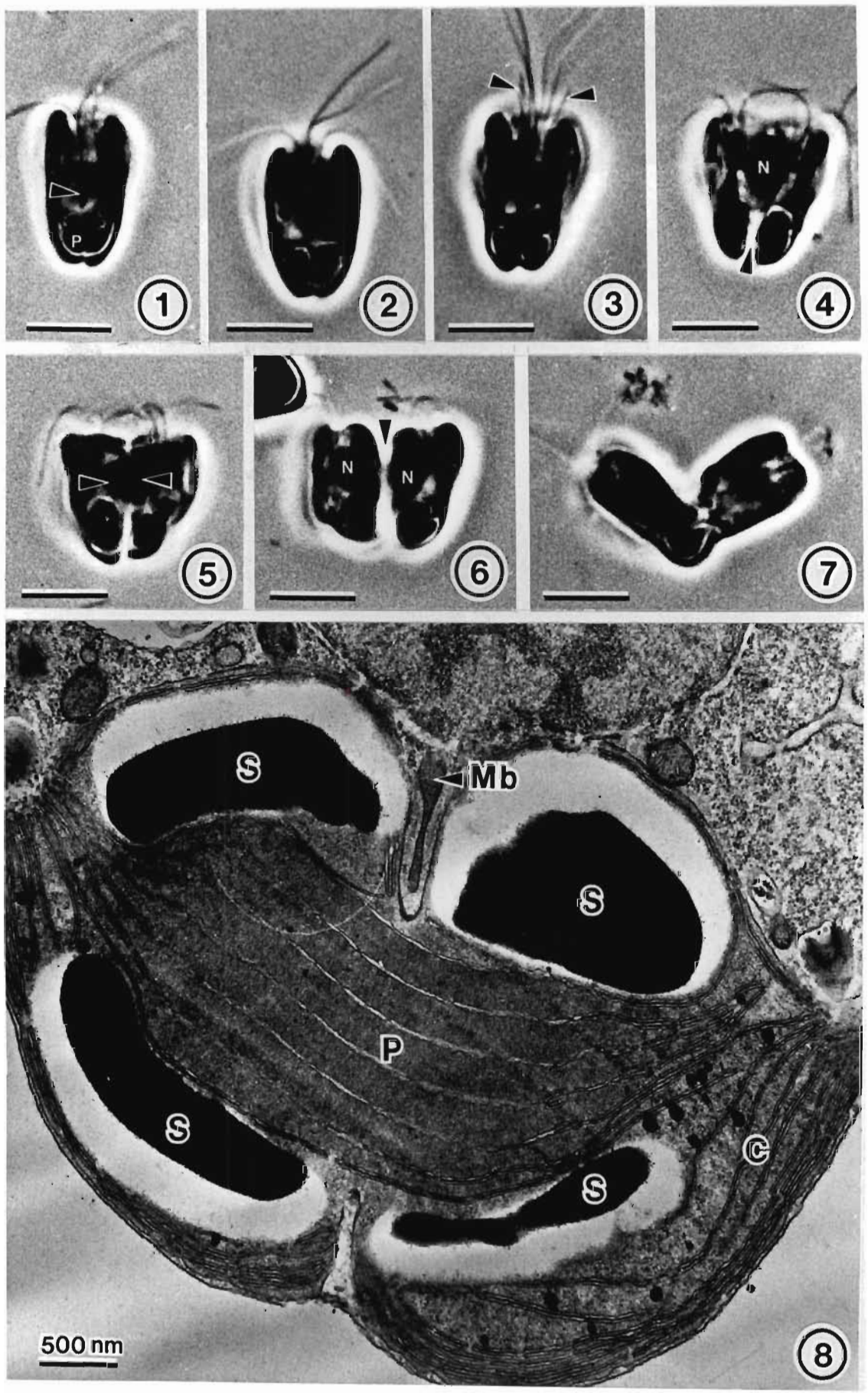
P
1
2
3
N
4
5
N
N
6
7
S
Mb
S
P
S
S
C
500 nm
8

PLATE 5.2

Chloroplast division

Figs. 1 - 3. Longitudinal sections through the posterior region of cells undergoing division.

Fig. 1. As the microbody (Mb) continues to elongate the anterior and posterior invaginations of the chloroplast envelope (arrowheads) grow toward each other and enter the pyrenoid (P).

Fig. 2. A lobe of the mitochondrion (M) is often seen in the anterior invagination of the chloroplast envelope.

Fig. 3. The anterior and posterior invaginations of the chloroplast envelope fuse in the centre of the pyrenoid (P) to cleave the chloroplast.

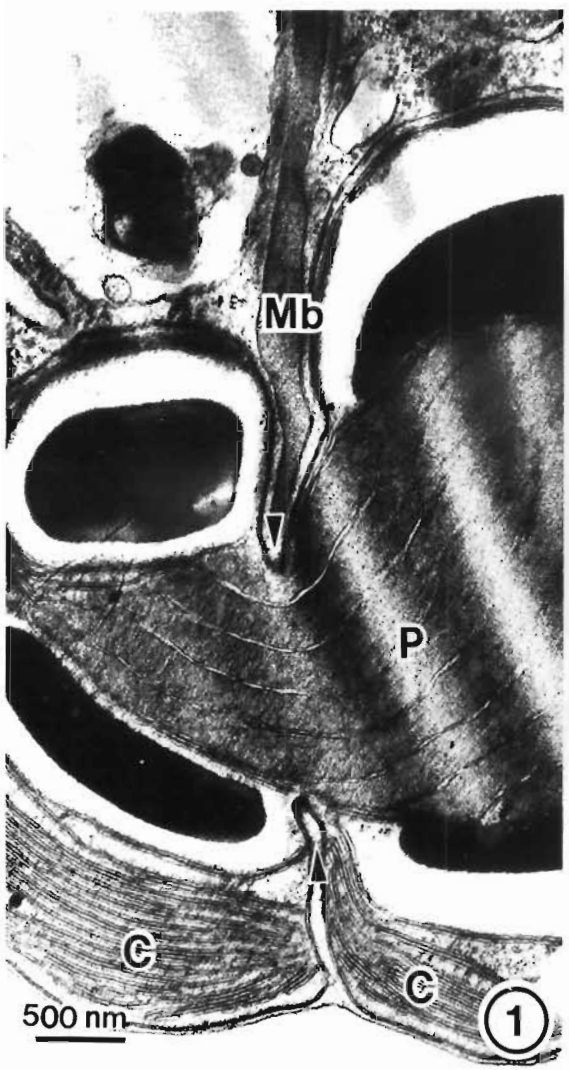
Mb
P
C
C
500 nm
1

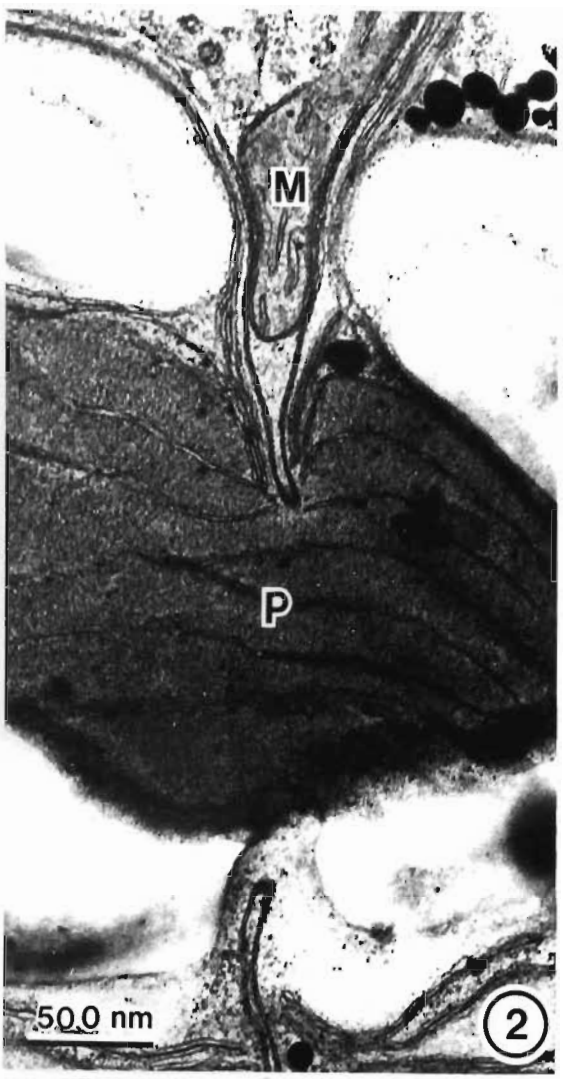
M
P
500 nm
2

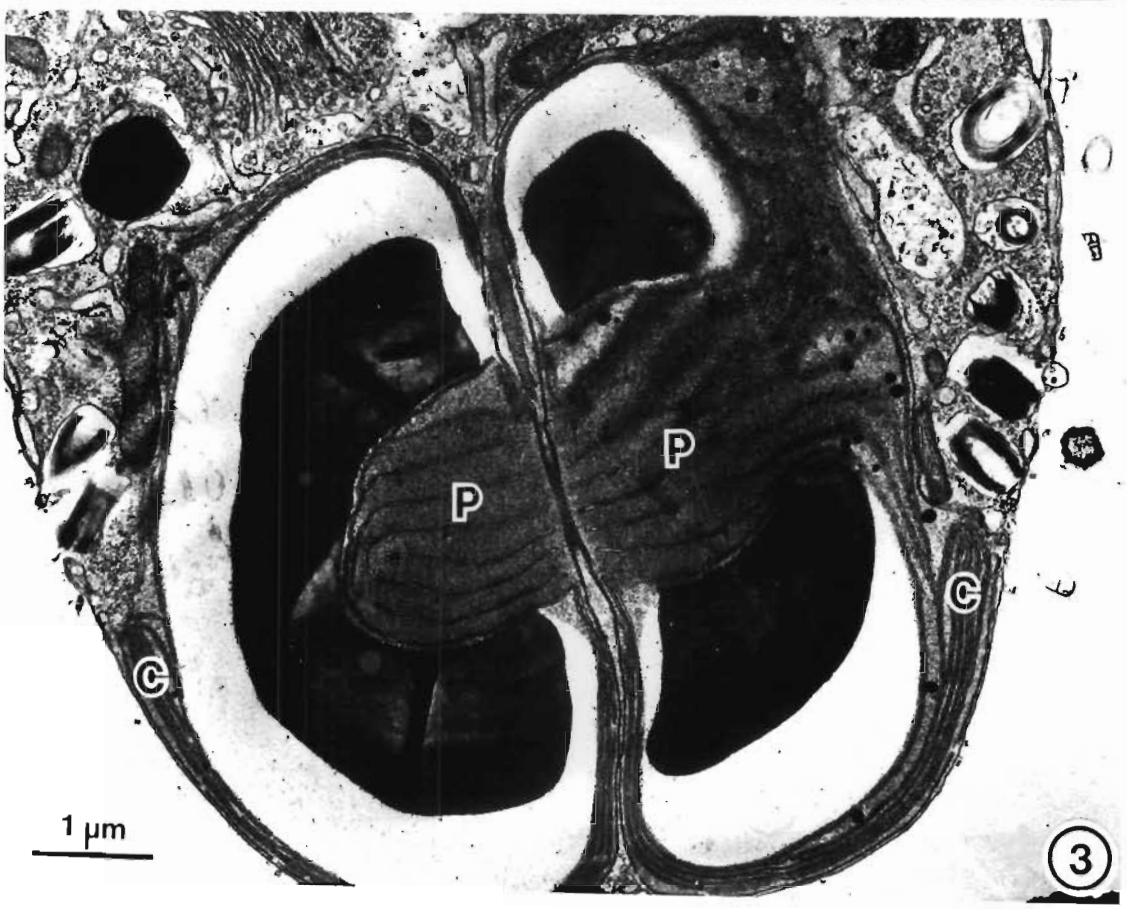
P
P
C
C
1 µm
3

PLATE 5.3

Chloroplast division and replication of the flagellar basal bodies

Fig. 1. A longitudinal section through a cell showing the divided chloroplast (C) and centrally located nucleus (N).

Fig. 2. A transverse section through a dividing cell showing the replicated basal bodies.

Fig. 3. An oblique section through the anterior region of a cell showing the replicated flagellar basal body apparatus (Fba). The cell is in interphase as the nucleus (N) possesses a well defined nucleolus (No). The cell has two dictyosomes (D).

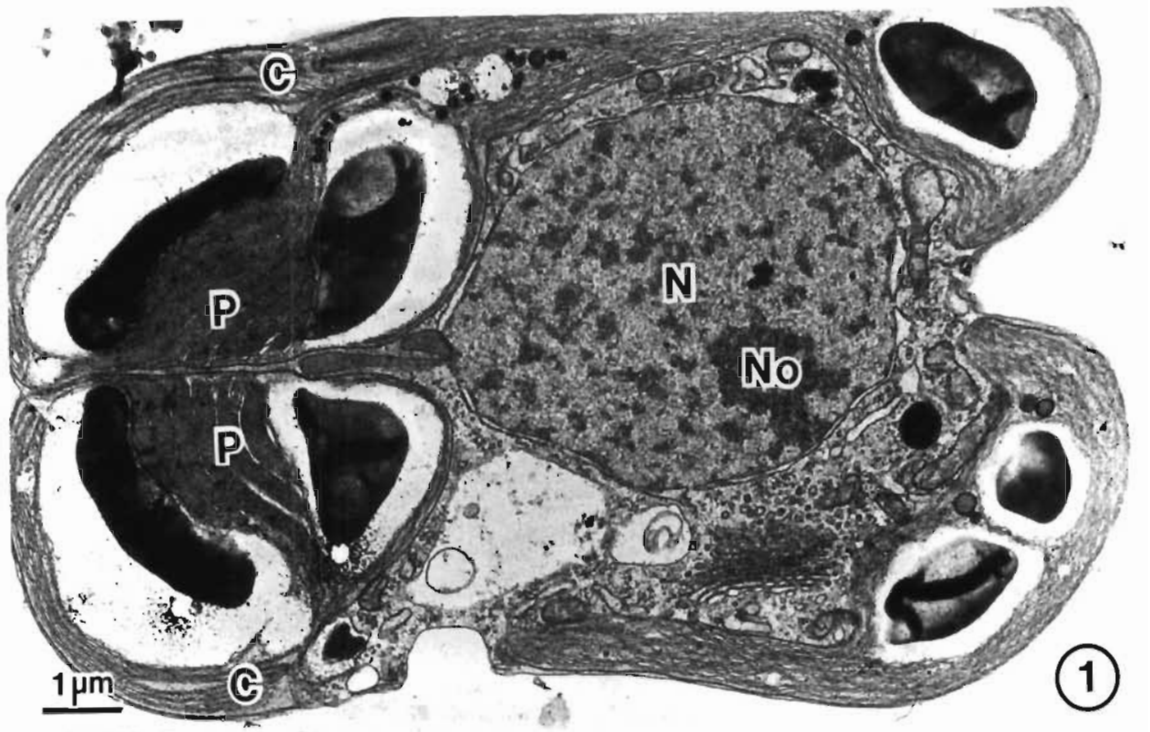
C
P
P
N
No
C
1µm
1


250 nm
2

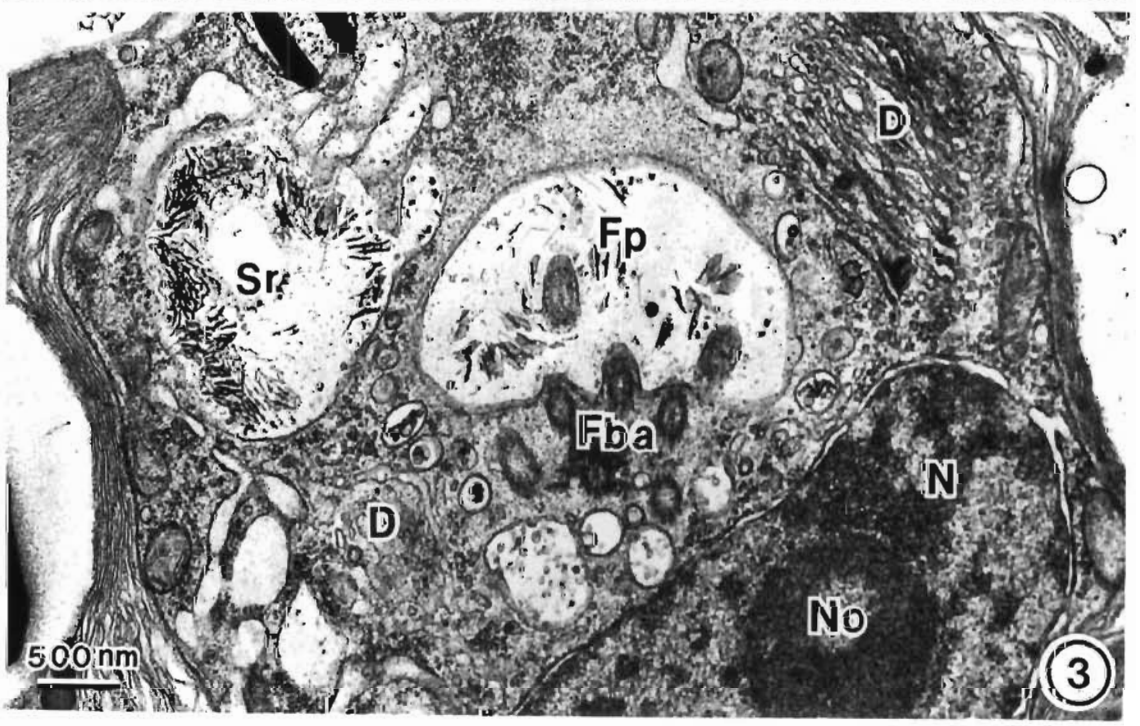
D
Fp
Sr
Fba
N
D
No
500 nm
3

PLATE 5.4

Replication of the flagellar basal bodies

Fig. 1. A transverse section through a dividing cell showing eight flagellar profiles (F) in the flagellar pit (Fp). The cell has two dictyosomes (D). Several small invaginations of the flagellar pit indicate sites where scales have been released. The membrane of the scale vesicles is incorporated into the plasmalemma.

Fig. 2. A longitudinal section through the anterior end of a dividing cell with 8 flagella (F) (only 4 seen). The base of the flagellar pit (Fp) has broadened to accommodate the replicated flagellar basal body apparatus (Fba). The duct (Du) of the scale reservoir remains connected with the flagella pit. The dense structures seen above and below the duct (arrowheads) represent the compound microtubular rootlet which encircles the duct of the scale reservoir.

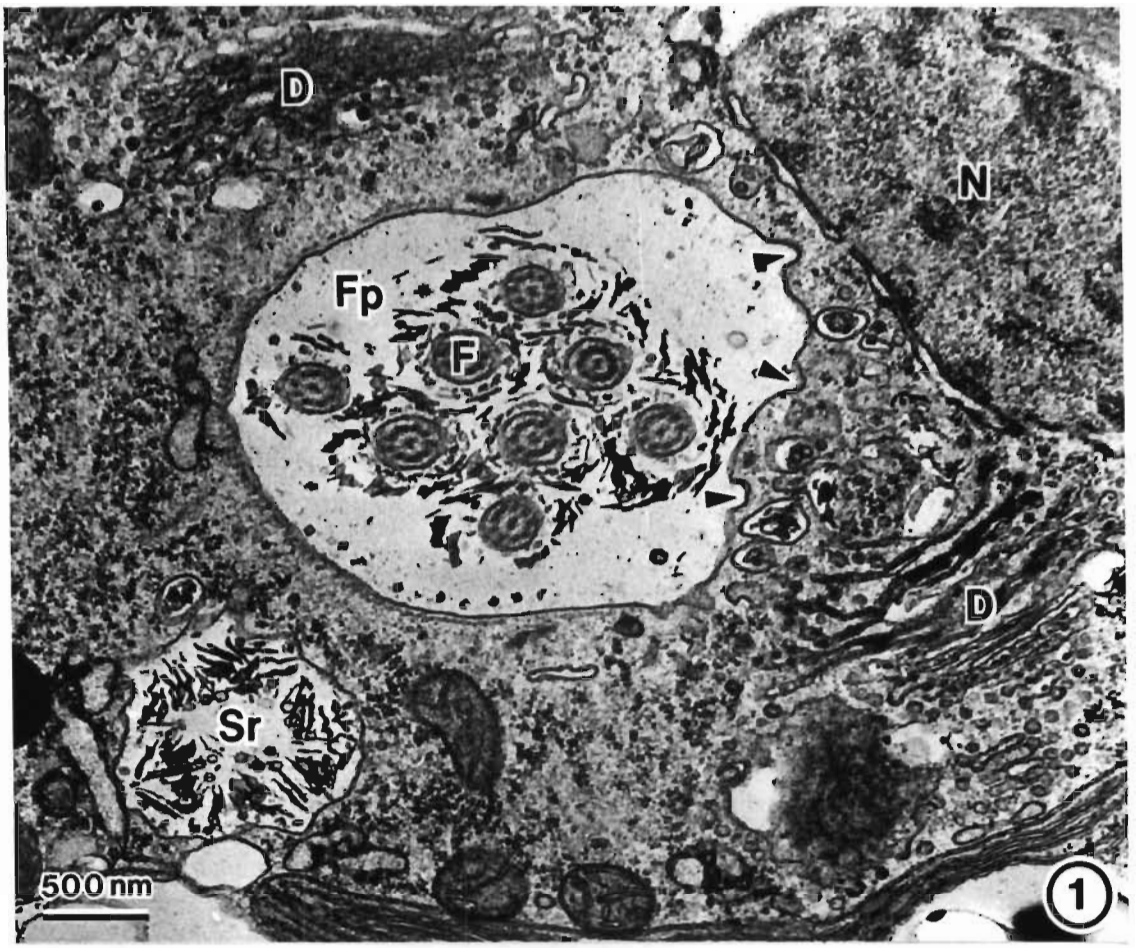
D
N
Fp
F
D
Sr
500 nm
1

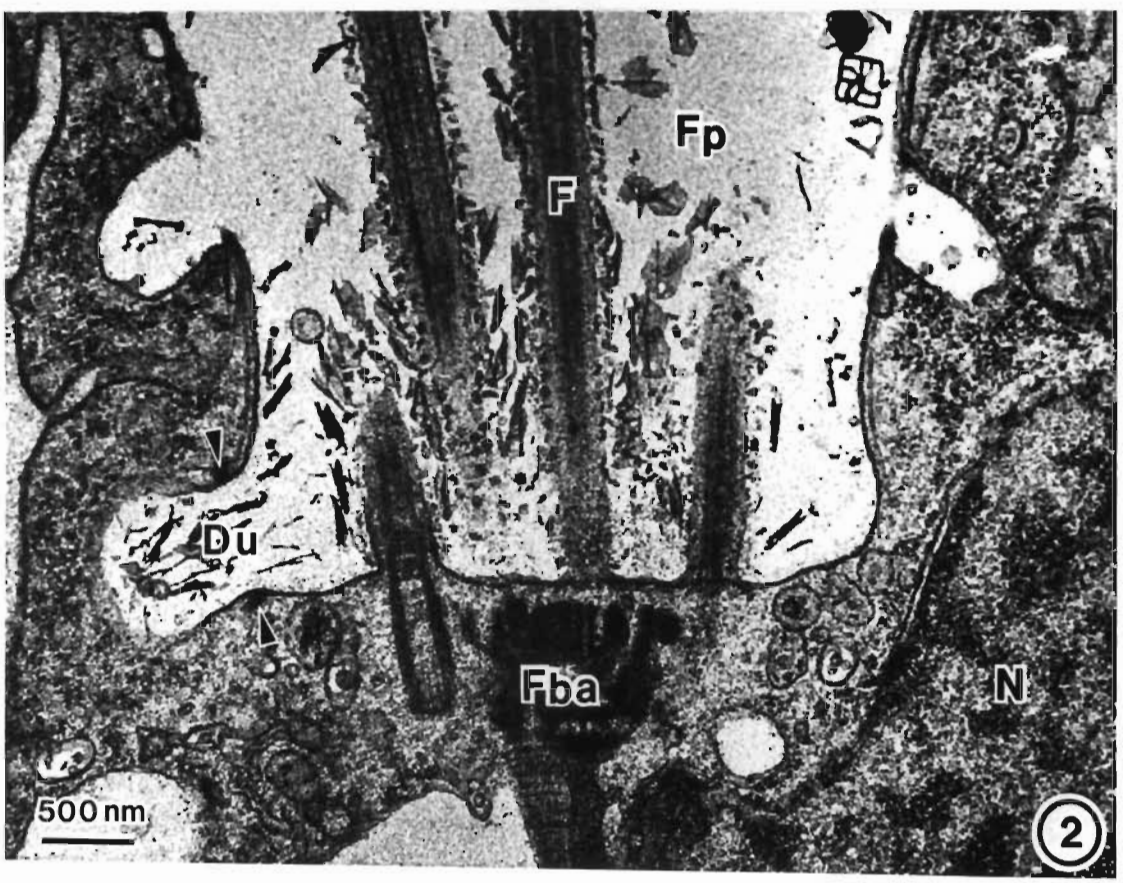
Fp
F
Du
Fba
N
500 nm
2

PLATE 5.5

Replication of the trichocysts, transformation of the rhizoplast; division of the dictyosome

Fig. 1. An oblique section through the anterior region of a dividing cell (only 6 flagella shown in the flagellar pit). Newly formed trichocysts (arrowheads) of narrow diameter are seen amongst older trichosysts (T).

Fig. 2. A median longitudinal section of a cell showing the microtubules (arrowheads) formed by the transformation of the rhizoplast. The microtubules originate near the flagellar basal bodies (Fb) and extend along one side of the nucleus (N). The chromatin of the nucleus begins to condense as the nucleus enters prophase.

Fig. 3. A transverse section of a cell showing two daughter dictyosomes (D) formed by separation of the parent dictyosome in the region indicated by the arrow.

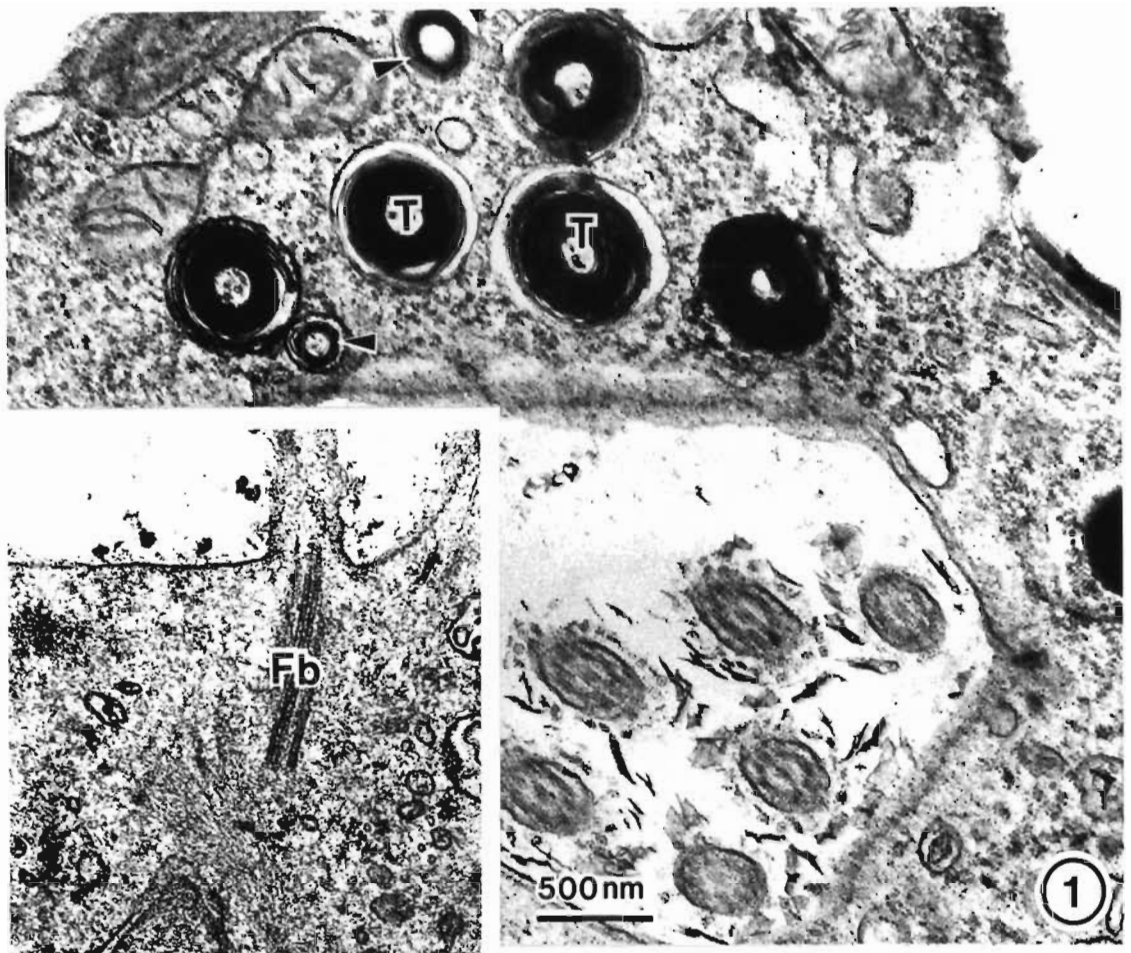
T
T
500 nm
1


Fb
N
500 nm
2

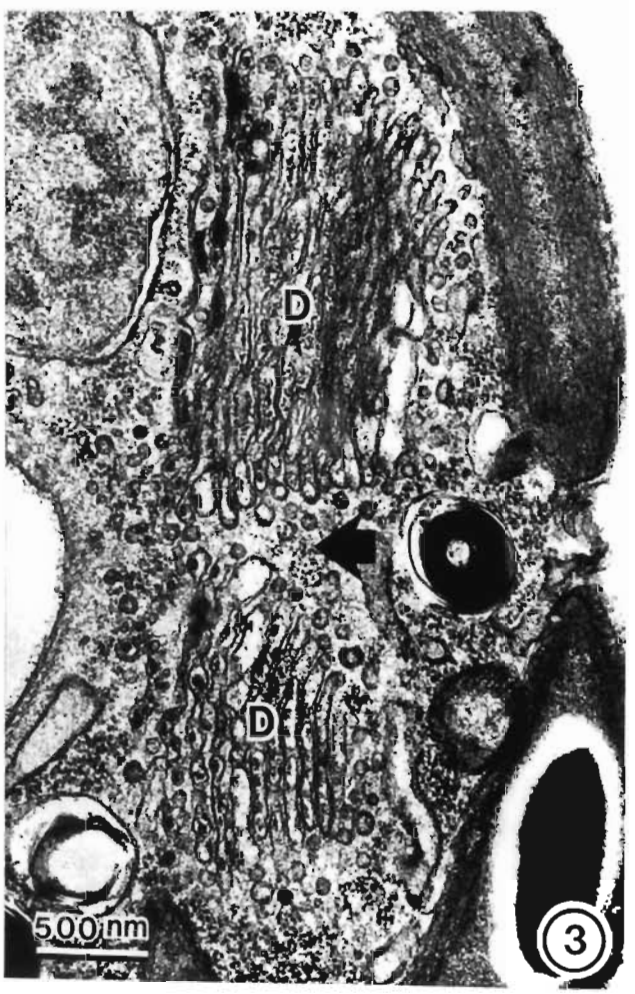
D
D
500 nm
3

PLATE 5.6

Prophase cells

Fig. 1. A transverse section of a dividing cell. The nucleus (N) is in prophase and four dictyosomes (D) are present in the cytoplasm.

Fig. 2. A transverse section of a cell showing that the scale reservoir remains connected with the flagellar pit (Fp). The nucleus (N) is in prophase and the cell has eight flagella (F) and four dictyosomes (D). The surface area of the scale reservoir is much reduced after the four flagella have been produced.

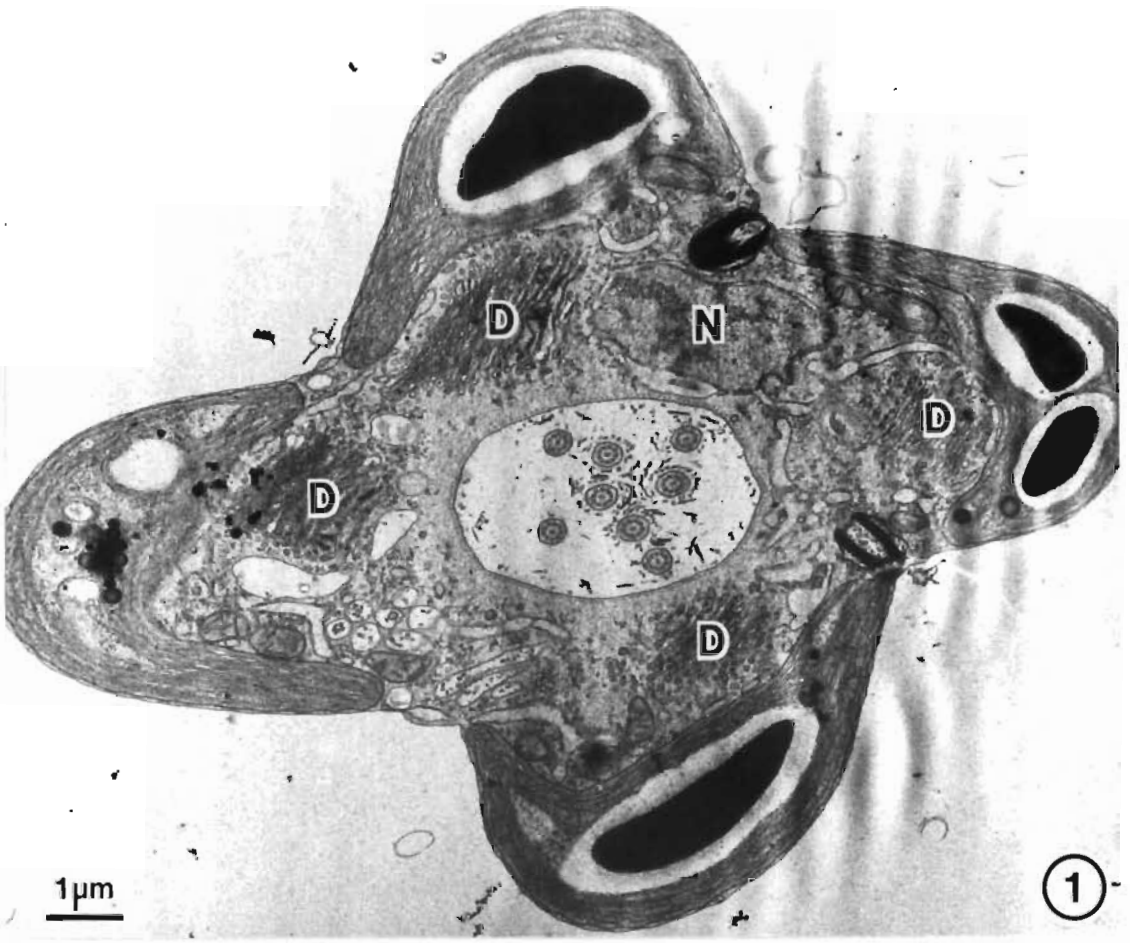

1

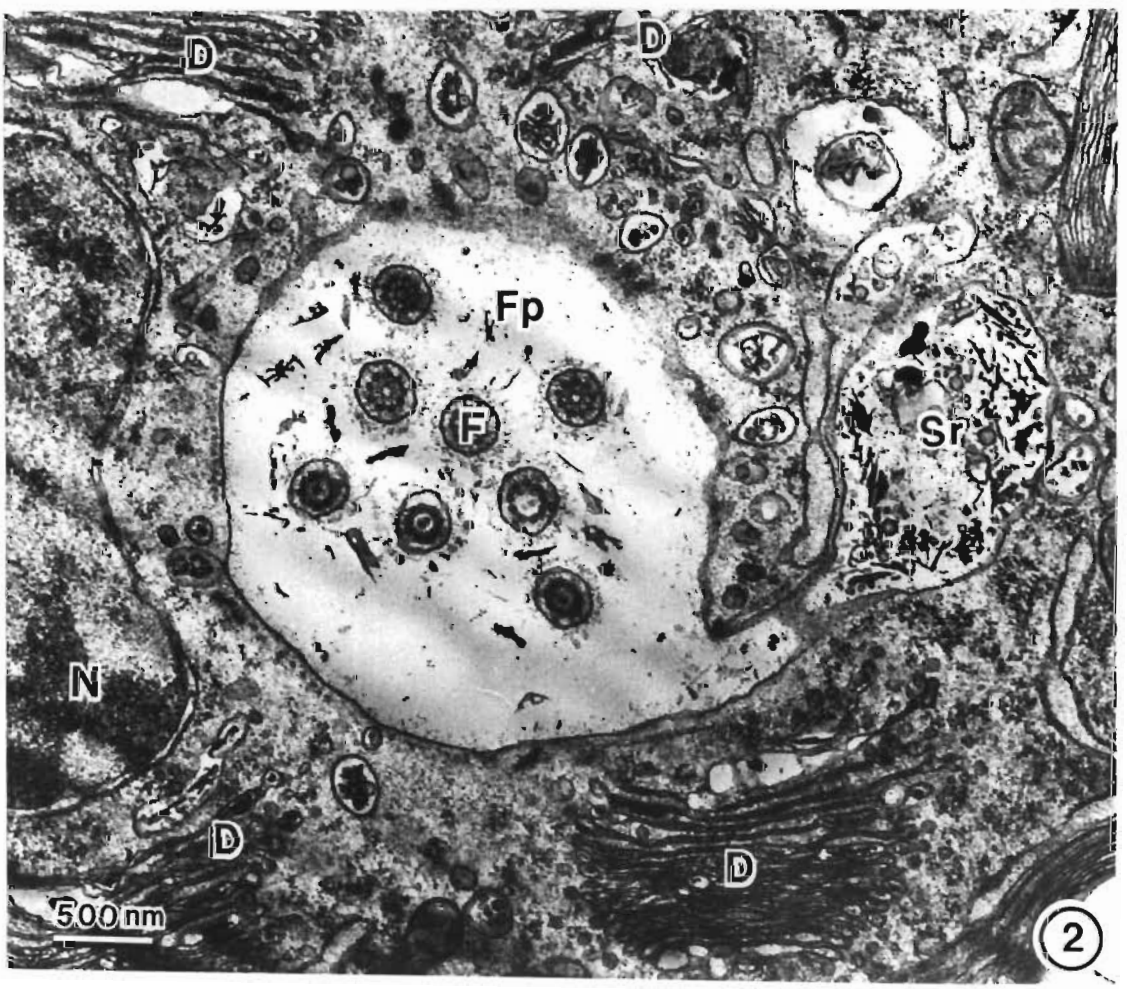

2

PLATE 5.7

Metaphase cells

Figs. 1 and 2. Longitudinal sections of dividing cells at metaphase.

Fig. 1. The replicated flagellar basal bodies have become widely separated and the nucleus (N) has taken up a position between the two flagellar pits (Fp). The nuclear envelope has almost disappeared and the chromatin begins to be organized in a metaphase plate.

Fig. 2. A well developed metaphase plate (Mp) is seen between two flagellar pits (Fp). The nuclear envelope has dispersed.

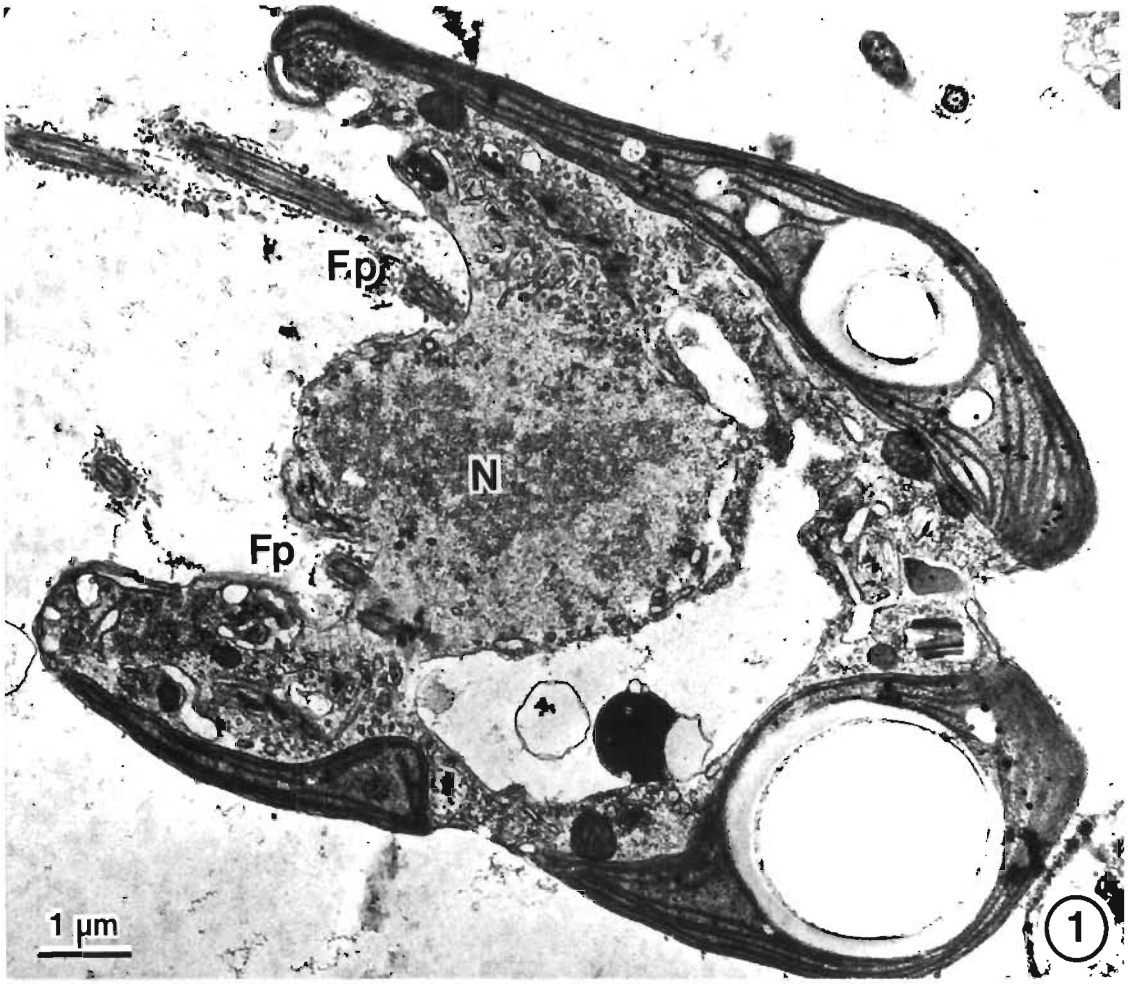
Fp
N
Fp
1 µm
1

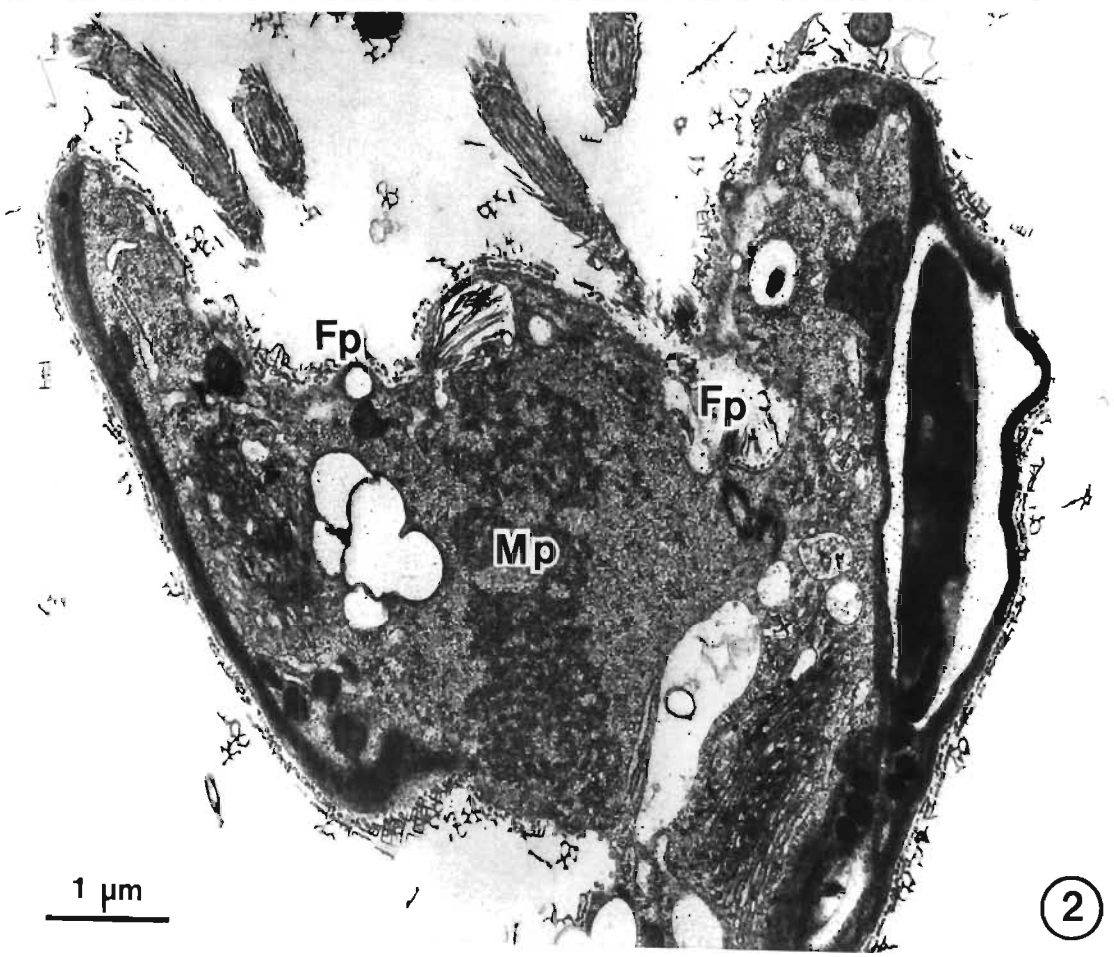
Fp
Fp
Mp
1 µm
2

PLATE 5.8

Metaphase cells

Figs. 1 and 2. Transverse sections of dividing cells at metaphase.

Fig. 1. A section through the middle of a cell showing a well defined metaphase plate (Mp). This is organized along the plane of cell division (arrowheads). The nuclear envelope becomes vesiculate and begins to disperse. Two lateral cleavage furrows (arrows) develop in the plane of cell division.

Fig. 2. A section through the anterior region of a cell showing the metaphase plate (Mp) situated between the two flagellar pits (Fp). The nuclear envelope is largely dispersed.

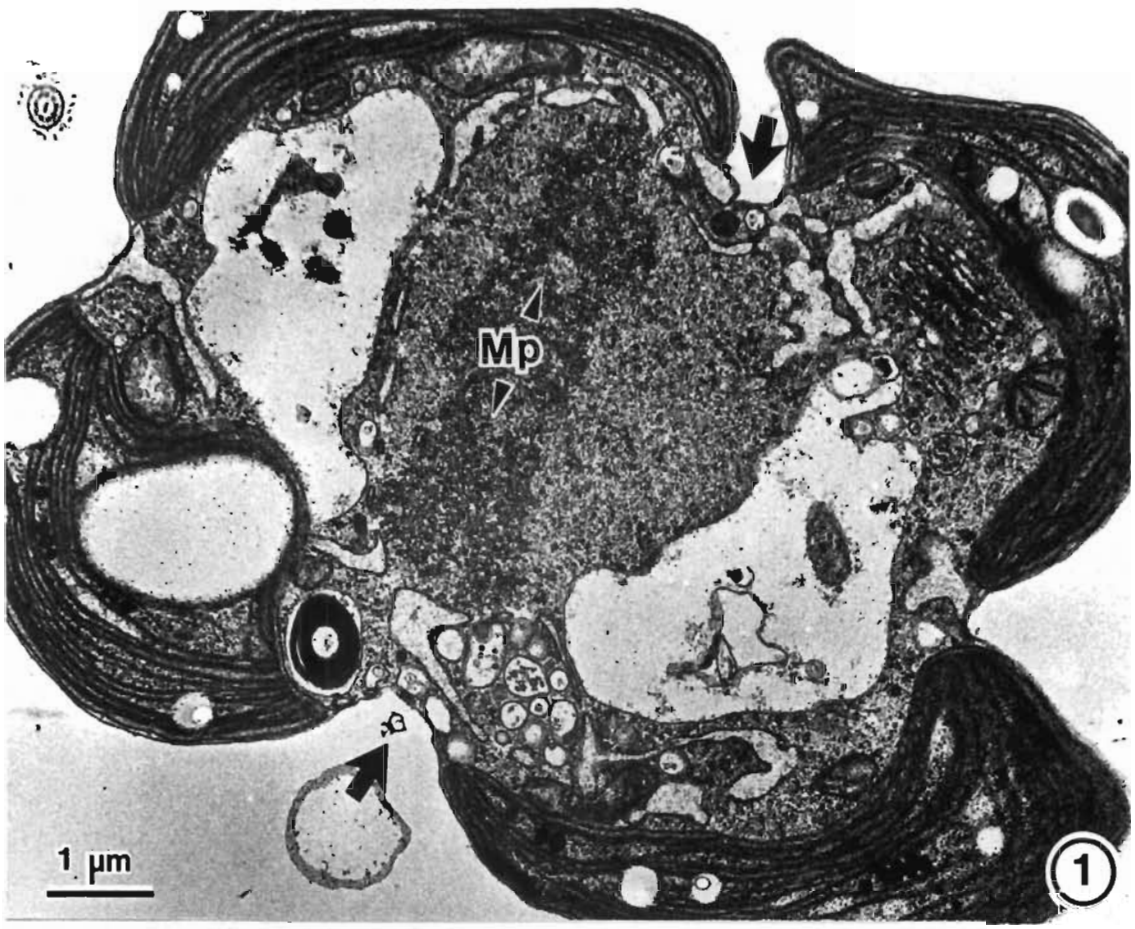
Mp
1 µm
1

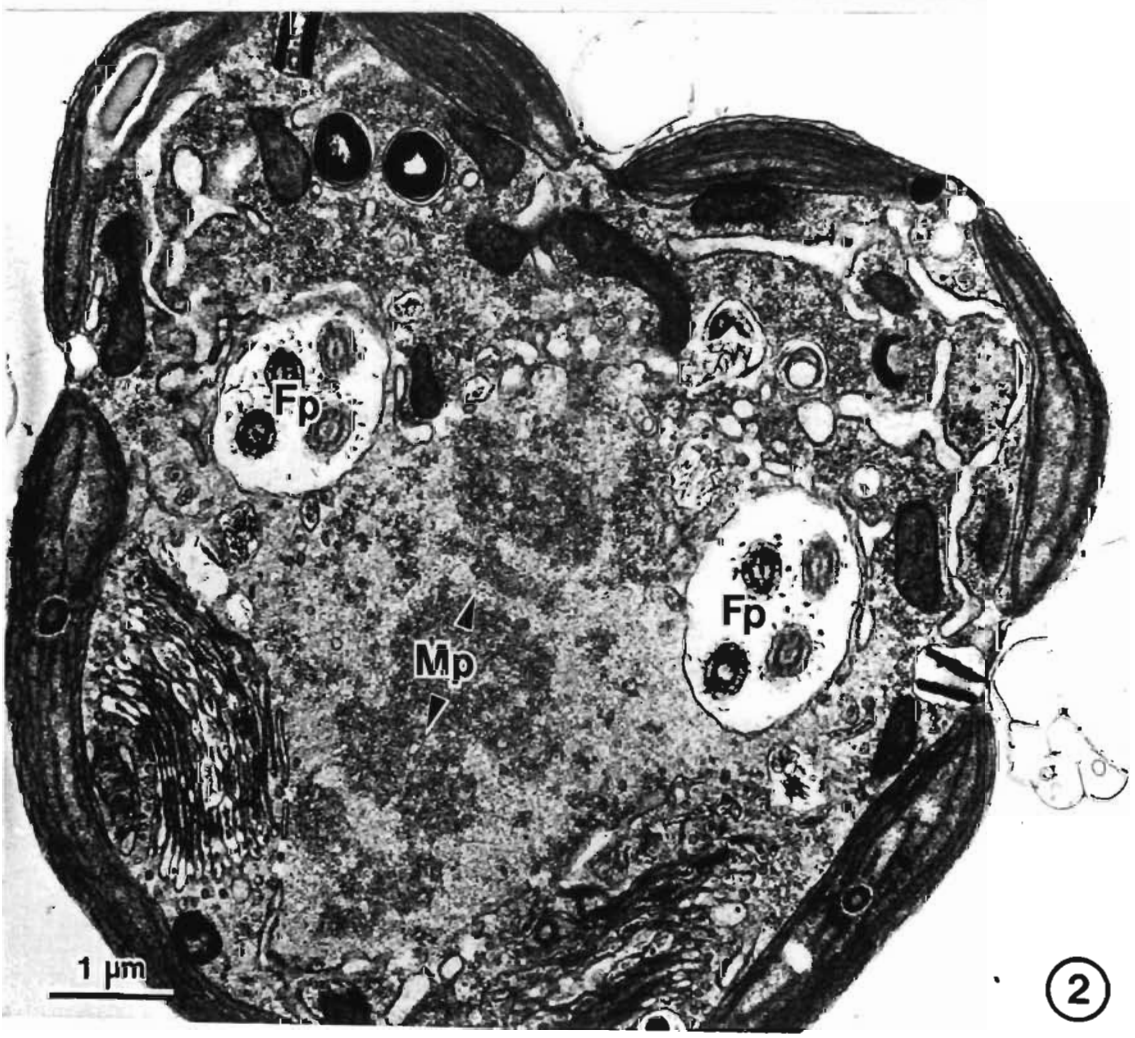
Fp
Fp
Mp
1 µm
2

PLATE 5.9

Spindle microtubules.

Fig. 1. A transverse section through a metaphase cell showing the spindle microtubules (arrowheads) radiating from the flagellar basal bodies (Fb) toward the metaphase plate (Mp).

Fig. 2. A longitudinal section through a metaphase cell showing the spindle microtubules (arrowheads) radiating from the flagellar basal bodies (Fb). Some spindle microtubules connect the flagellar basal bodies with the kinetochores (K). of the chromosomes. Other spindle microtubules (arrow) extend through the metaphase plate (Mp). These are the "pole-to-pole" microtubules and connect the separated basal bodies.

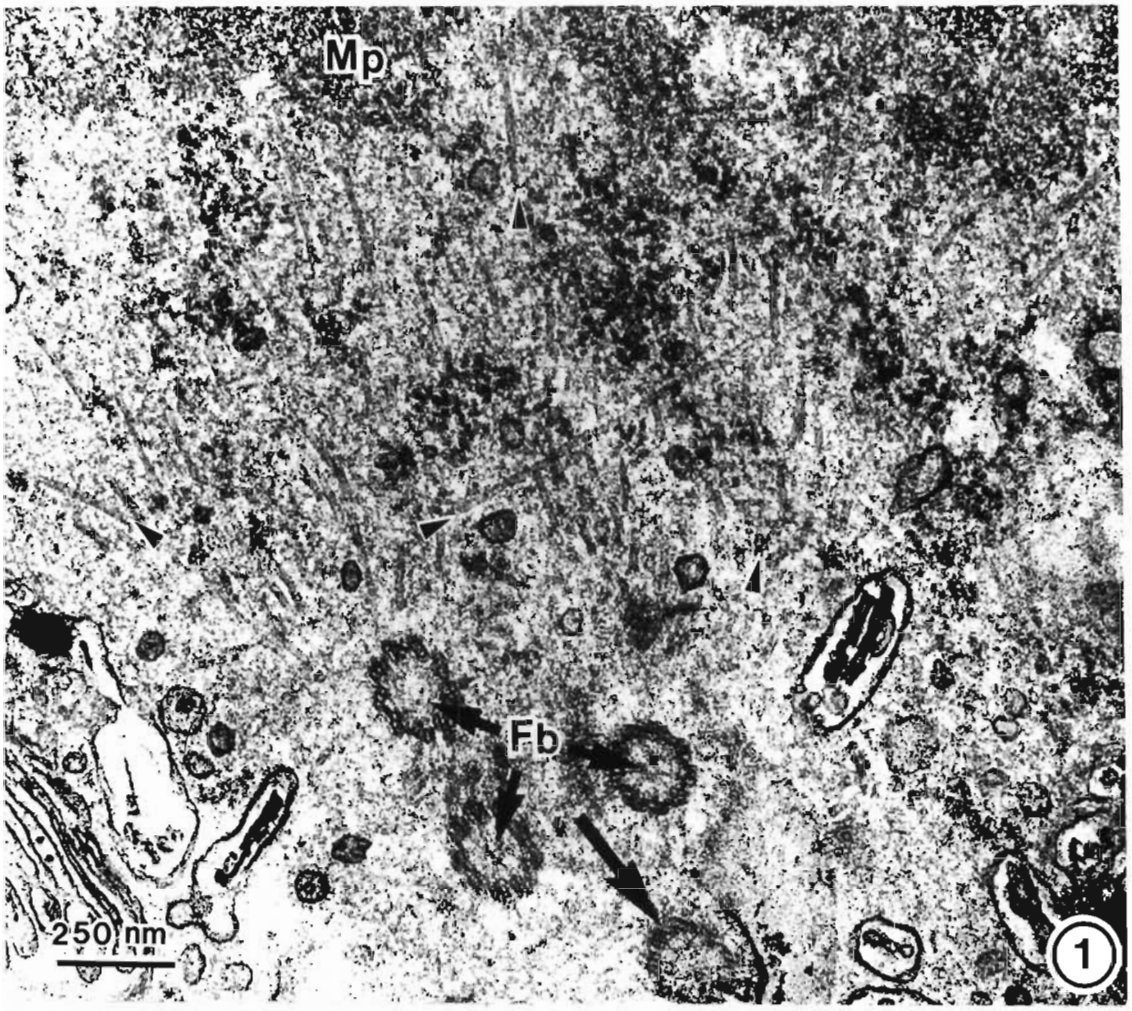
Mp
Fb
250 nm
1

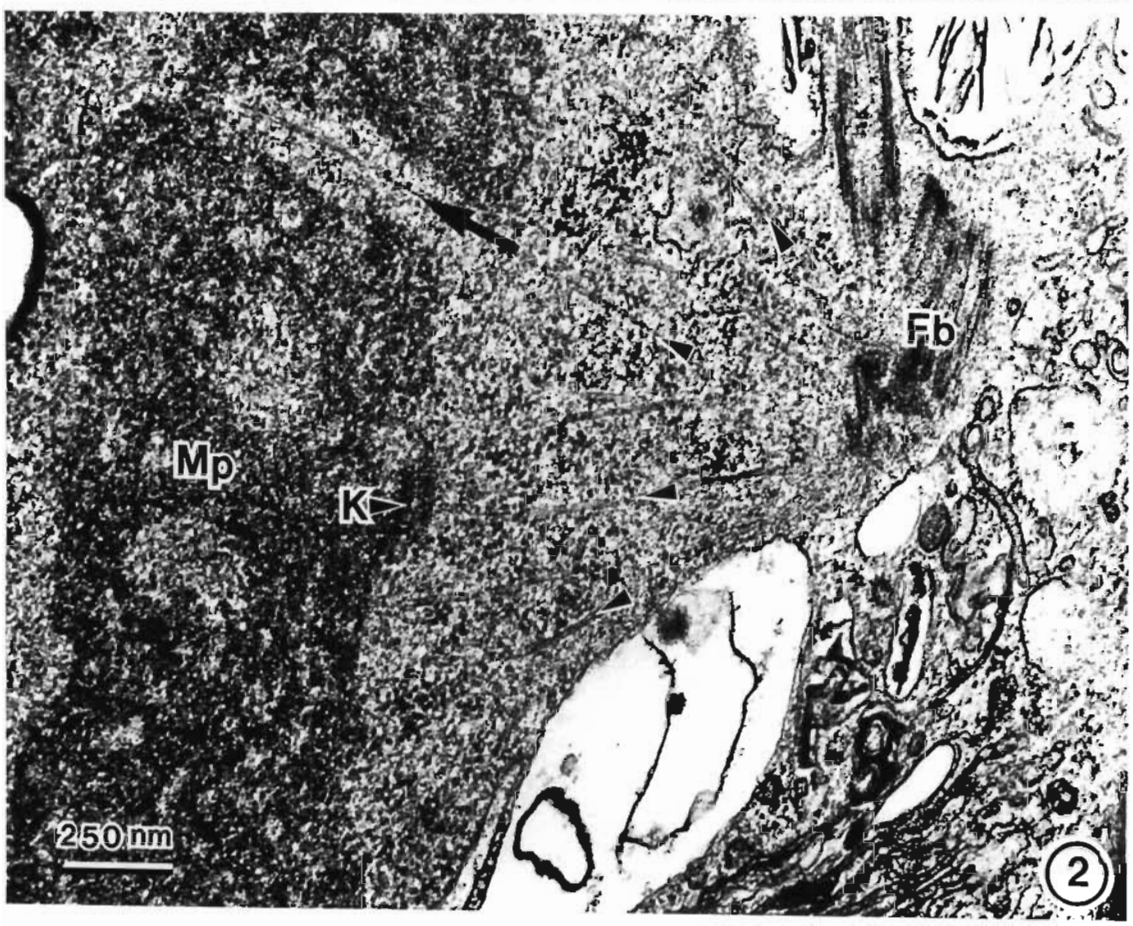
Fb
Mp
K
250 nm
2

PLATE 5.10

Cytokinesis and anaphase

Fig. 1. A longitudinal section through a dividing cell showing the development of an anterior cleavage furrow (arrow). The scale reservoir (Sr) remains connected with one of the flagellar pits.

Fig. 2. A longitudinal section through an anaphase cell. The chromatin masses in the nucleus (N) begin to separate in the direction shown by the arrowheads. A posterior cleavage furrow (arrow) becomes pronounced. Endoplasmic reticulum forms an anterior and posterior boundary to the anaphase spindle.

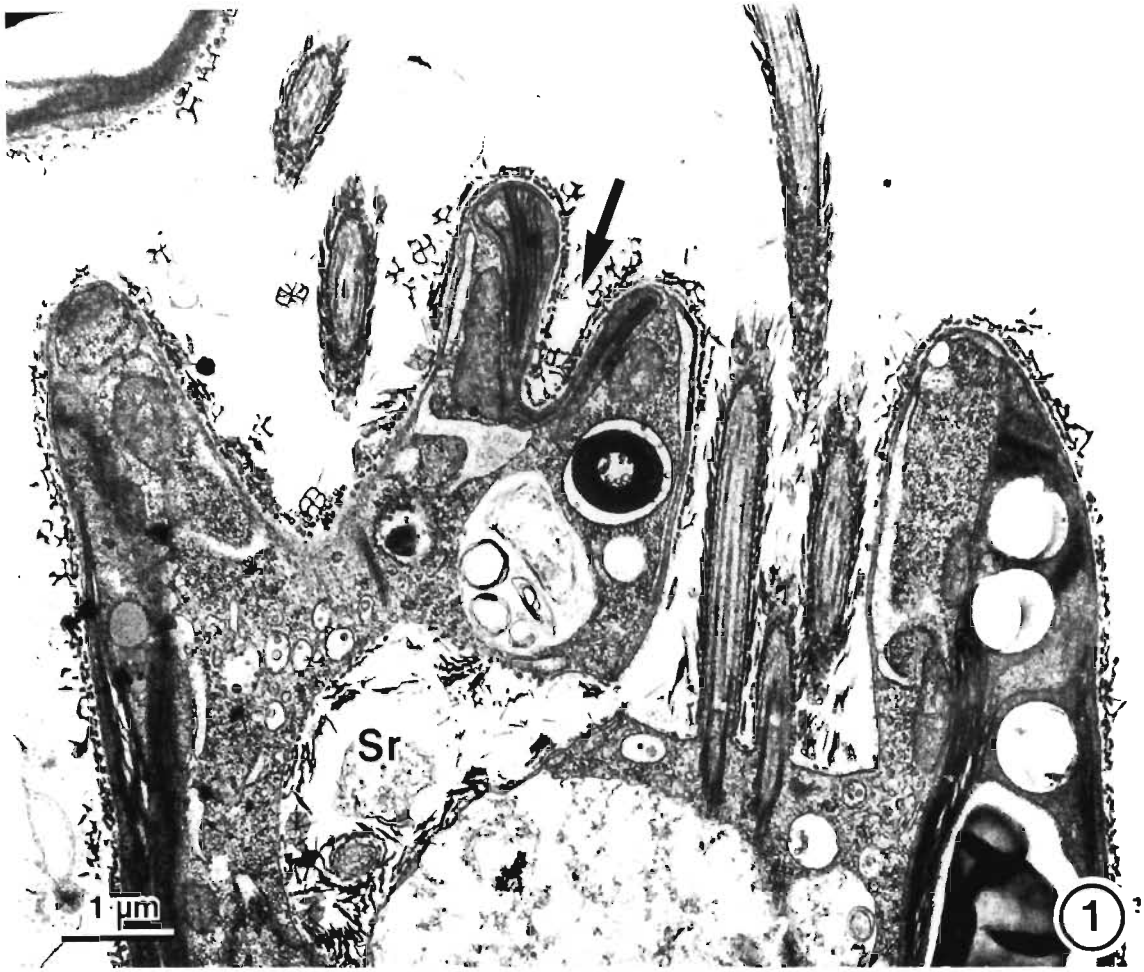
Sr
1 µm
1

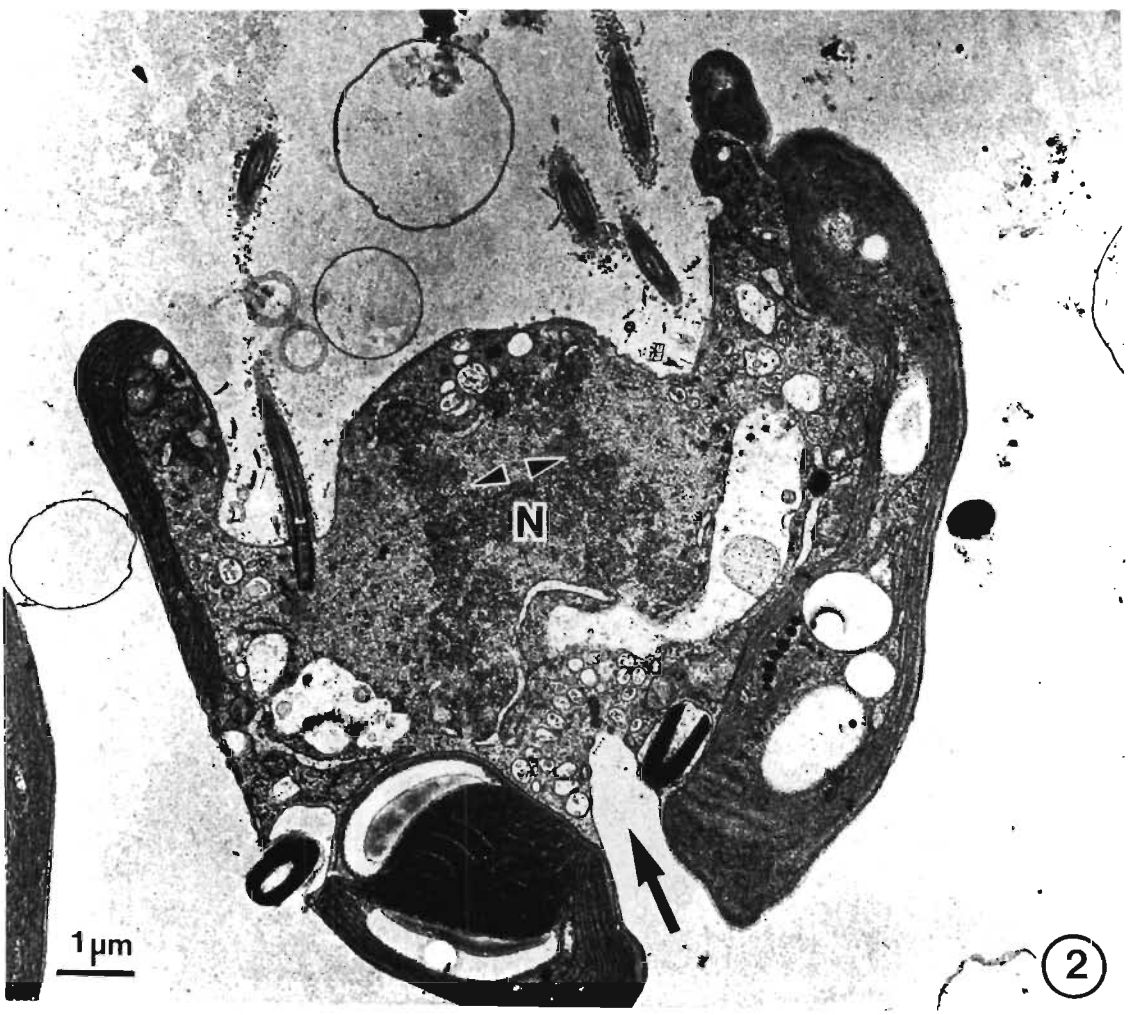
N
1 µm
2

PLATE 5.11

Telophase cells

Fig. 1. A section through a dividing cell with the nuclei (N) in telophase. The two flagellar pits (Fp) are widely separated.

Fig. 2. A section through the telophase nuclei (N) of a dividing cell. The daughter nuclei lie close to one another. There is no interzonal spindle at telophase nor is there a phycoplast.


Fp
N
N
Fp
1 μm
1

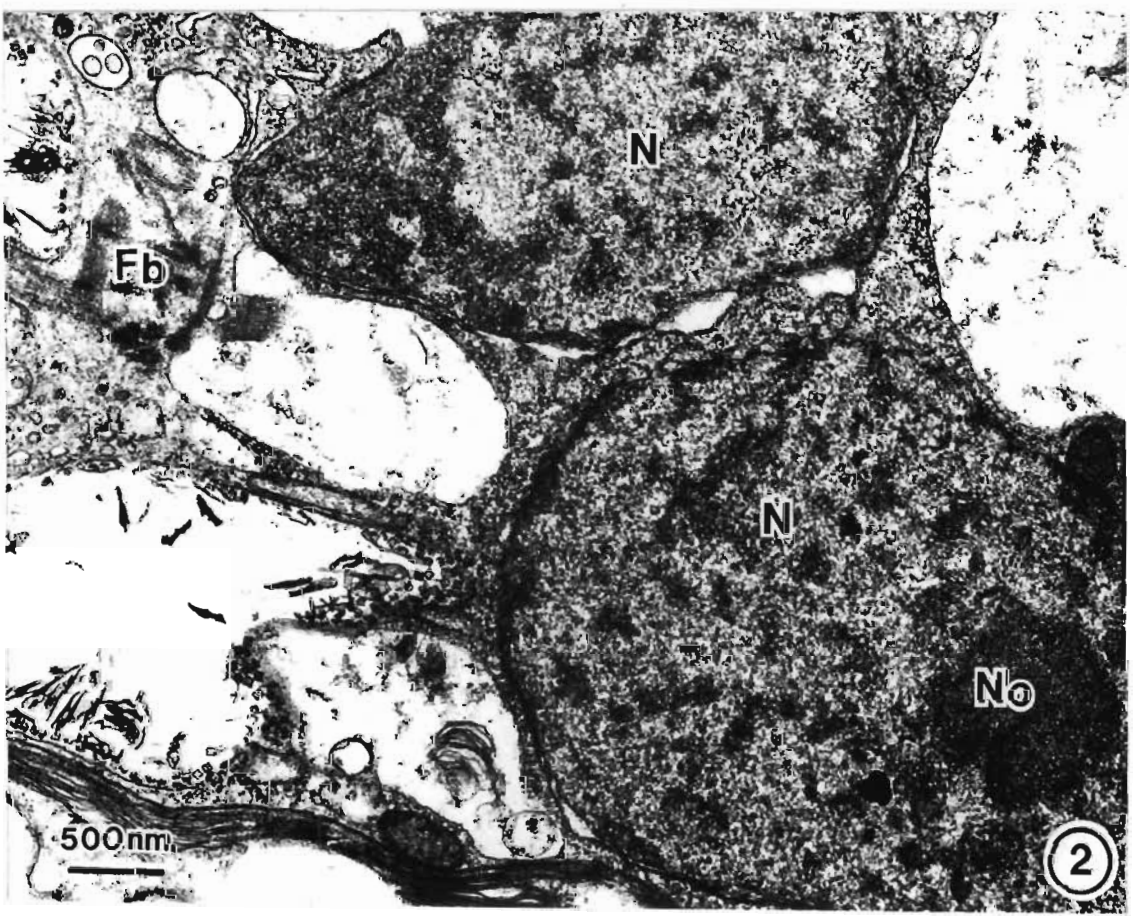
N
Fb
N
No
500nm
2

PLATE 5.12

SCALE PRODUCTION

Figs. 1 and 2. Two longitudinal sections of the dictyosome (D).

Fig. 1. The dictyosome (D) is comprised of approximately 20 cisternae. Scales are produced within the cisternae. There is a progressive development of the scales as they move toward the mature face (mf) of the dictyosome. Generally the first 5 cisternae at the forming face (ff) of the dictyosome do not contain any recognizable scale material. Mature scales (B_3, B_2 and F_2) are seen at the mature face of the dictyosome. Small electron dense vesicles (arrowheads) which are derived from the peridictyosomal endoplasmic reticulum (ER), fuse with the cisternae in peripheral regions of the dictyosome.

Fig. 2. A section of a dictyosome (D) showing scale profiles (B_3, B_2, F_4 and F_3) within the cisternae. At the mature face of the dictyosome the cisternae fragment so that scales are released in membrane bound vesicles (arrowhead).

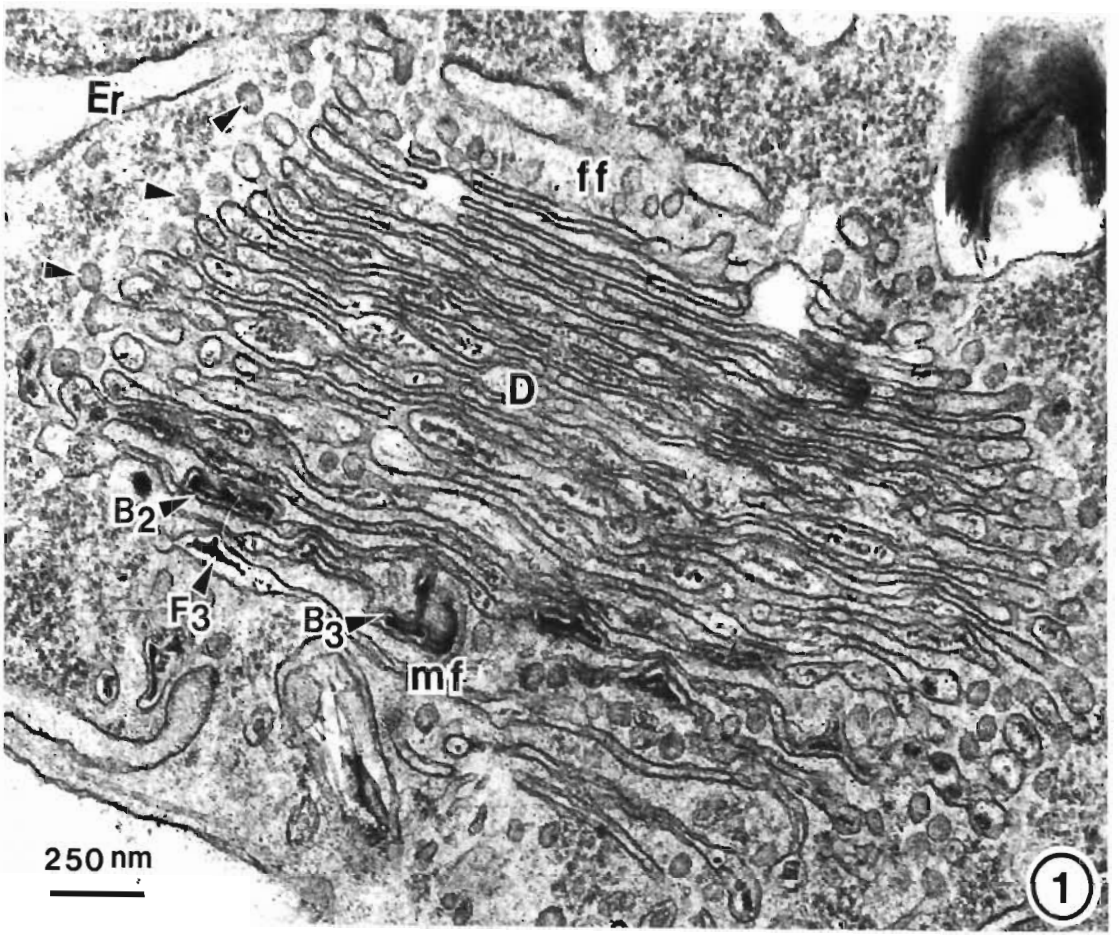
Er
ff
D
B2
F3
B3
mf
250 nm
1

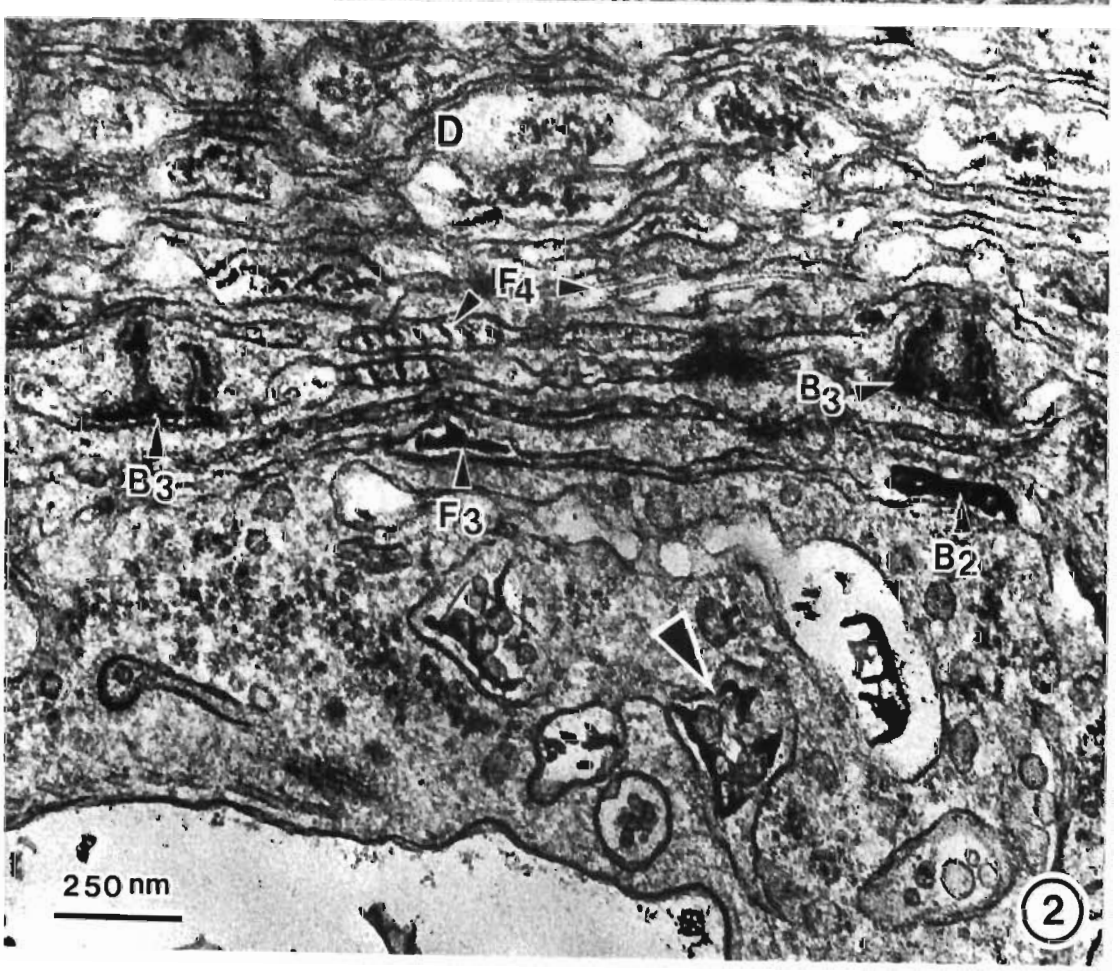
D
F4
B3
B3
F3
B2
250 nm
2

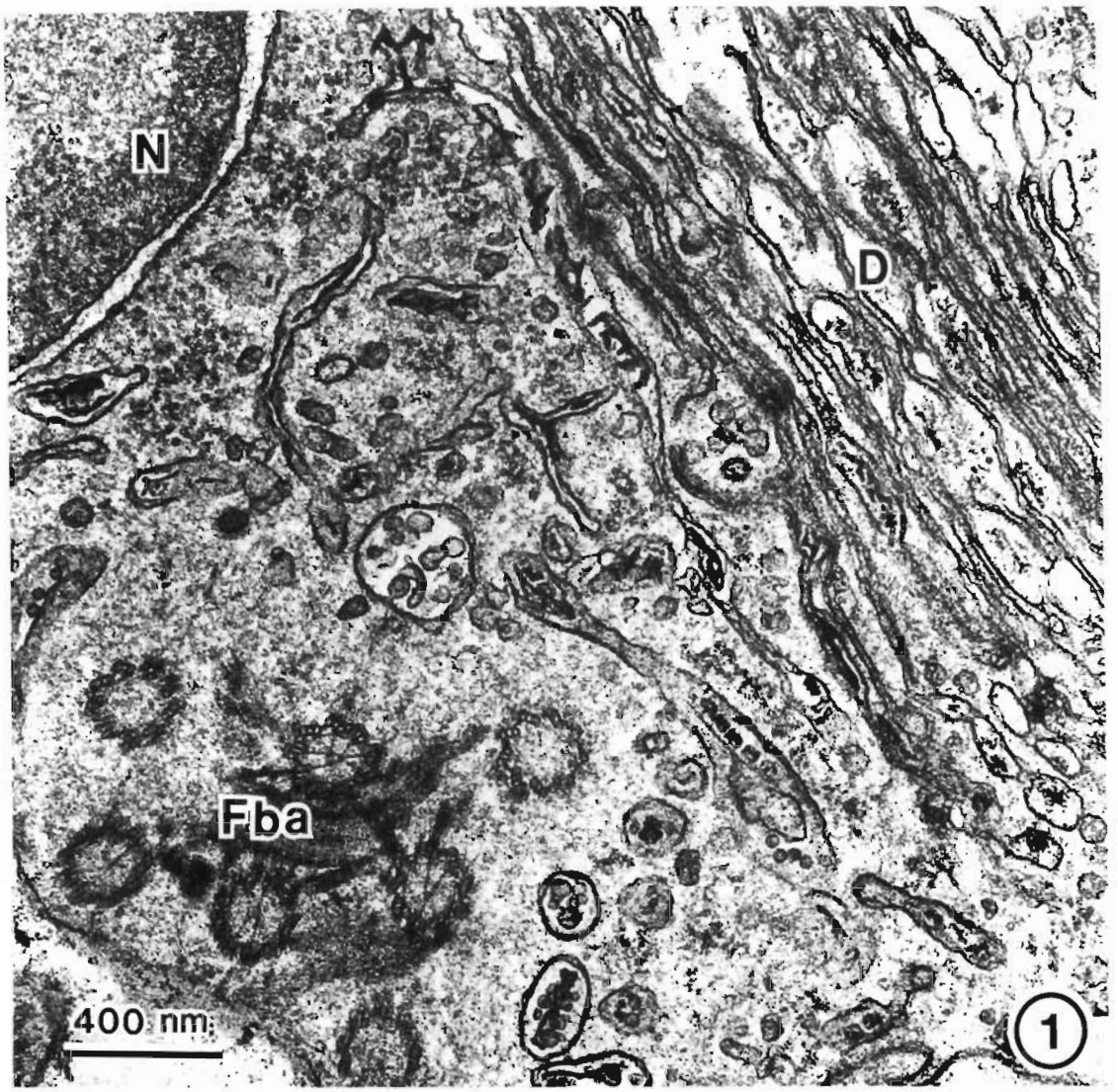
N
D
Fba
400 nm
1

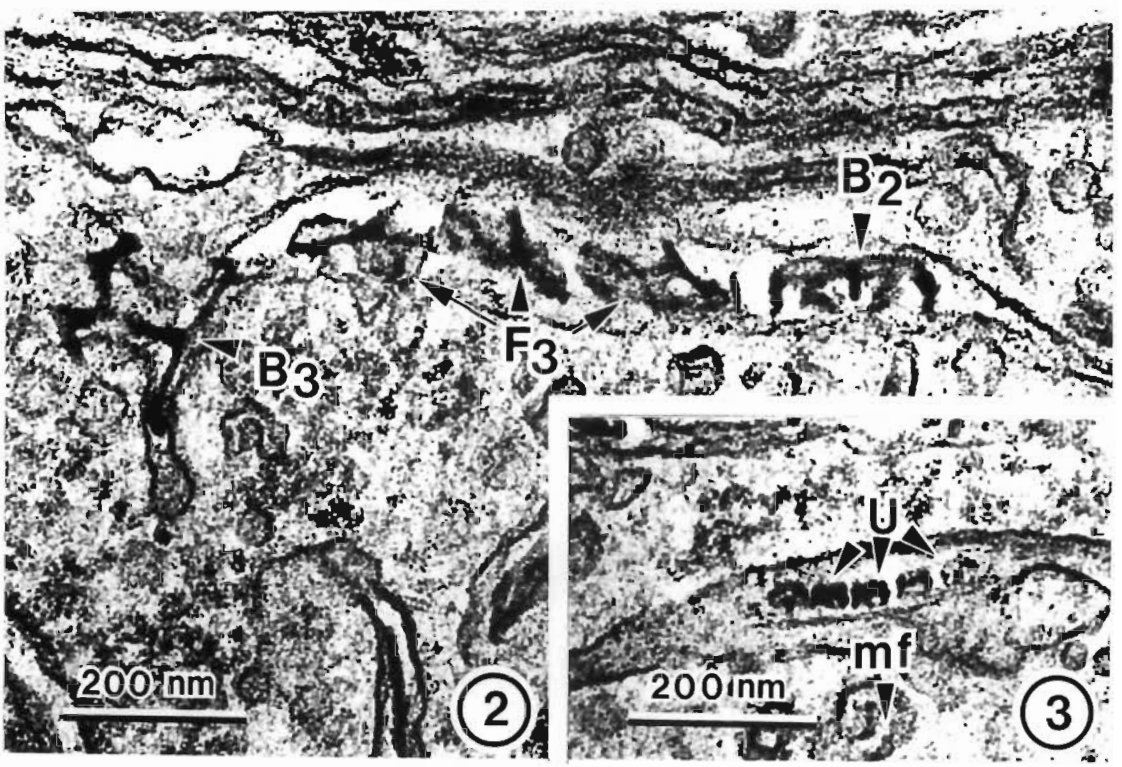
B2
F3
B3
200 nm
2
U
mf
200 nm
3

PLATE 5.15

Morphogenesis of the B_3, B_2 and F_3 scales

(Scale bar on all micrographs = 100 nm)

Figs. 1-11. Morphogenesis of the B_3 scale.

Fig. 1. A snowflake structure with eight radiating arms and associated pinnate appendages.

Fig. 2. Four radiating arms become thickened to form a cruciate structure (This stage is also represented in the development of the B_2 scale).

Fig. 3. The cruciate structure becomes more prominent and is associated with the α cisternal membrane.

Fig. 4 The transient arms of the B_3 scale become detached to form the rounded corners of the scale.

Figs.5-11 The α cisternal membrane remains closely associated with the B_3 scale throughout its development. As the scale develops three dimensionally the α membrane accommodates the growing scale (Figs. 6-8, 11).

Fig. 6 At this stage the B_3 and B_2 scales appear identical in L/S.

Figs. 12-16 Morphogenesis of the B_2 scale.

Fig. 12 Early in the development of the B_2 scale the α cisternal membrane forms a boundary around the scale.

Figs.13-16 As the B_2 scale develops the α cisternal membrane remains in close association with the scale in all parts. The knee-shaped substructure on the proximal surface of the scale develops from the subordinate arms of the scale (figs. 13 and 14).

Figs. 17-20 Morphogenesis of the F_3 scale.

Fig. 17 Two profiles of an asymmetrical snowflake structure which develops into the F_3 scale. The scale has seven radiating arms possessing pinnate appendages.

Figs.18 and 19. The pinnate appendages of the F_3 scale anastomose (fig. 18) and then additional scale material is deposited onto this skeleton to produce the characteristic plate-like appearance of the F_3 scale. The α cisternal membrane is also closely associated with the developing F_3 scale.

Fig. 20 The F_3 scale develops three dimensionally along the dorsal spine only.

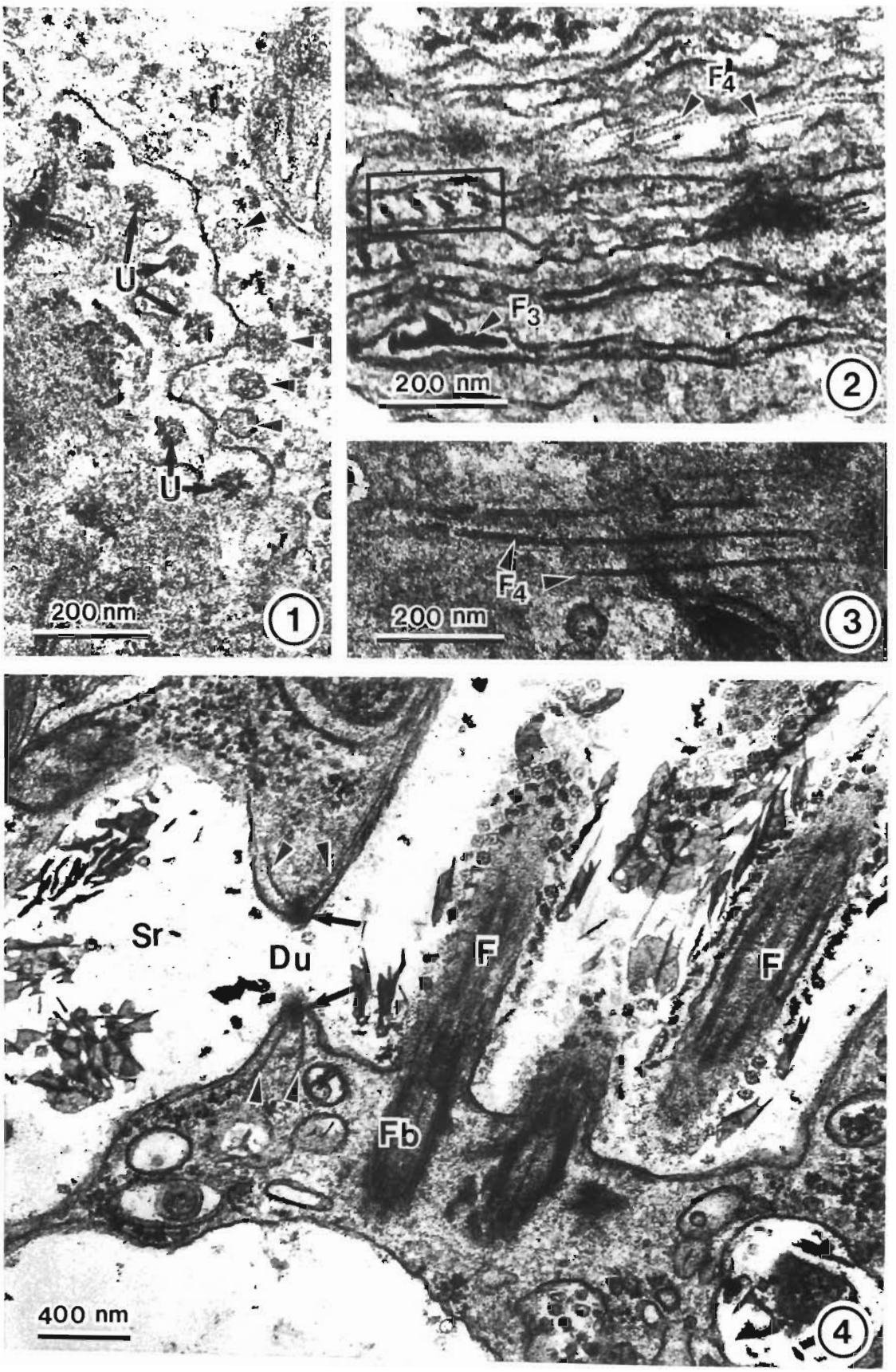
U
U
200 nm
1
F4
F3
200 nm
2
F4
200 nm
3
Sr
Du
F
F
Fb
400 nm
4

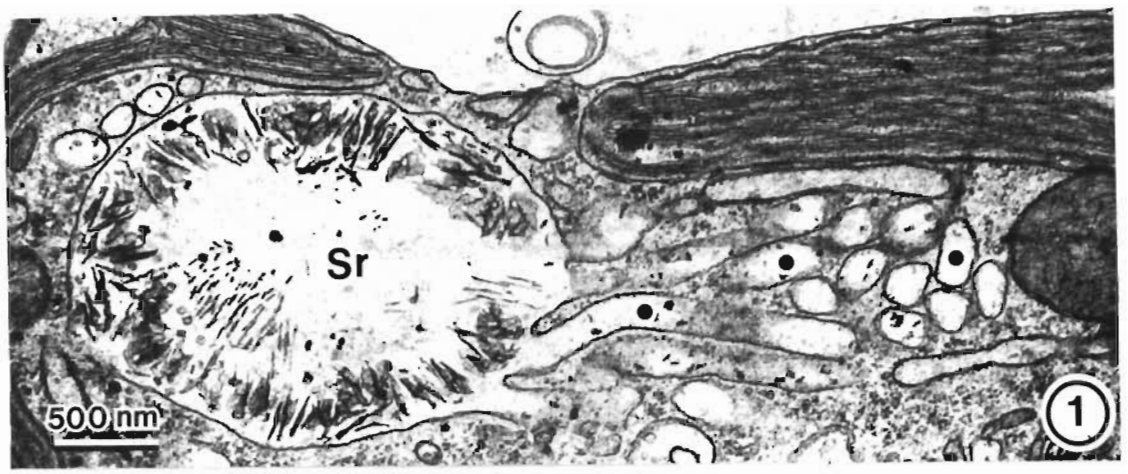
Sr
500 nm
1

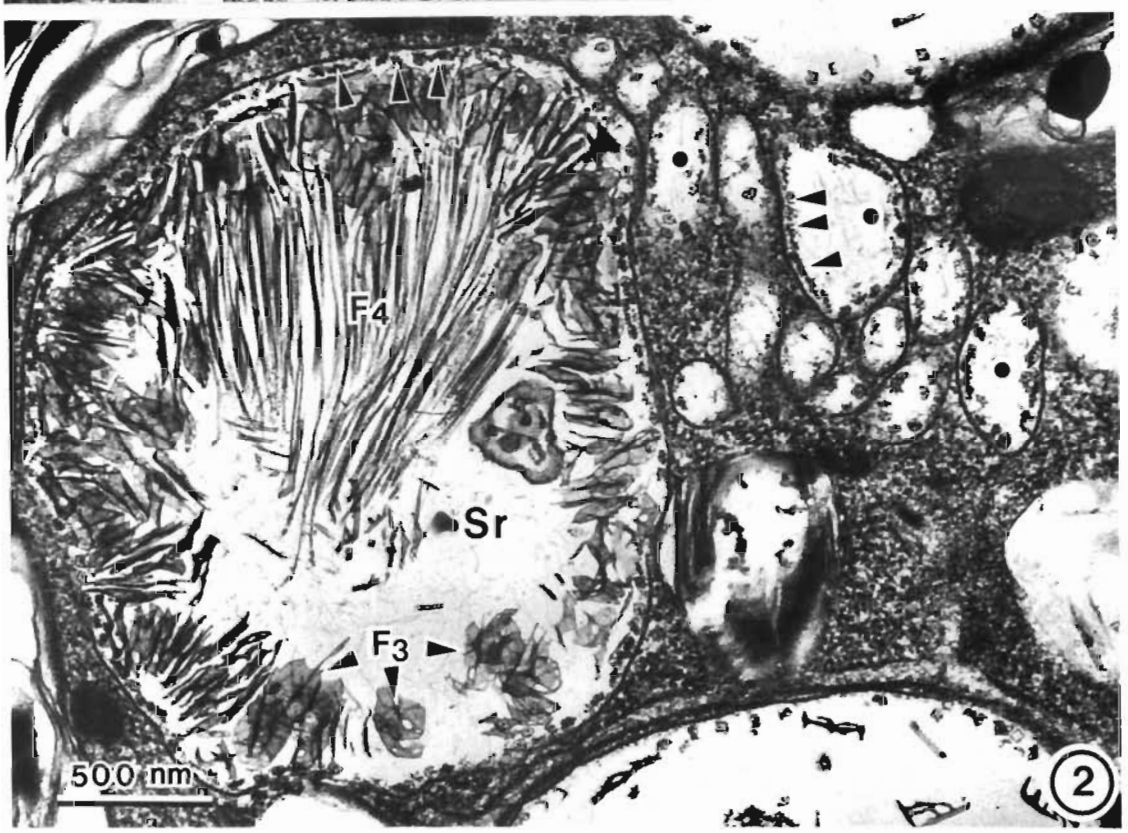
F4
Sr
F3
500 nm
2

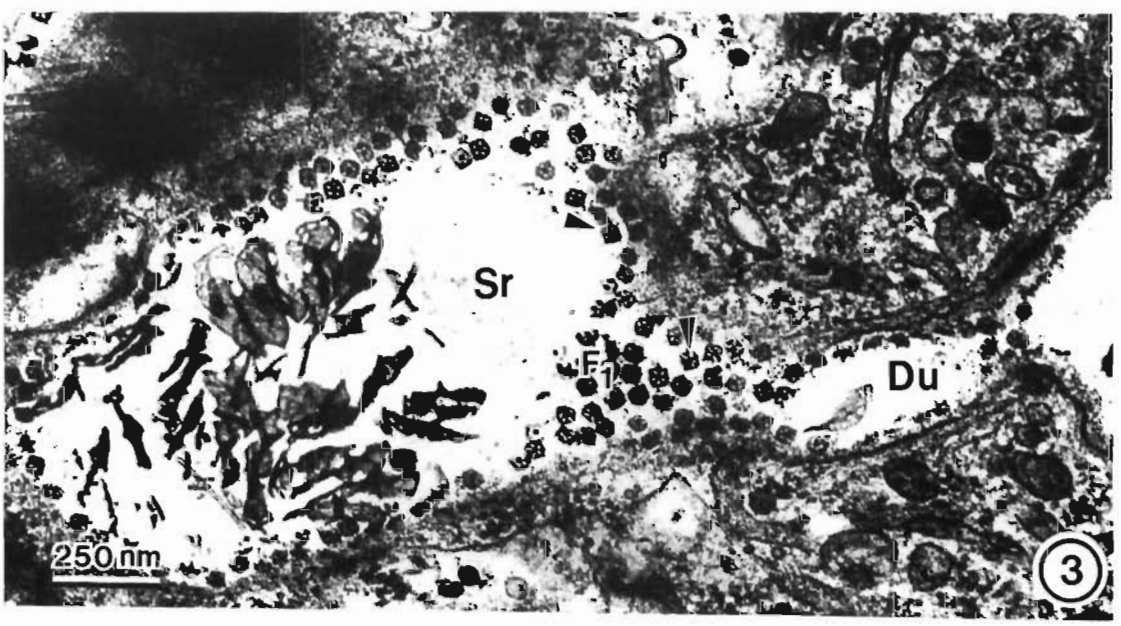
Sr
F1
Du
250 nm
3

PLATE 5.18

Scale release

Figs. 1 and 2. Two oblique sections through the flagellar pit (Fp) region showing predominantly body scales contained in vesicles beneath the plasmalemma. Numerous depressions in the plasmalemma (arrowheads) indicate sites of recent scale releases. The membrane of the scale vesicles is incorporated into the plasmalemma.


Fp
400 nm
1

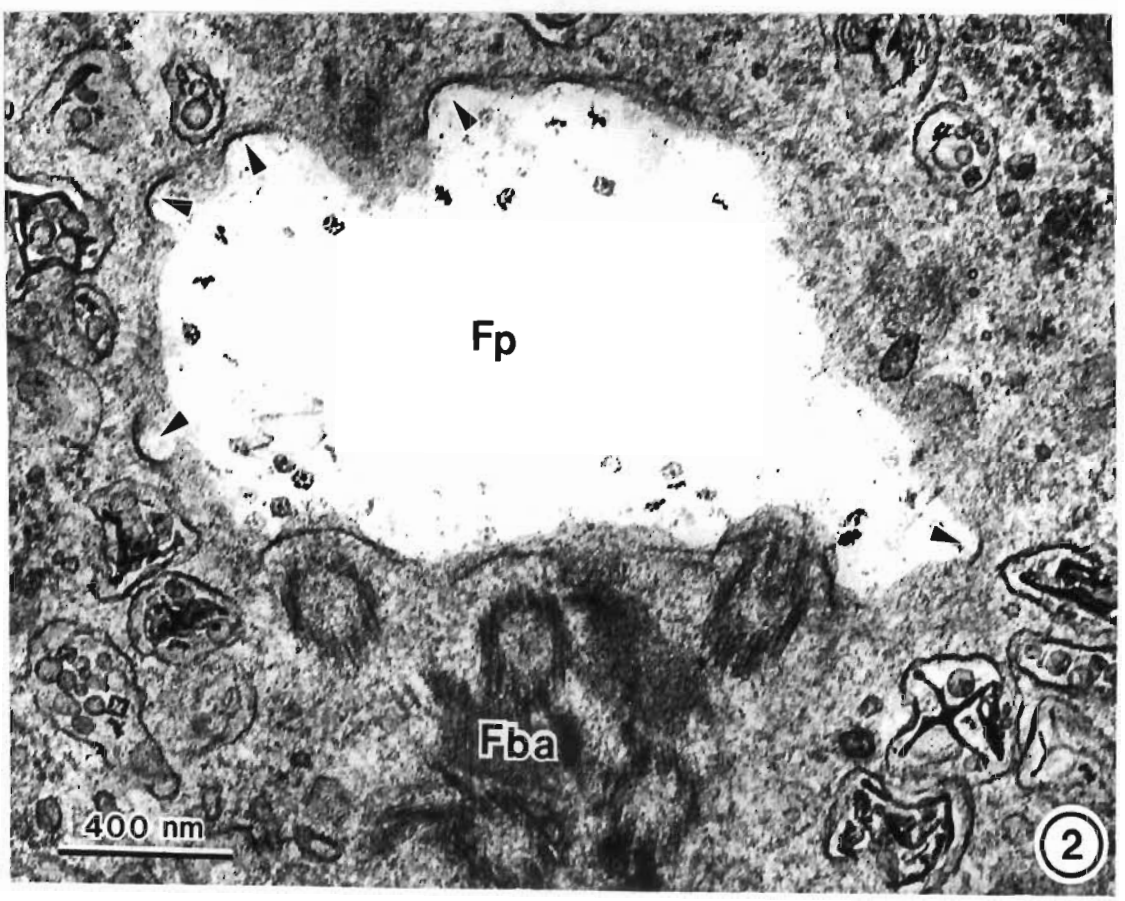
Fp
Fba
400 nm
2

PLATE 6.1

Isolation of Scales

Fig. 1. A heavy metal shadowed preparation of the cell slurry obtained after cells had been lysed with distilled water and sonicated for 10 min. Note the intact bacteria (B) and scales (B_1, B_2, B_3 and F_3) amongst the cell debris (CD).

Fig. 2. A dense pellet of scales from scale fraction A obtained after differential centrifugation (Au/Pd shadowed prep.).

Fig. 3. A diluted sample of scales from scale fraction A showing the individual scales and the purity of the fraction. The standard symbols for different scale types are used (Au/Pd shadowed prep.).

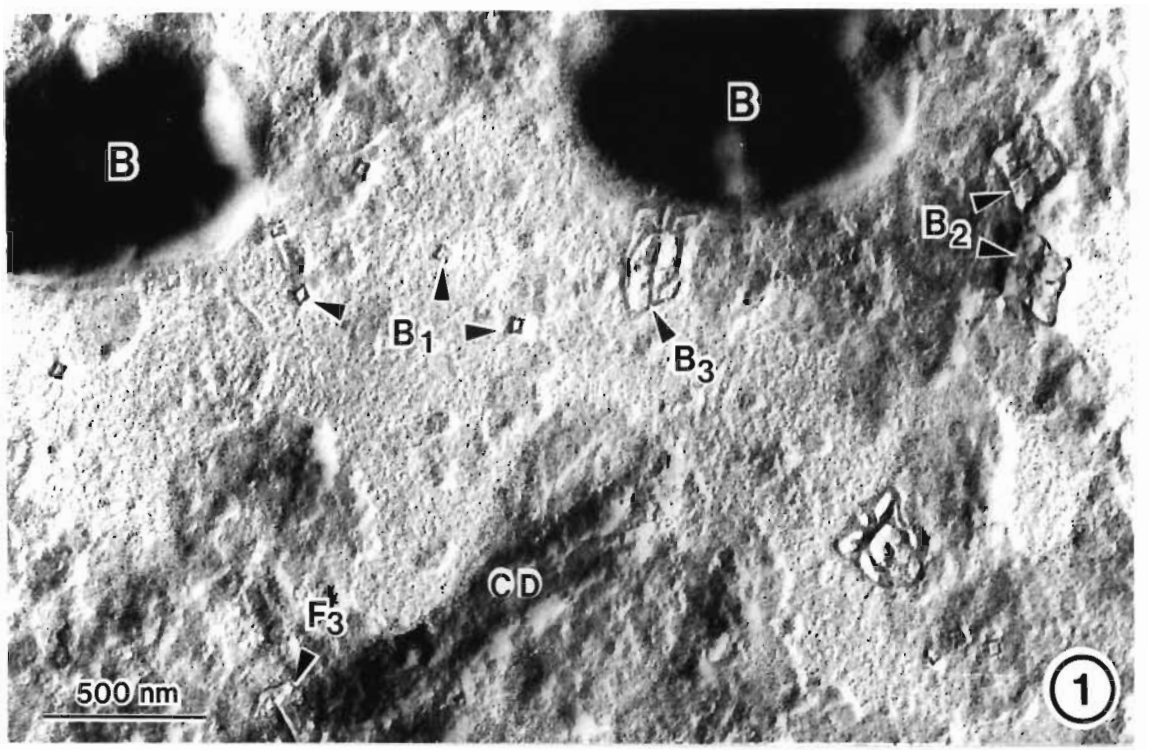
B
B
B2
B1
B3
CD
F3
500 nm
1


1 µm
2

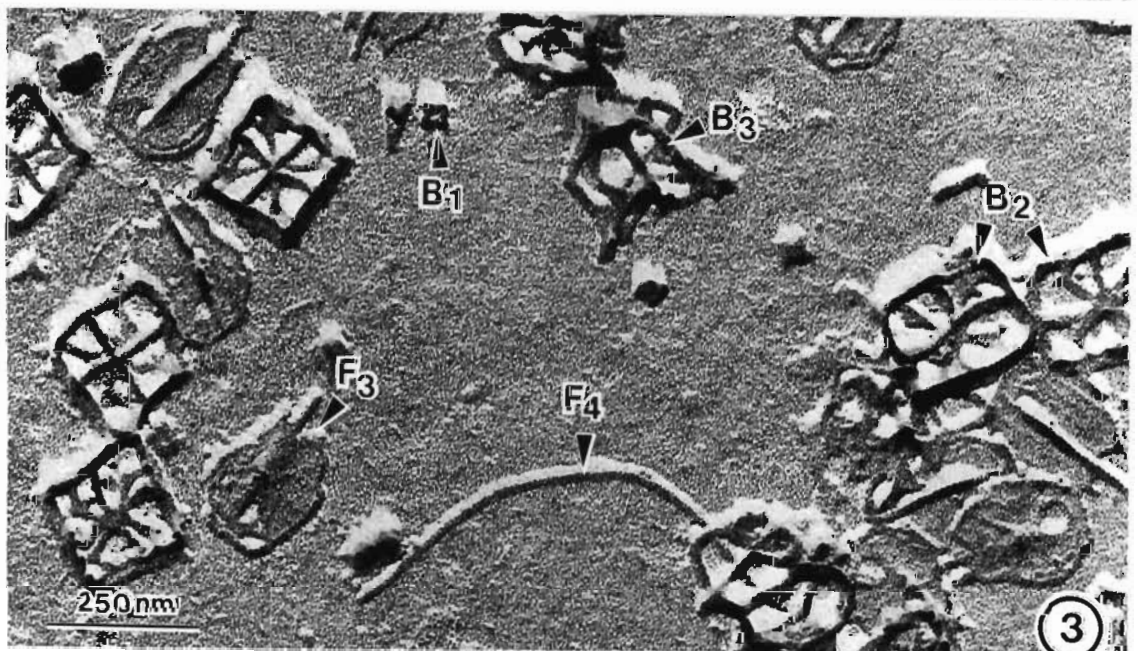
B3
B1
B2
F3
F4
250 nm
3

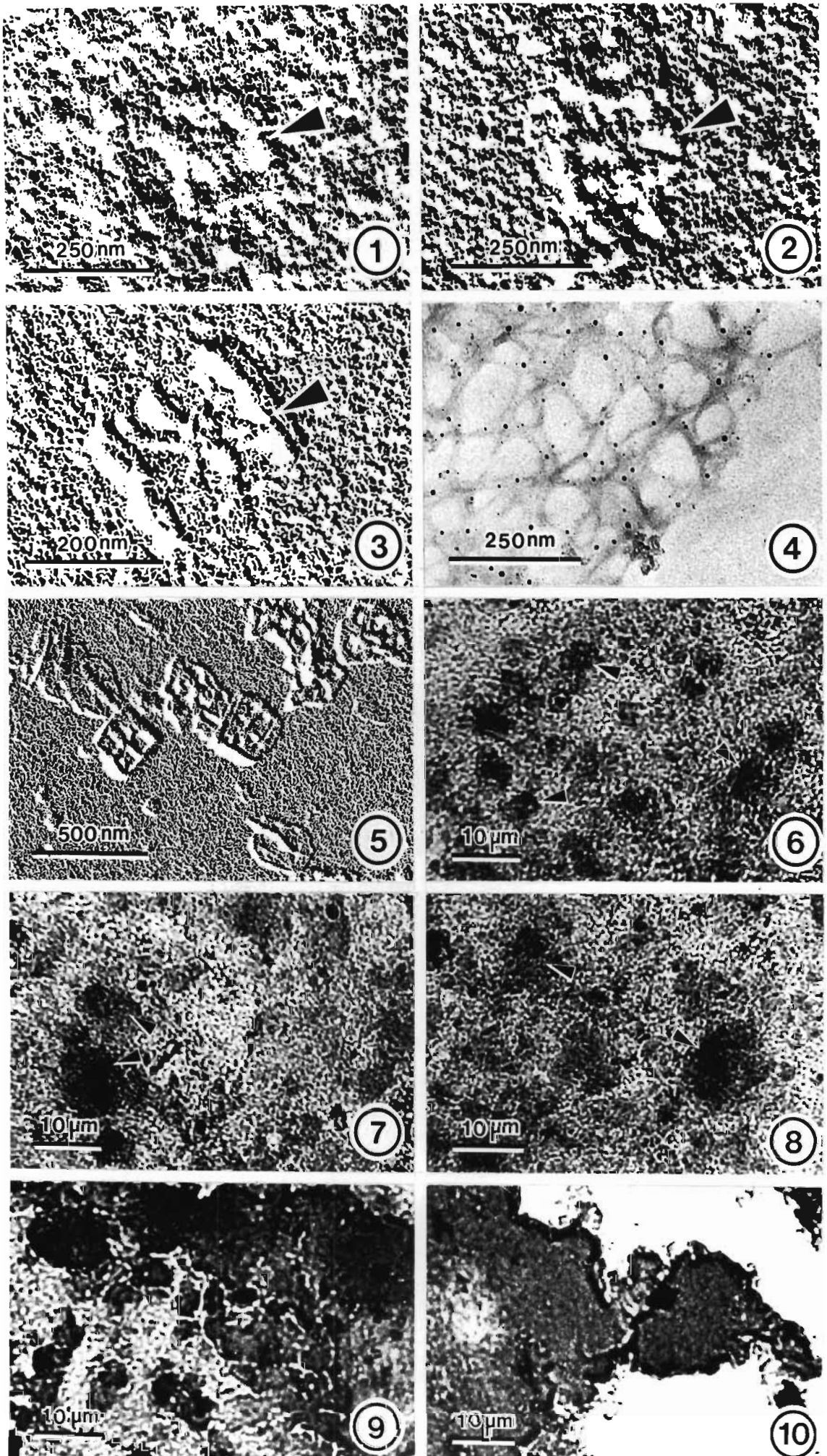
250 nm
1
250nm
2
200nm
3
250nm
4
500nm
5
10 µm
6
10 µm
7
10 µm
8
10 µm
9
10 µm
10

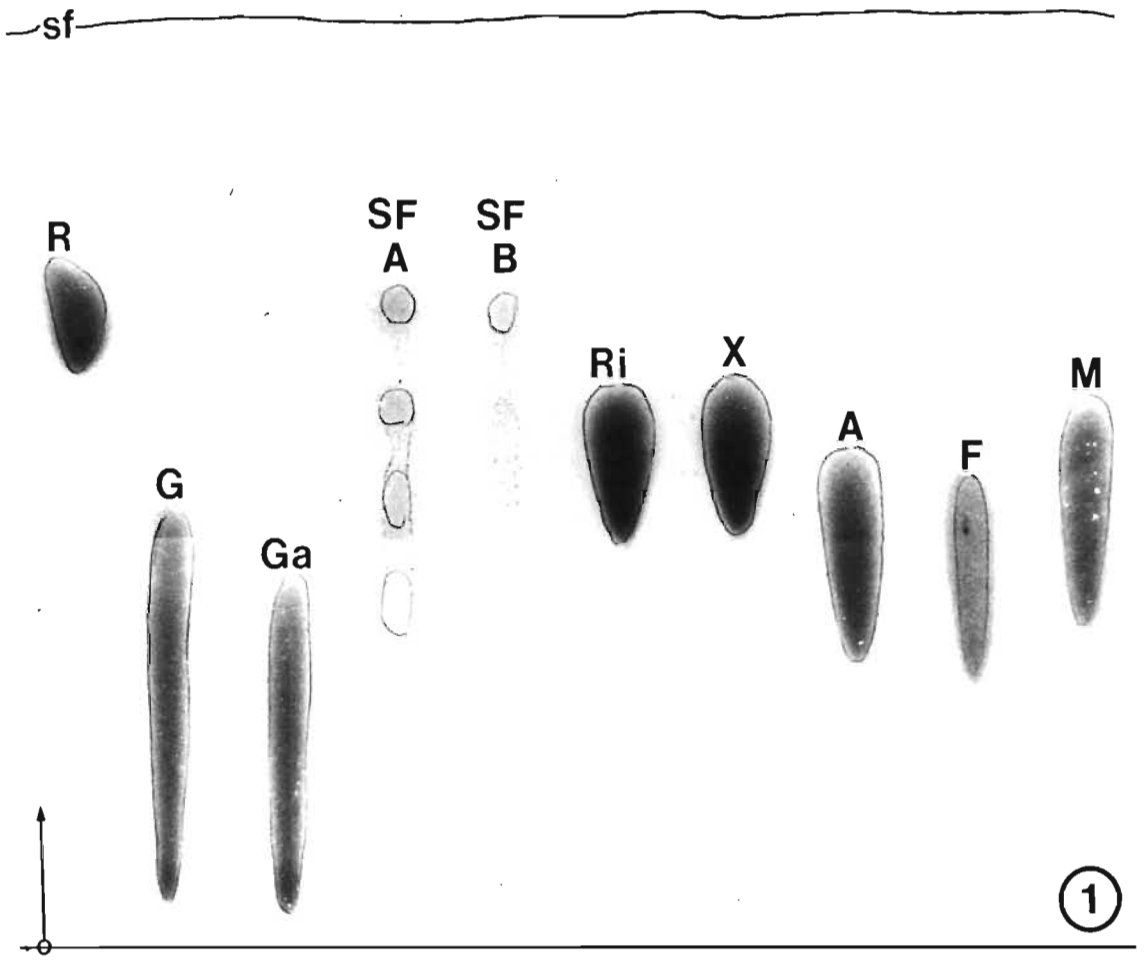
sf
R
SF A
SF B
Ri
X
M
A
F
G
Ga
1

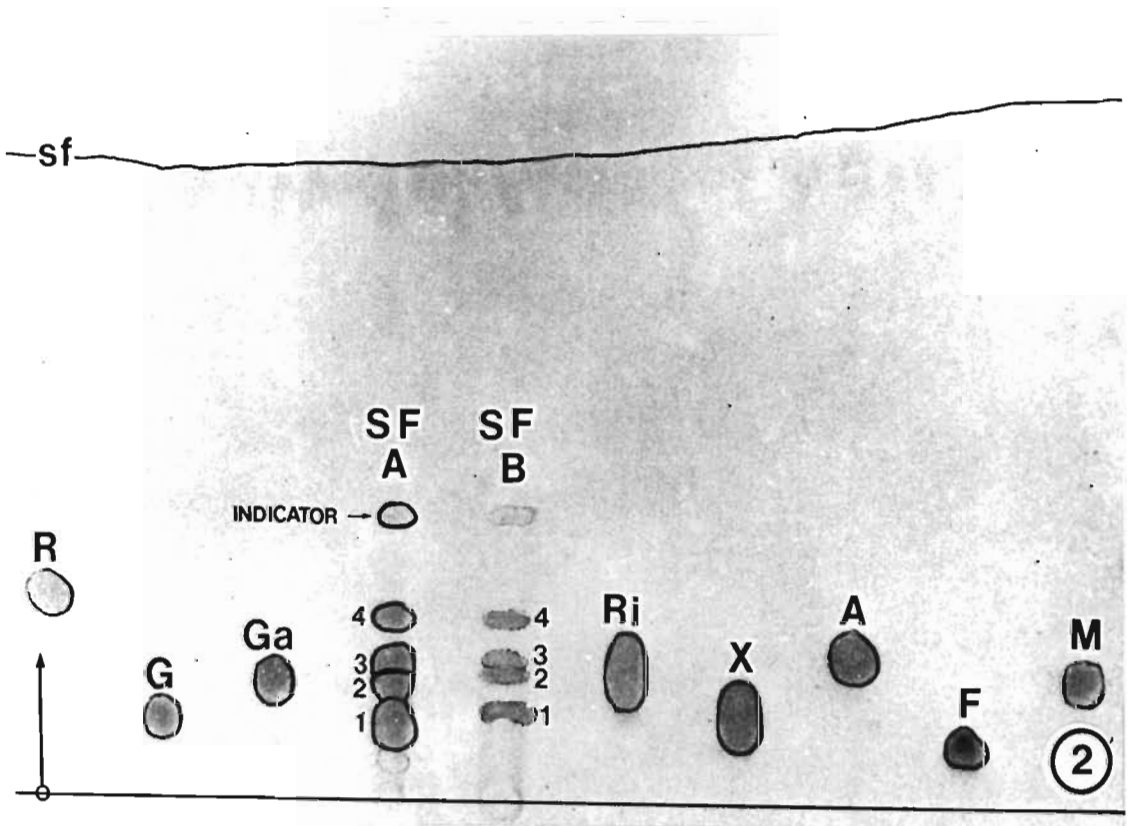
sf
SF A
SF B
INDICATOR
R
4
3
2
1
Ri
A
M
X
F
G
Ga
2

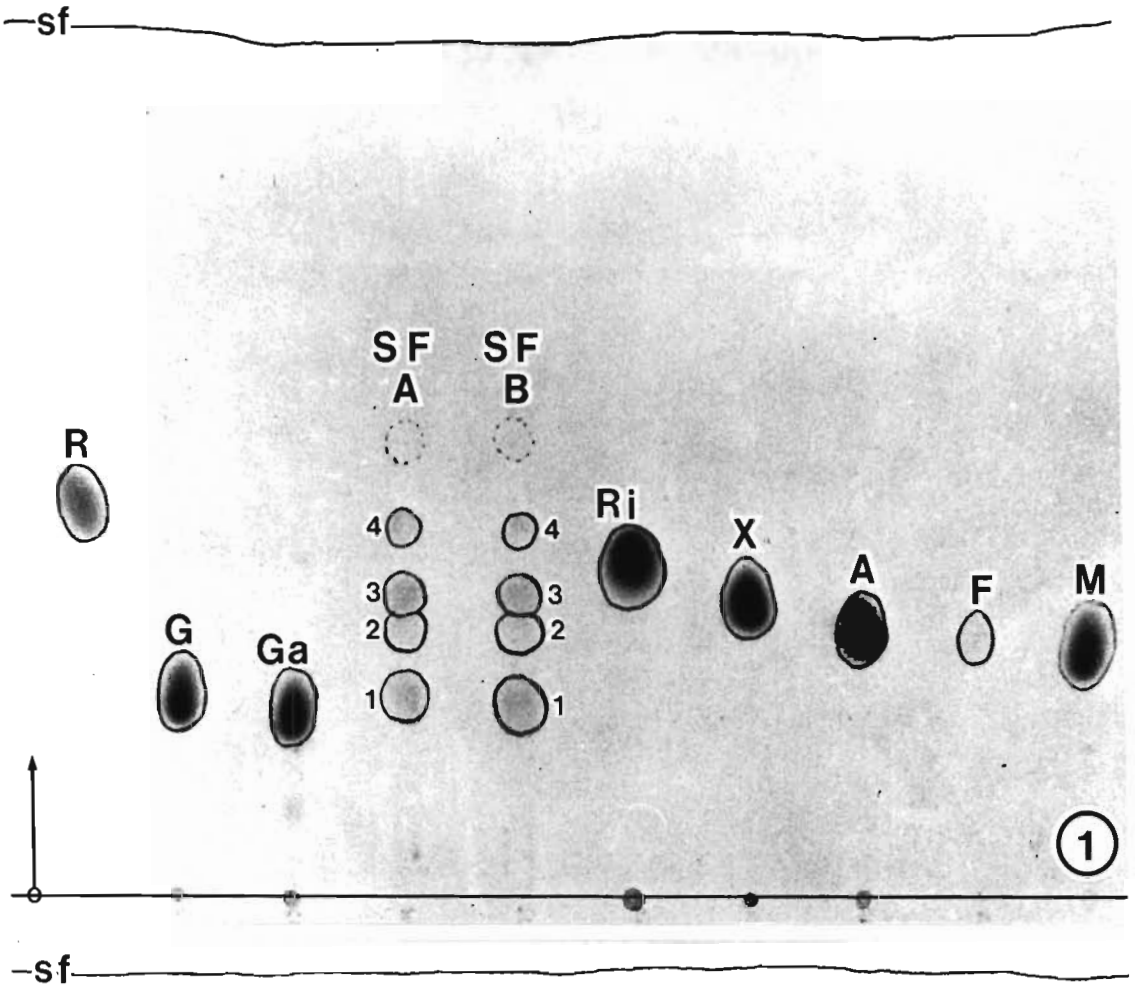
sf
SF A
SF B
R
G
Ga
4
3
2
1
Ri
X
A
F
M
1
sf

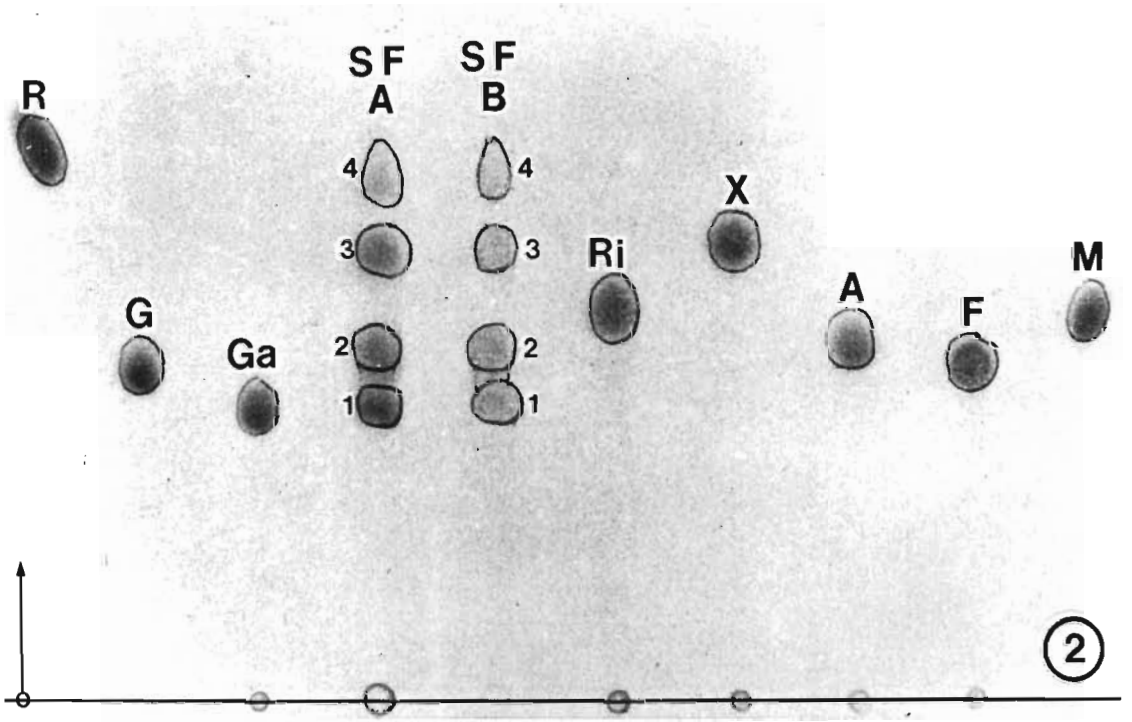
SF A
SF B
R
G
Ga
4
3
2
1
Ri
X
A
F
M
2

PLATE 6.5

Thin layer chromatography

Abbreviations as for Plate 6.3

Fig. 1. A thin layer chromatogram developed twice in the same direction in the BAEW solvent system. This procedure did not prove to be successful because the relatively concentrated reference sugars ran more slowly than scale hydrolysate residues. Plate sprayed with aniline hydrogen phthalate.

Fig. 2. A thin layer chromatogram showing the presence of fructose (f) in the scale fraction B hydrolysate after the acid resistant residue was rehydrolysed in 5N H_2SO_4. This sugar was recognized by its colour reaction with naphthoresorcinol/H_3PO_4. All sugars in scale fraction A ran more slowly than the reference sugars. The reason for this could be because the hydrolysate was applied too heavily at the origin.

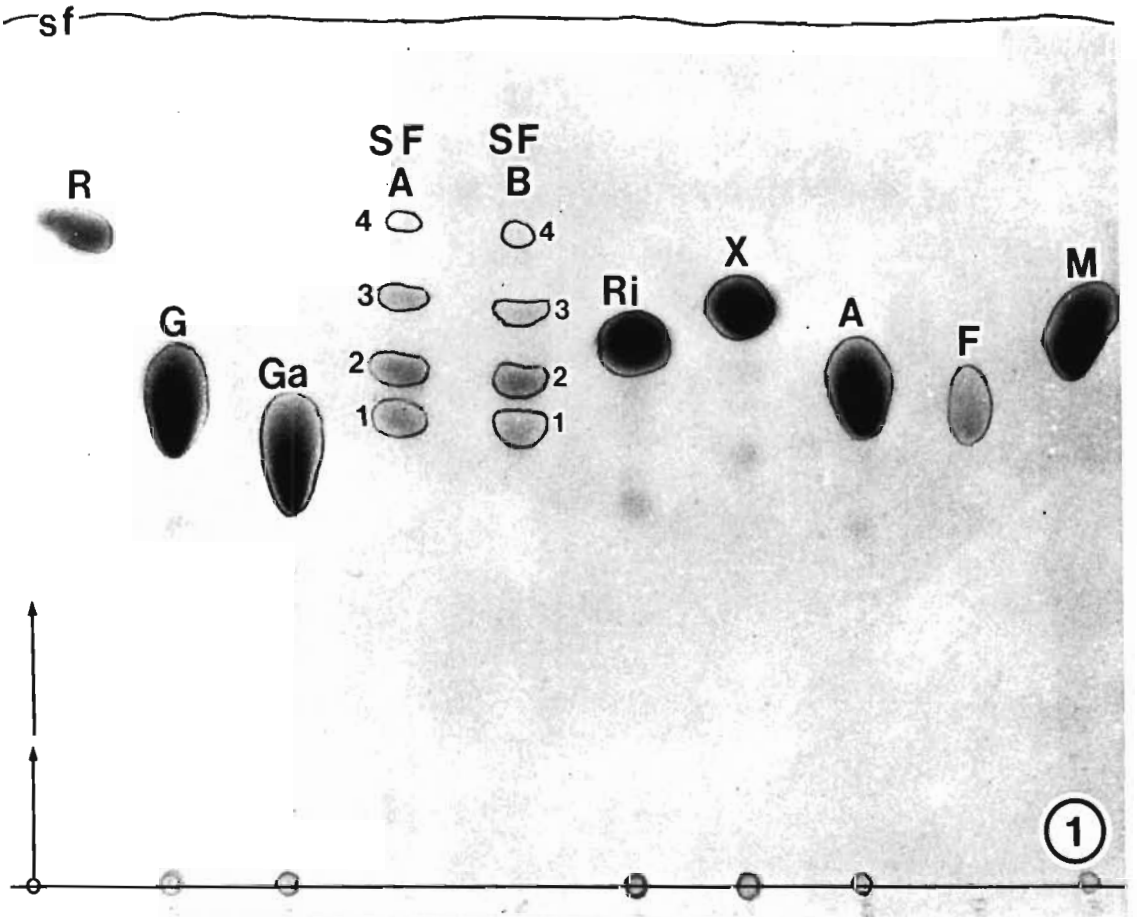
sf
R
G
Ga
SF A
4
3
2
1
SF B
4
3
2
1
Ri
X
A
F
M
1

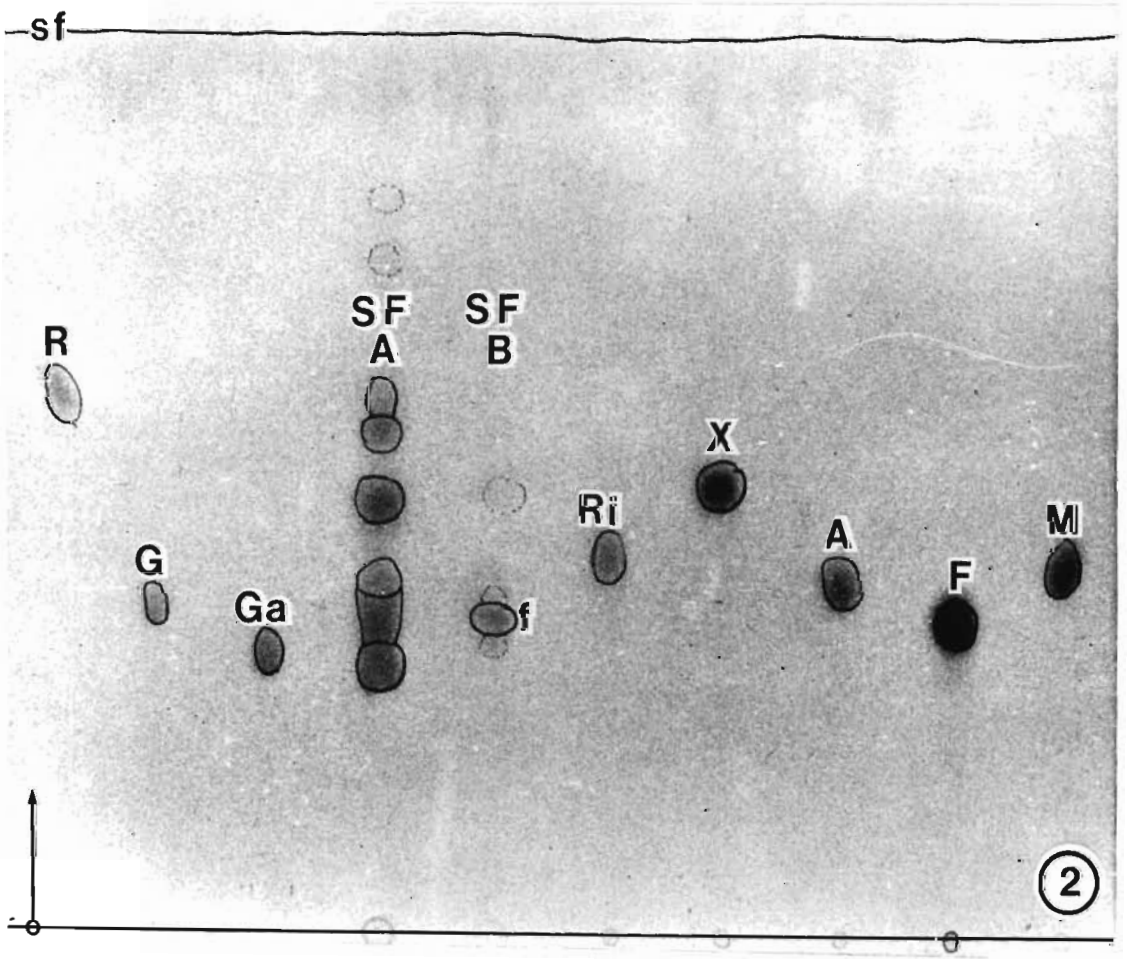
sf
R
G
Ga
SF A
SF B
f
Ri
X
A
F
M
2

PLATE 7.1

Life-history - structure and division of l-cells

Scale bar on all micrographs = lO μm.

Fig. l A lateral view of a large l-cell (LC) surrounded by smaller t-cells (TC). Note the lipid globules (L.) in the cell (bright field).

Fig. 2. A lateral view of a newly formed l-cell showing the four flagella (F) emerging from the anterior flagellar pit. The cell is pyriform in shape and has a parietal chloroplast (C) containing a posterior pyrenoid (P) and an eyespot (E). Though the cell contains starch granules in the chloroplast lobes no lipid material is present. (bright field).

Fig. 3. An apical view of a settled l-cell. Note the 4 large starch grains (S) in the chloroplast lobes. (bright field).

Fig. 4. A flattened l-cell with 2 eyespots (arrowheads). (phase contrast).

Fig. 5. An osmotically lysed l-cell with 4 eyespots (arrowheads), one in each of the chloroplast lobes. (phase contrast).

Figs. 6-lO. Cell division stages (phase contrast).

Fig. 6 The first sign of cell division is marked by the division of the chloroplast. This is evident in the region of the pyrenoid (arrowhead).

Fig. 7- 9 The flagellar apparatus replicates and 4 new flagella are formed. These increase in length so that the cell has 8 isokont flagella.

Fig. lO Cytokinesis begins anteriorly and the two flagellar poles move apart.

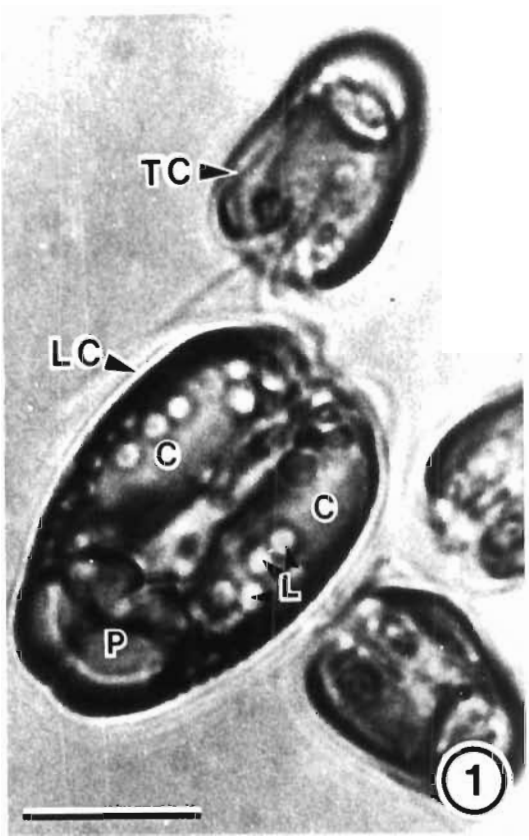
TC
LC
C
C
L
P
1

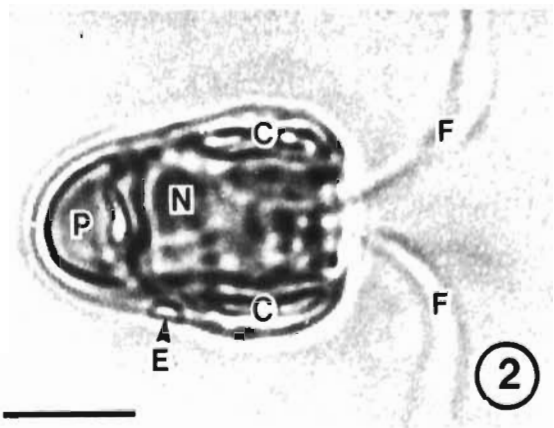
C
F
P
N
C
F
E
2

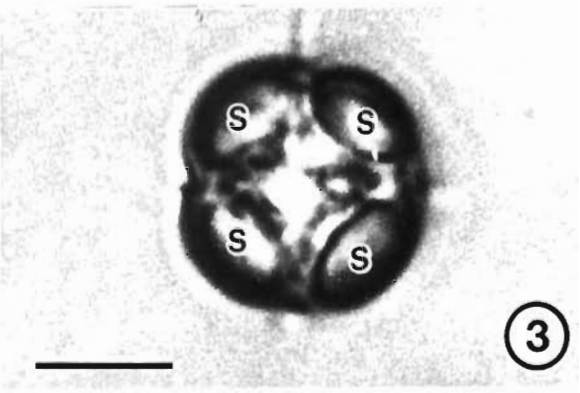
S
S
S
S
3

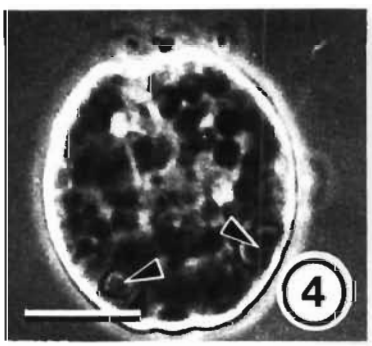
4


5


6


7

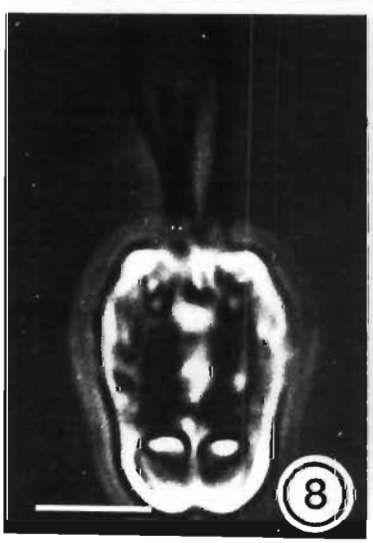
8

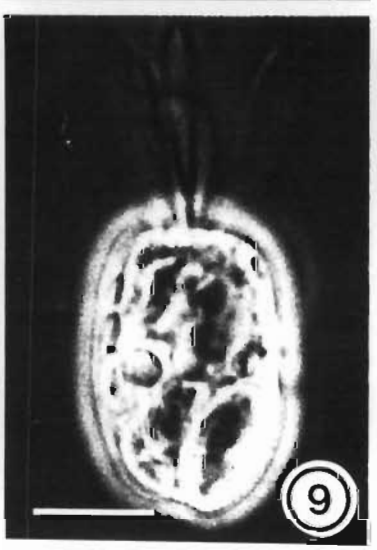
9

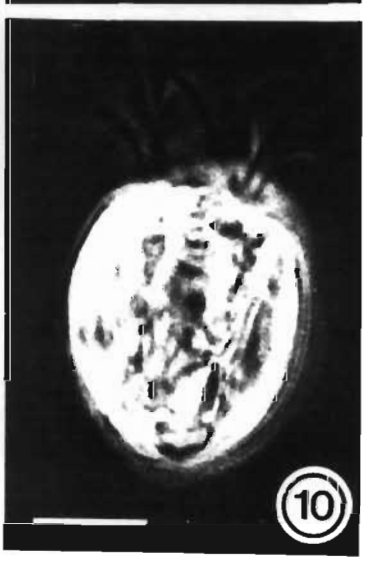
10

PLATE 7.2

Cell division in 1-cells, pleomorphic cells.

Scale bar on all micrographs = 10 µm.

Figs. 1-6 Later stages in cell division. (phase contrast).

Fig. 1 and 2. The flagellar poles continue to move apart and a longitudinal cleavage line (arrowheads) is apparent.

Fig. 3 An apical view of a dividing 1-cell showing the cleavage line (arrowheads). Note the four large starch grains (S) within the cell.

Figs. 4 and 5. Late stages in cytokinesis with the cells in a "back-to-back" stage. Daughter lobes are attached in the region of the pyrenoid.

Fig. 6 An asymmetrical daughter 1-cell with two large starch grains (S).

Figs. 7-12 Pleomorphic cells (phase contrast)

Fig. 7 Cytokinesis is sometimes arrested early so that the flagellar poles do not move apart.

Fig. 8 In other cells cytokinesis progresses more rapidly at the posterior end.

Fig. 9 Where cytokinesis is arrested late in the division process a permanent bilobed or back-to-back stage results.

Figs. 10 and 11. Some cells with incomplete cytokinesis have one cell lobe larger than the other.

Fig. 12 One lobe of a bilobed cell may divide subsequently to give rise to a trilobed pleomorph.

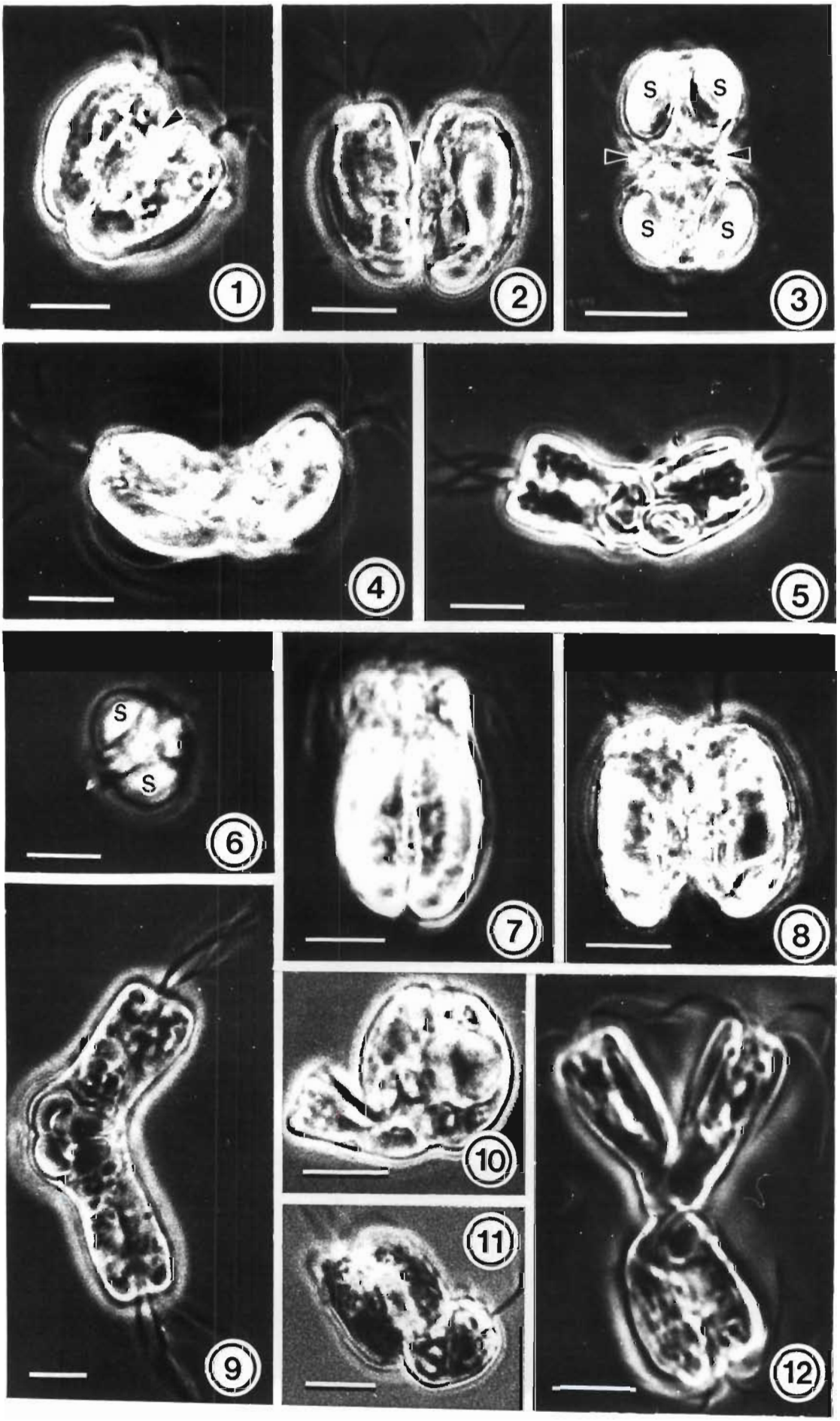
S
S
S
S
S
S
1
2
3
4
5
6
7
8
9
10
11
12

PLATE 7.3

Encystment and excystment

Scale bar on all micrographs = 10 µm.

Encystment

Figs. 1 and 2 The 1-cell begins to round-off and the flagella shorten as they are resorbed. (phase contrast)

Fig. 3 The non-motile 1-cell rounds-off further to form the immature cyst. (phase contrast)

Figs. 4 and 5. Mature cysts with large reserves of storage material. The cyst has a thick cell wall. (bright field).

Fig. 6 Four large starch grains (S) are seen in the cyst. (bright field).

Fig. 7 Cysts often have a "fuzzy" outer surface where bacteria are attached to the cyst wall. (phase contrast).

Excystment

Fig. 8. The first sign of germination is noted when the protoplast begins to move away from one pole of the cyst. (bright field).

Fig. 9 The chloroplast then divides (bright field).

Fig. 10 Following the division of the chloroplast the protoplast divides and the cyst wall appears to lose its rigidity. (phase contrast).

Fig. 11 The cyst wall ruptures and the divided protoplast is extruded from the cyst. (phase contrast).

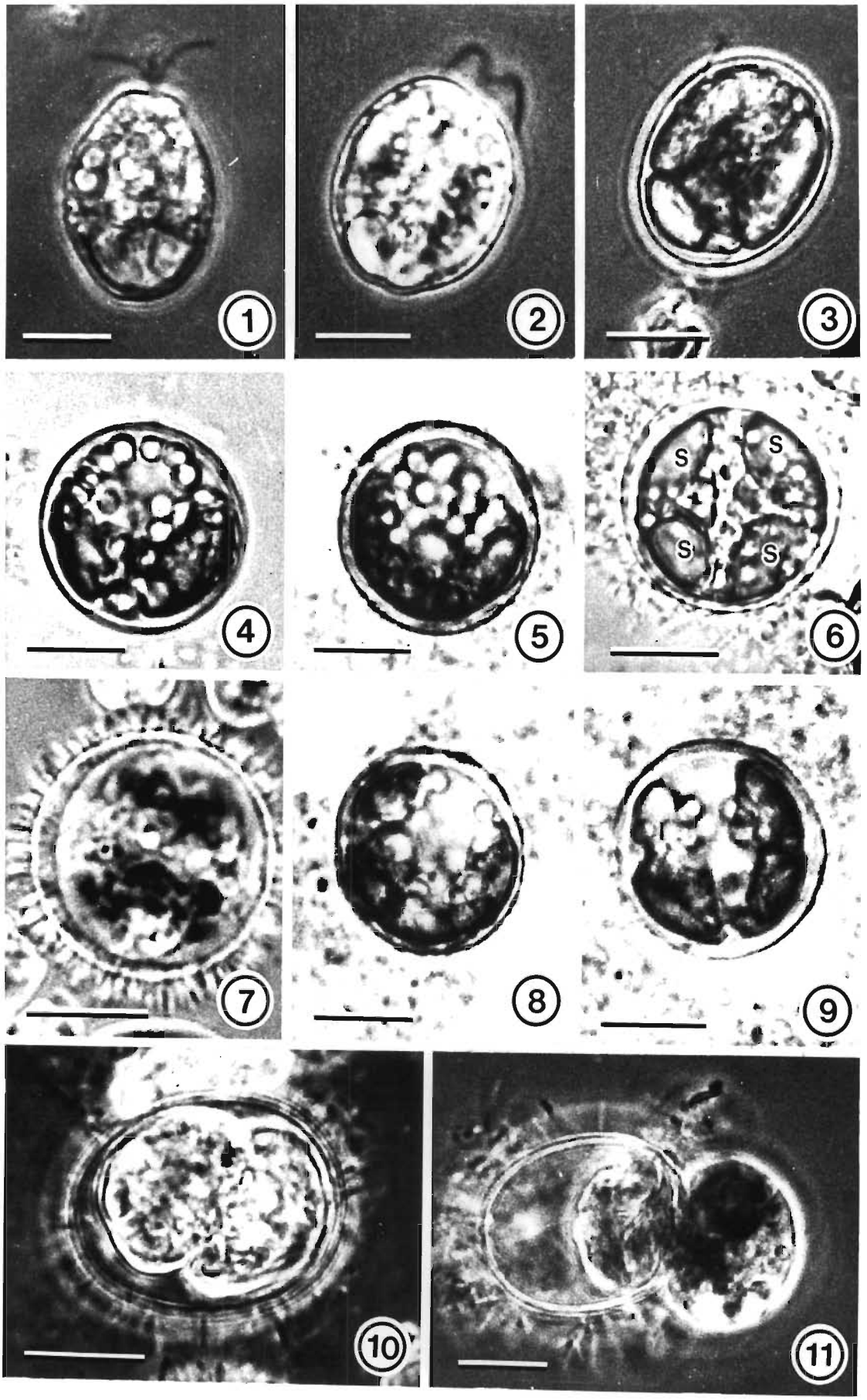
1
2
3
4
5
S
S
S
S
6
7
8
9
10
11

PLATE 7.4

Excystment

Scale bar on all micrographs = 10 µm.

Fig. 1 The daughter protoplasts released from the cyst are contained in a parental sac. (phase contrast).

Fig. 2 The two daughter protoplasts become motile and four flagella (arrowheads) are seen emerging from an anterior flagellar pit. (phase contrast).

Fig. 3 One of the cells divides (arrowhead) before the other. (phase contrast).

Figs. 4 and 5. These micrographs show three motile cells within the parental sac. The larger cell divided subsequently. (bright field).

Fig. 6 A parental sac containing four motile cells. Most often the motile cells are released from the parental sac at this stage. (bright field).

Figs. 7 and 8. Occasionally the motile cells within the parental sac underwent further divisions so that five (Fig. 7) or six (Fig. 8) motile cells were seen in the parental sac. (bright field).

Fig. 9 A field of encysted cells which developed in mucopolysaccharide material found on the base of the culture flask. (phase contrast).

Fig. 10 Motile t-cells and l-cells were often seen to become attached to the mucopolysaccharide material. (phase contrast).

Fig. 11 An unusual non-motile cell type seen in one culture. The cells had large vacuoles. (phase contrast).

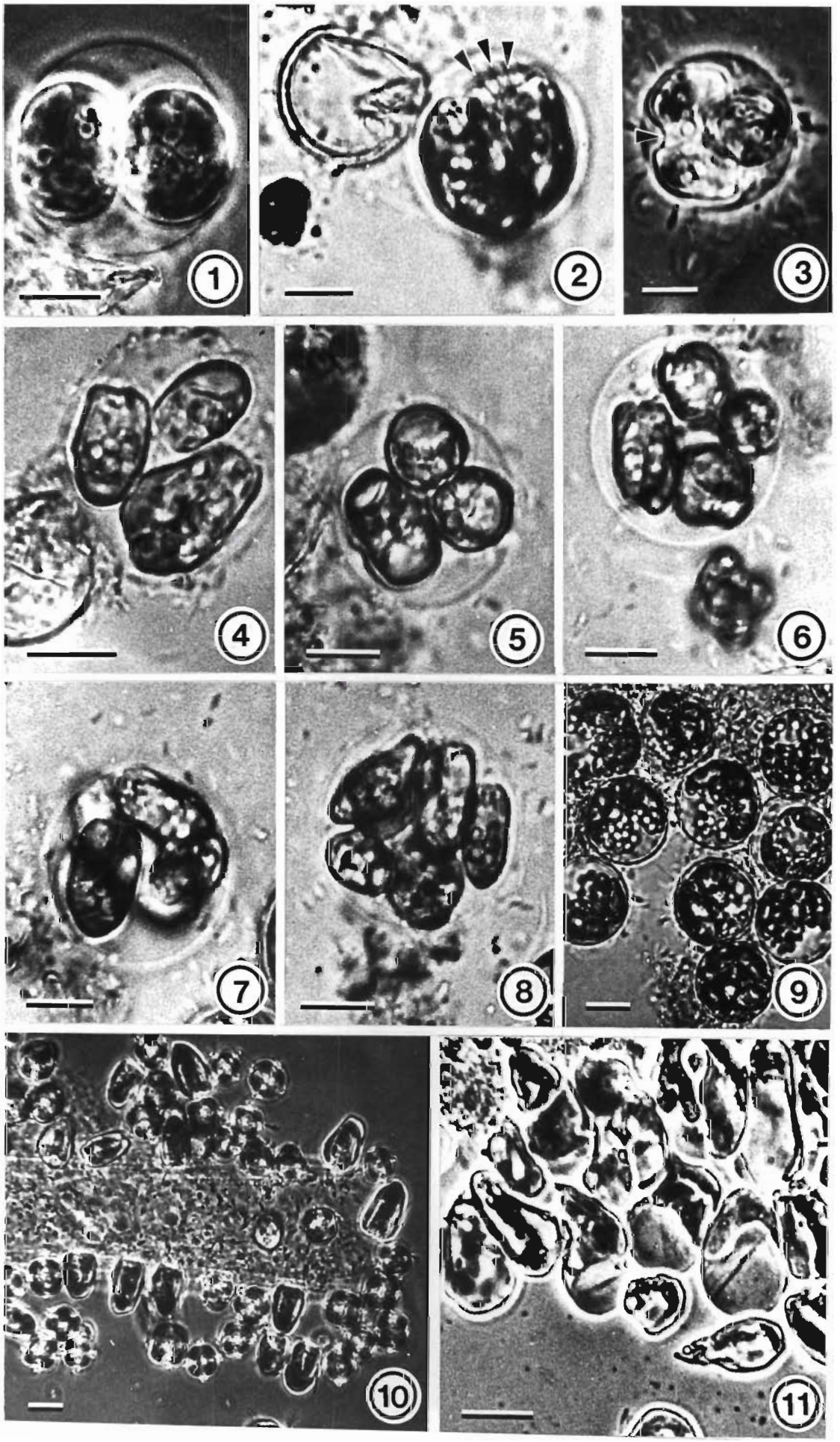
1
2
3
4
5
6
7
8
9
10
11

PLATE 7.5

Structure of l-cells.

Fig. 1 A longitudinal section through an l-cell showing the large reserves of starch (S) and lipid (L). The cell has a parietal chloroplast (C) which contains an eyespot (E) and a posteriorly situated pyrenoid (P). A large vacuole (V) occupies a central position within the cell. Trichocysts (T) are present around the opening of the anterior flagellar pit (Fp). A scale-boundary identical to that reported for t-cells covers the l-cell.

Fig. 2 A transverse section through the flagellar pit region of an l-cell. The four lobes of the chloroplast (C) are seen in the four lobes of the cell body. Numerous lipid globules (L) and trichocysts (T) are seen surrounding the flagellar pit (Fp). Four flagellar profiles (F) are seen within the flagellar pit.

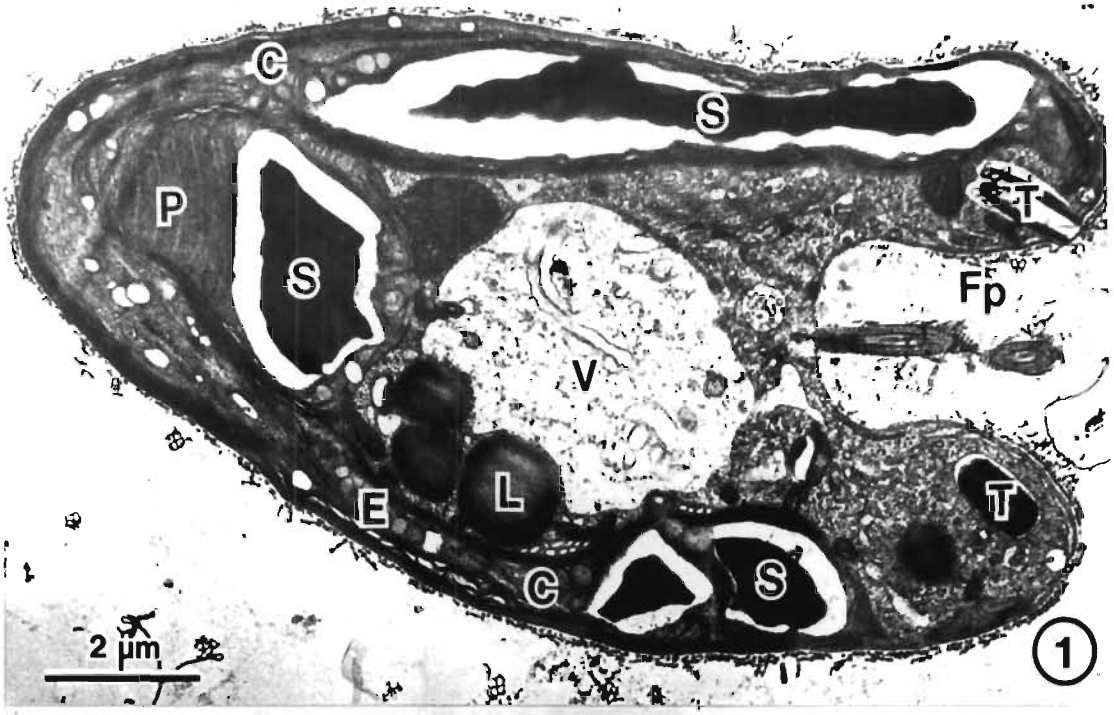
C
S
P
S
T
Fp
V
E
L
T
C
S
2 µm
1

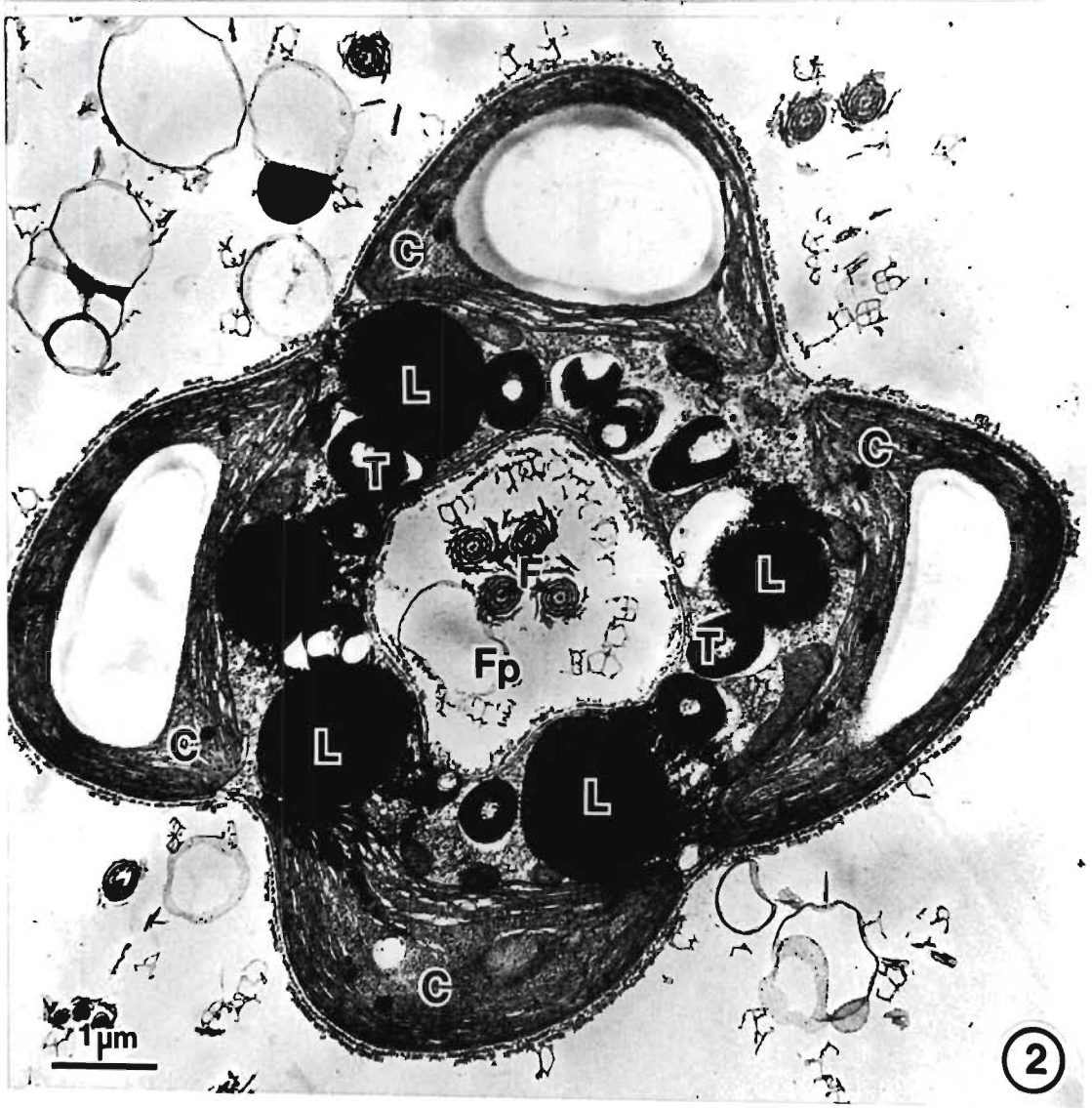
C
L
T
C
F
L
Fp
T
C
L
L
C
1 µm
2

PLATE 7.6

Structure of l-cells

Fig. l A transverse section through an l-cell showing the flagellar basal body apparatus (Fba), nucleus (N), vacuole (V), two dictyosomes (D) and scale reservoir (Sr). The cell has lipid (L) and starch (S) reserve material. Trichocysts (T) are also situated between the lobes of the chloroplast.

Figs. 2 and 3. Two micrographs showing the association of the compound microtubular rootlet (R_2 C) with the duct (Du) of the scale reservoir. The micrographs show the microtubular rootlet surrounding the duct of the scale reservoir (arrowheads). Fig. 2 is a detailed view of the flagellar basal body apparatus of the cell shown in Fig. l.

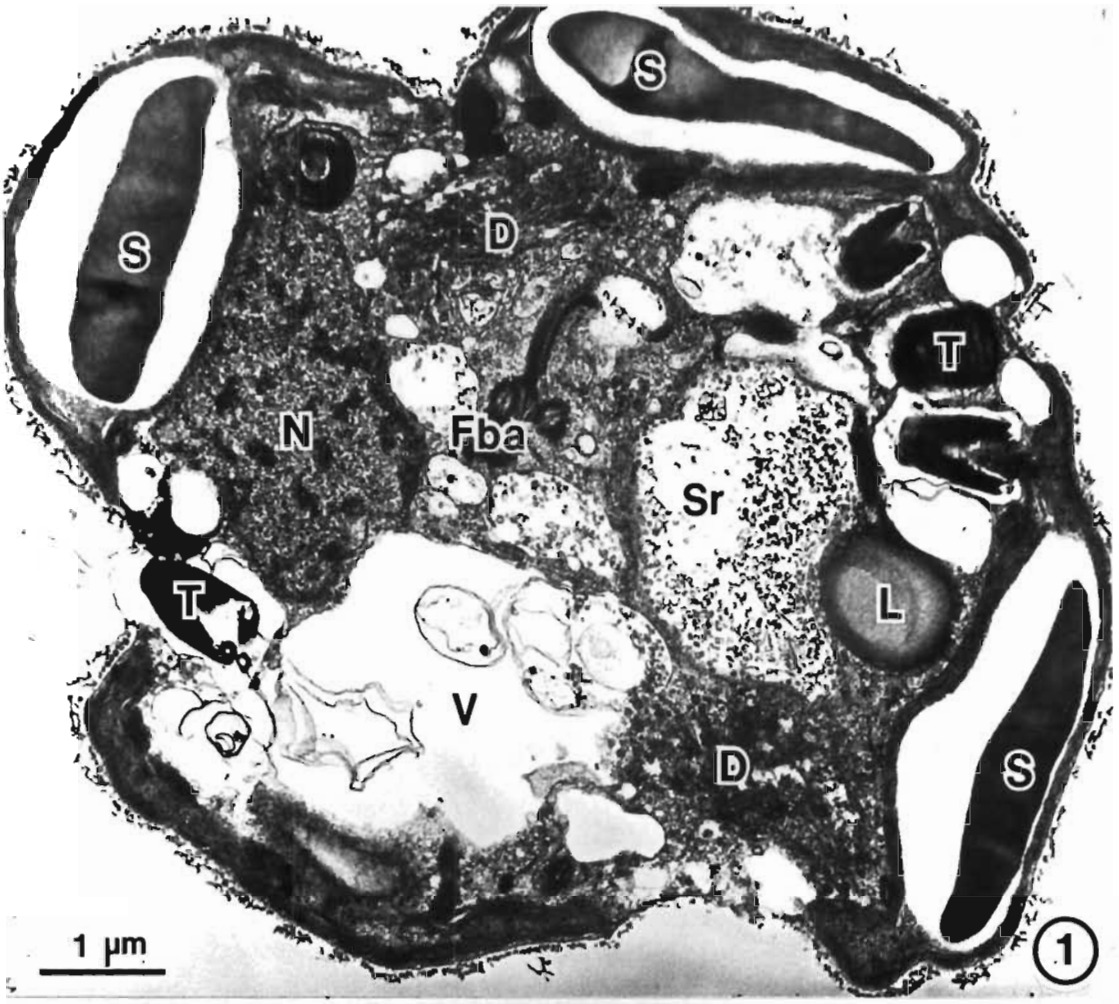
S
S
D
T
N
Fba
Sr
T
L
V
D
S
1 µm
1

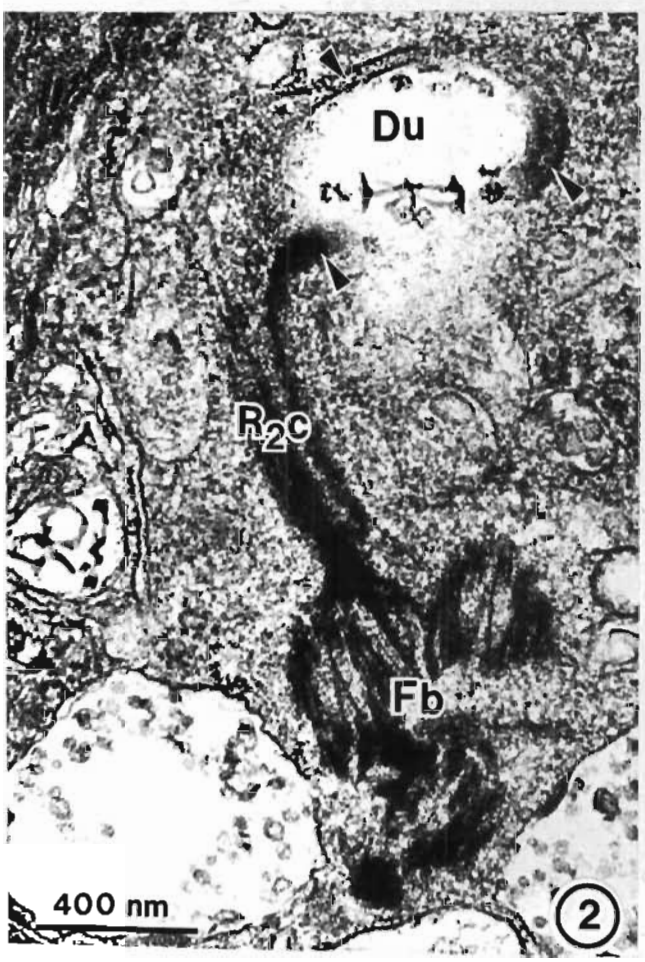
Du
R2C
Fb
400 nm
2


Du
Fb
400 nm
3

PLATE 7.7

Comparison of an l-cell and t-cell, origin of lipid globules.

Fig. 1 A micrograph showing an l-cell (LC) and t-cell (TC) in transverse section. Note the size difference between the two cell types. The l-cell has much starch (S) and lipid (L) storage material not seen in the t-cell.

Figs. 2-6 Micrographs showing the development of lipid globules.

Figs. 2 and 3. Early in the development of the lipid globule many spheroidal particles were seen to accumulate within a vesicle.

Fig. 4 As the spheroidal particles fused the first sign of lipid (L) deposition was seen.

Fig. 5 An almost mature lipid globule containing much lipid (L) material. The lipid was osmiophilic and stained densely.

Fig. 6 A mature lipid globule (L) surrounded by endoplasmic reticulum (Er).


L
S
S
LC
TC
3 µm
1

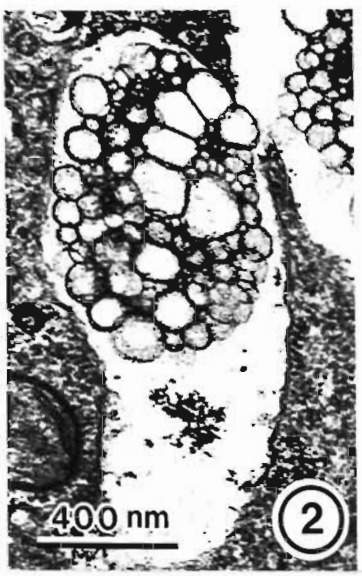
400 nm
2


400 nm
3

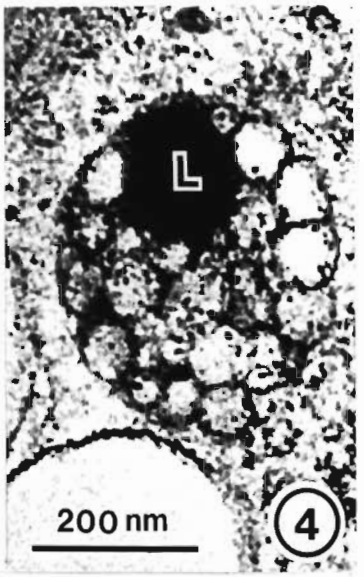
L
200 nm
4

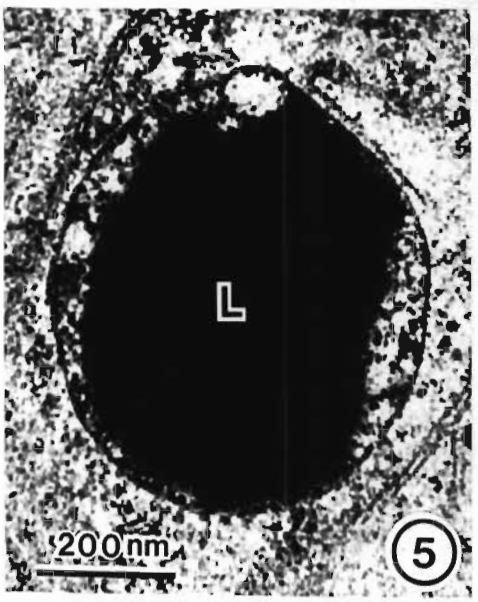
L
200 nm
5

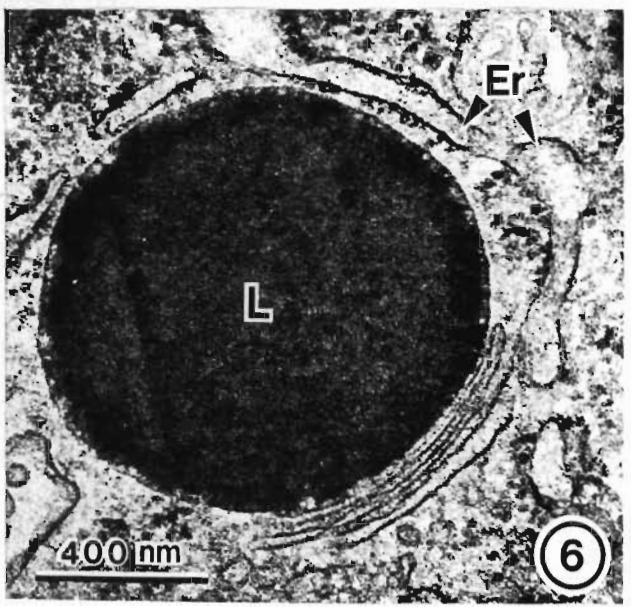
Er
L
400 nm
6

PLATE 7.8

Cell division in l-cells

Fig. 1 A longitudinal section through a dividing l-cell. The chloroplast (C) has divided and cleaved the pyrenoid (P). The base of the flagellar pit (Fp) has broadened to accommodate the replicated flagellar basal bodies.

Fig. 2 A transverse section through the anterior region of a dividing l-cell. The flagellar pit has eight flagellar profiles (F). The cell has only two dictyosomes (D) at this stage.

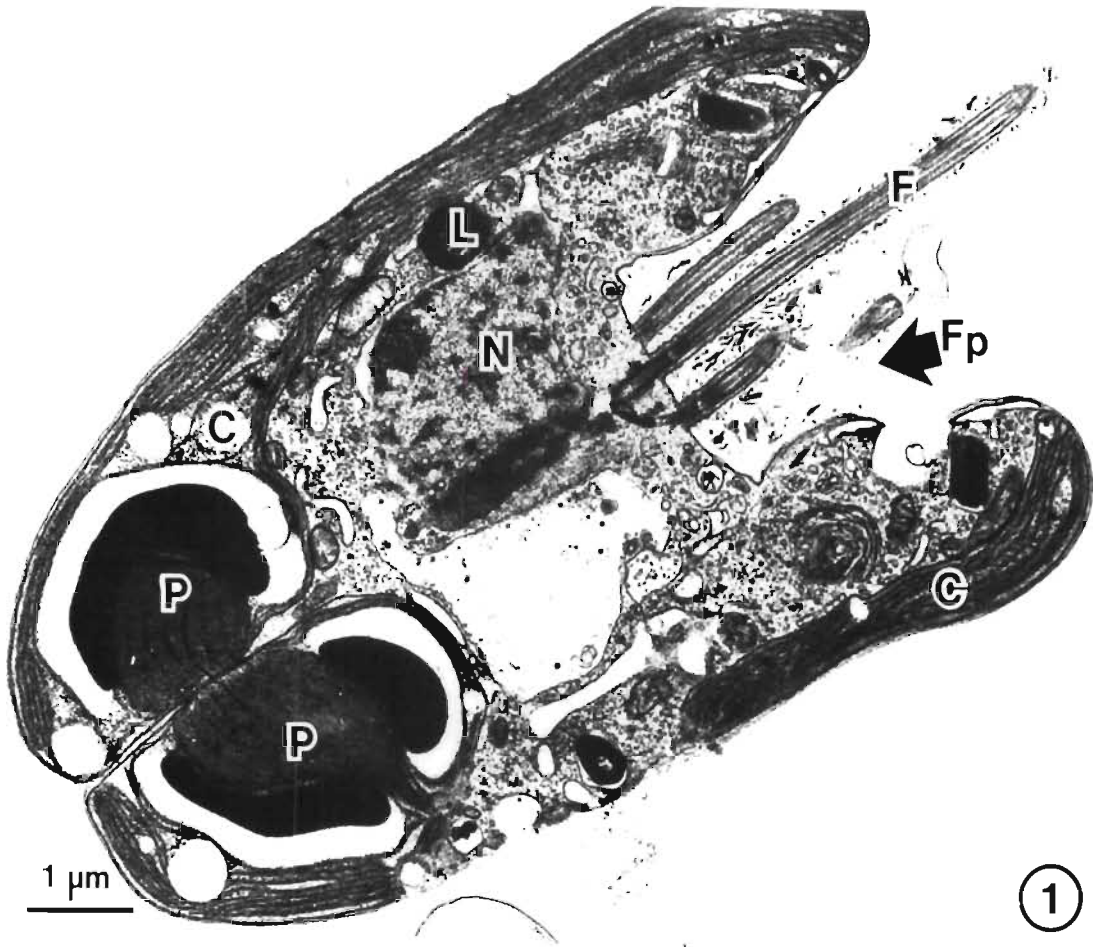

1

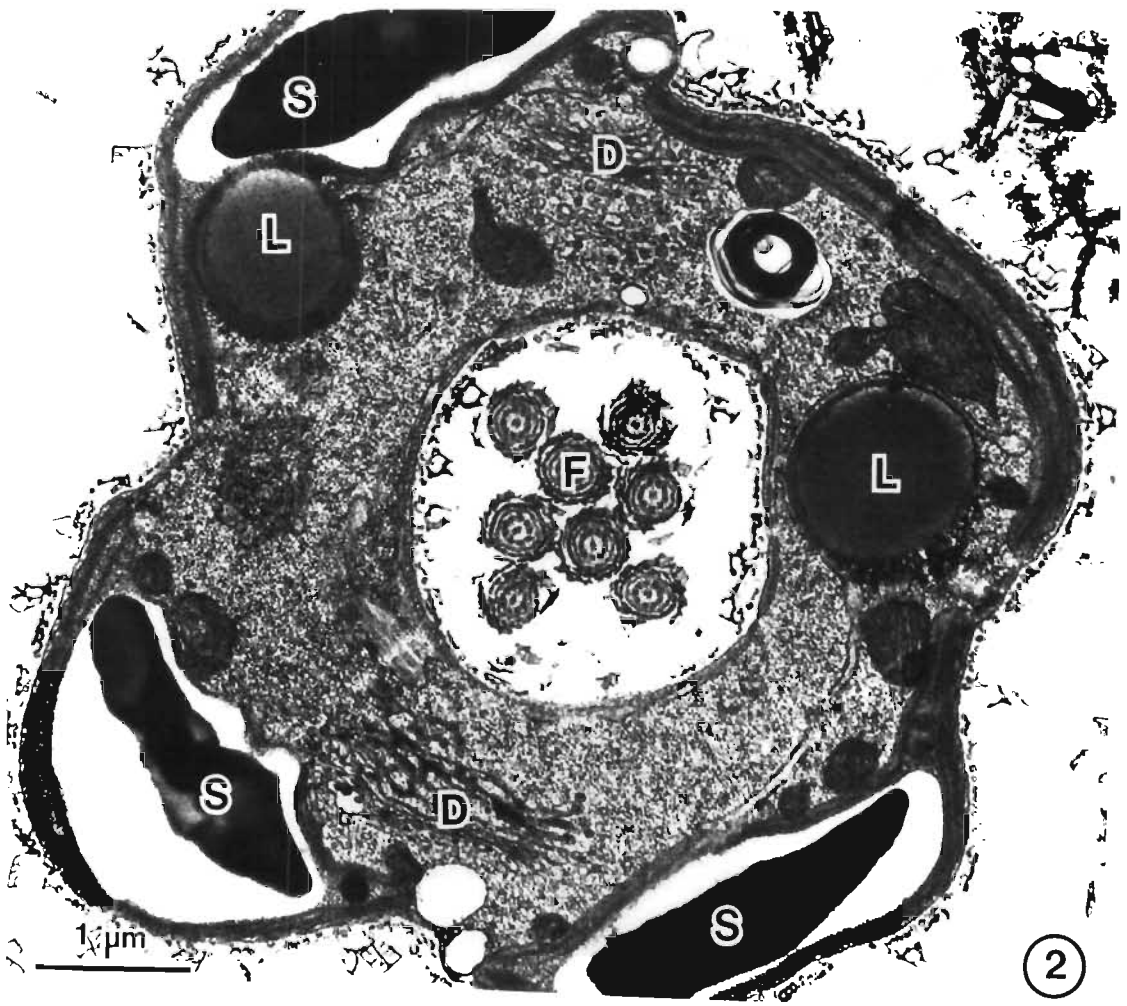

2

PLATE 7.9

Cell division in l-cells

Fig. 1 A section through the anterior region of an l-cell that is undergoing cytokinesis. The two flagellar pits (Fp) have become separated and two lateral cleavage furrows (arrows) are well developed.

Figs. 2 and 3. A transverse section through a dividing l-cell showing the two telophase nuclei (N). Spindle microtubules are not seen between daughter nuclei at telophase (Fig. 3).

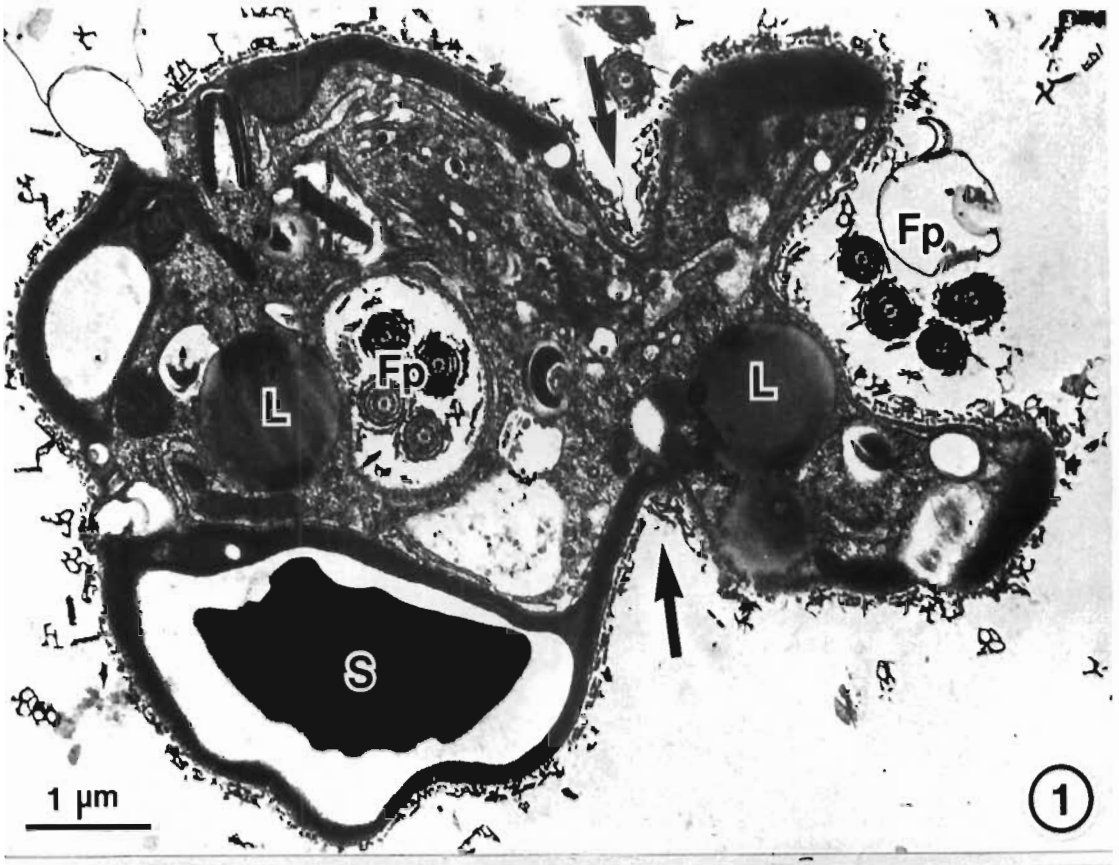
Fp
L
Fp
L
S
1 µm
1

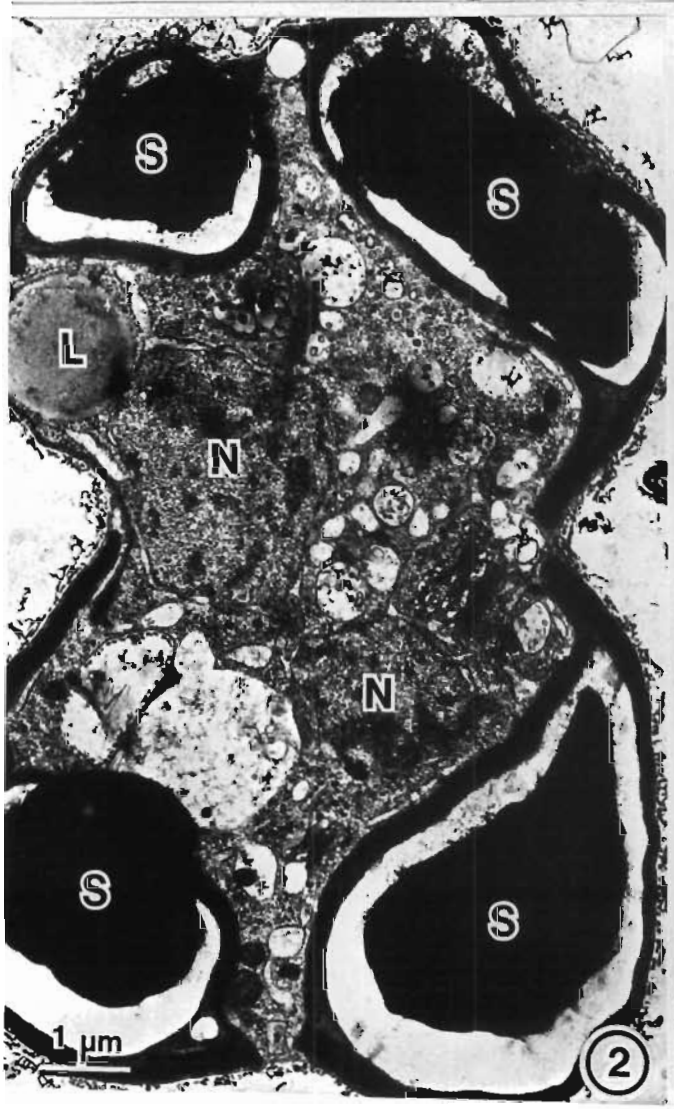
S
S
L
N
N
S
S
1 µm
2

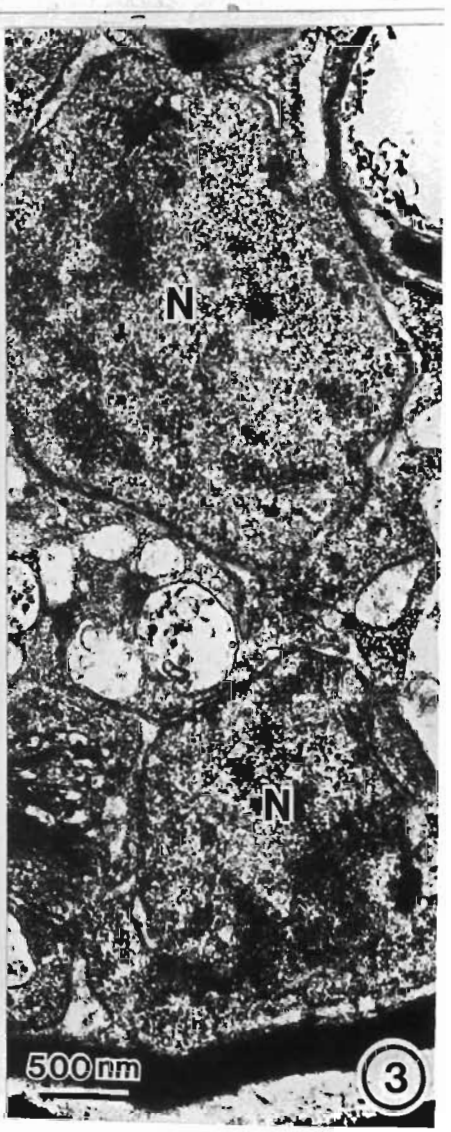
N
N
500 nm
3

PLATE 7.10

The mature l-cell

Fig. 1 A longitudinal section through a mature l-cell. Although the cell has lost its flagella, it is still called an l-cell because it is covered with a scale boundary. When the cell wall begins to be deposited the cell could be called an immature cyst. The l-cell depicted here has large reserves of starch (S) and lipid (L). The scale reservoir (Sr) and vacuole (V) are seen within the cytoplasm.

Fig. 2 A detailed view of the scale reservoir (Sr) shown in Fig. l. In the mature l-cell both body and flagellar scales are stored in the scale reservoir. The vacuole (V) and scale reservoir are separated by a thin cytoplasmic partition.

Fig. 3 A section through an immature cyst showing scales, and trichocyst and membrane fragments in vesicles within the cytoplasm. At this stage it is very difficult to distinguish between the scale reservoir and vacuole because both organelles may accumulate scales.

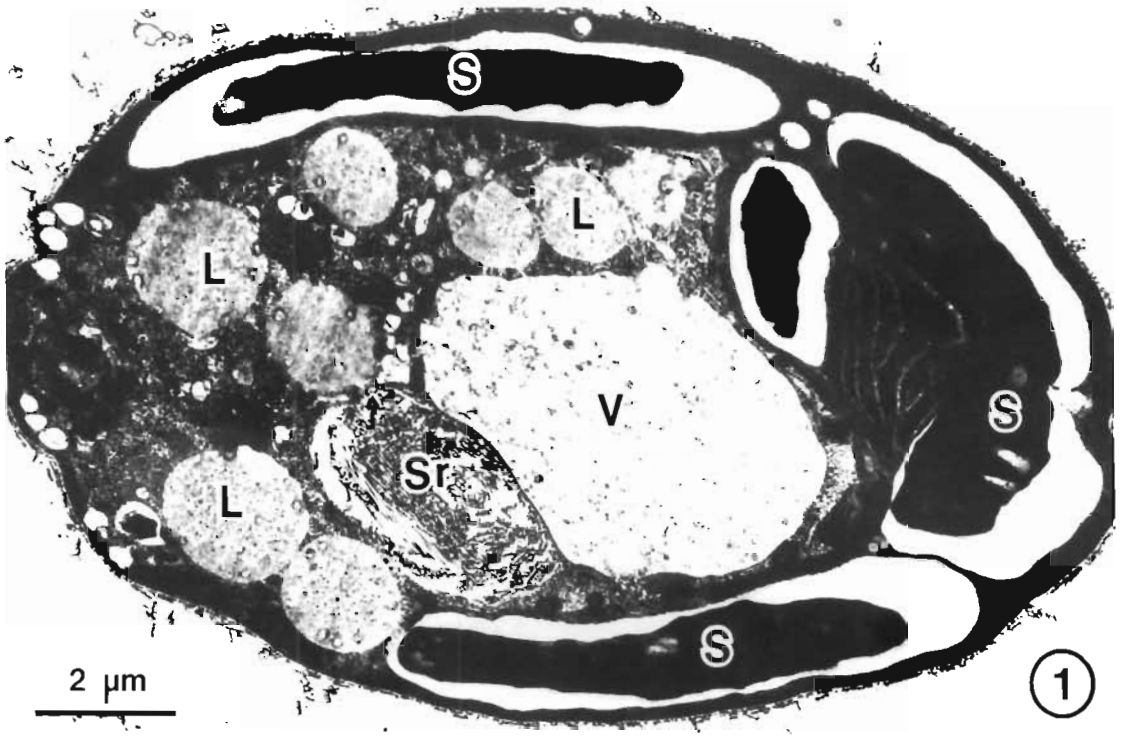
S
L
L
V
S
Sr
L
S
2 µm
1


V
Sr
500 nm
2


500 nm
3

PLATE 7.11

The immature cyst

Fig. 1 A section through an immature cyst. The cell has a single centrally situated nucleus (N). Four large starch grains (S) are seen in the chloroplast and numerous lipid globules (L) are packed into the cytoplasm. The immature cyst has a thin electron translucent cell wall.

Fig. 2 A section of the peripheral region of an immature cyst. An electron translucent cell wall layer (W_1) is deposited beneath the scales (Sc) in the scale-boundary. Scales are soon lost from the surface of the cell.

Fig. 3 Bacteria (B) are often seen attached to the cell wall (W_1). Bacteria may be partly responsible for removing scales once the deposition of the cell wall begins.

Fig. 4 A section through a bacterium (B) with many scales attached to its outer surface.

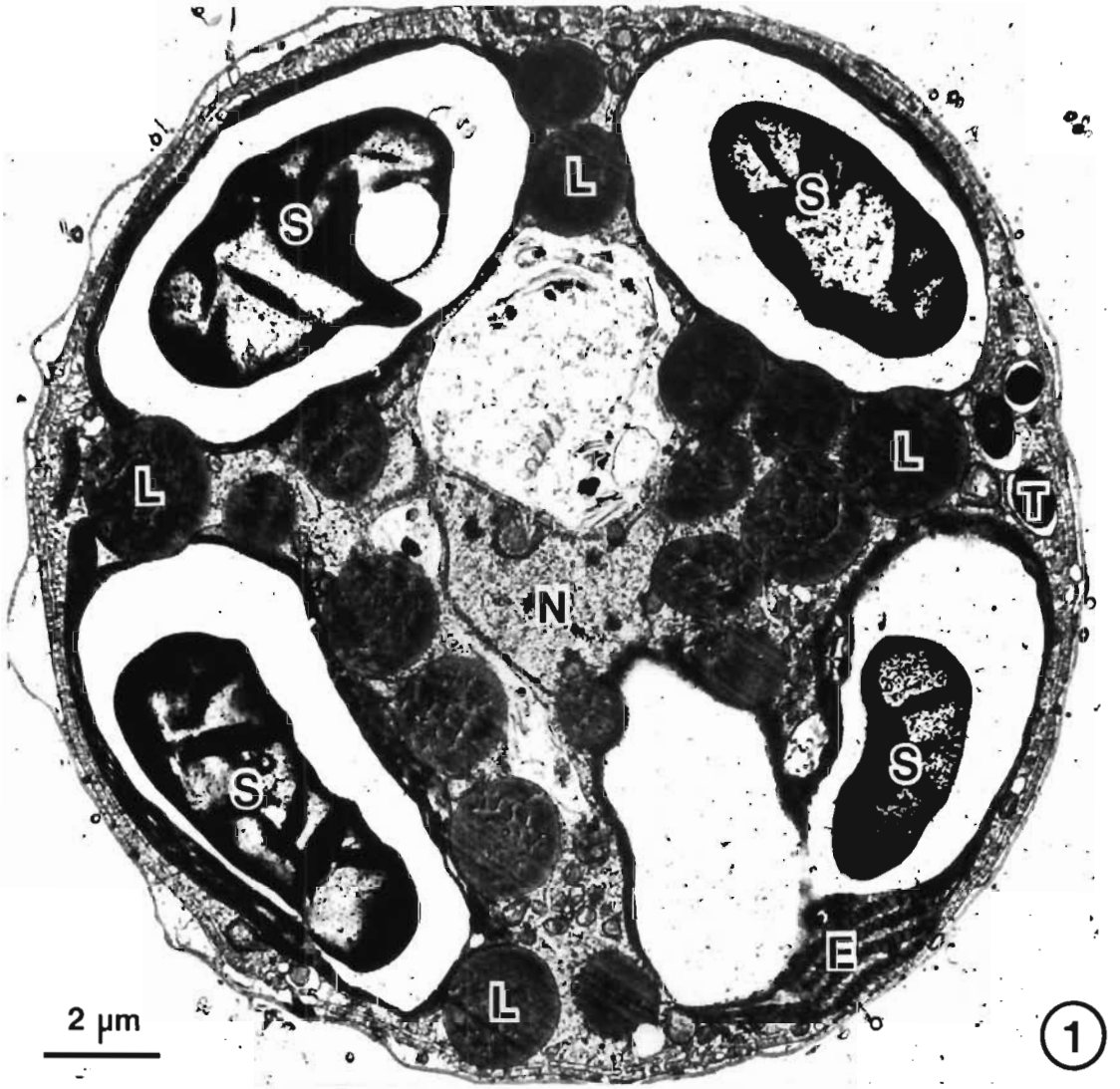
S
L
S
L
T
L
N
S
S
E
L
2 µm
1

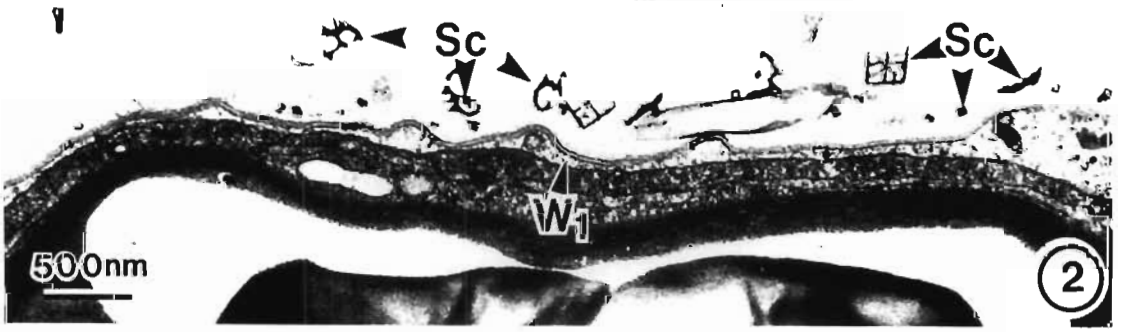
Sc
Sc
W1
500nm
2

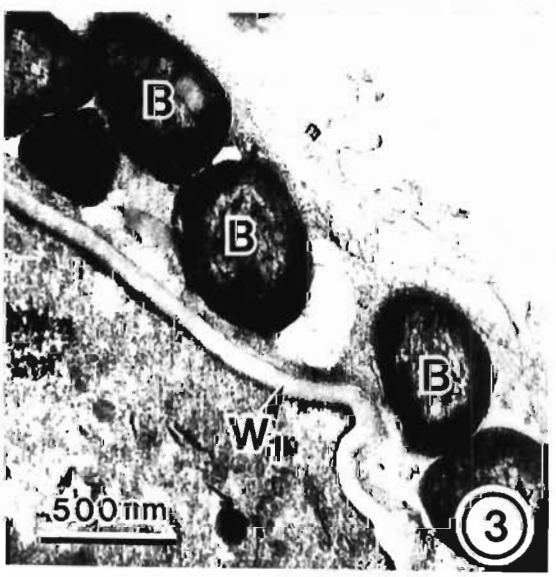
B
B
B
W1
500nm
3

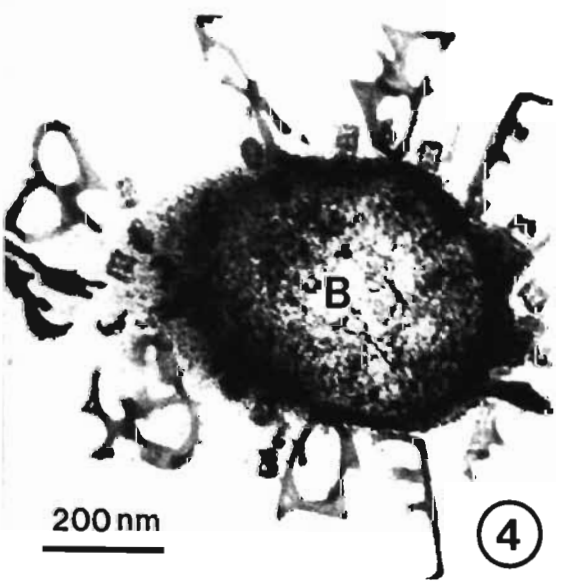
B
200nm
4

PLATE 7.12

Cell wall deposition

Fig. 1 A section through an immature cyst. The first layer of the cyst wall (W_1) has been deposited. A peripheral network of endoplasmic reticulum (Er) is always present beneath the plasmalemma throughout cell wall deposition. A dictyosome (D), which is seen associated with the Er, may be playing a role in synthesizing cell wall material.

Figs. 2 and 3. Following the deposition of the electron translucent layer of the cell wall an electron dense inner cell wall layer (open arrows) is deposited. At this stage the dictyosomes (D) release vesicles with dense contents (arrowheads).

Fig. 4 A section of the cyst wall showing the electron translucent outer layer (W_1) and electron dense inner layer W_2). In this preparation the innermost layer of the W_2 wall layer has delaminated (open arrows).

Fig. 5 A section of the cell wall of a mature cyst. The outer layer of the cyst wall (W_1) has small irregularly arranged projections (open arrow). The inner layer of the cyst wall (W_2) is often thickened in places (asterisk).

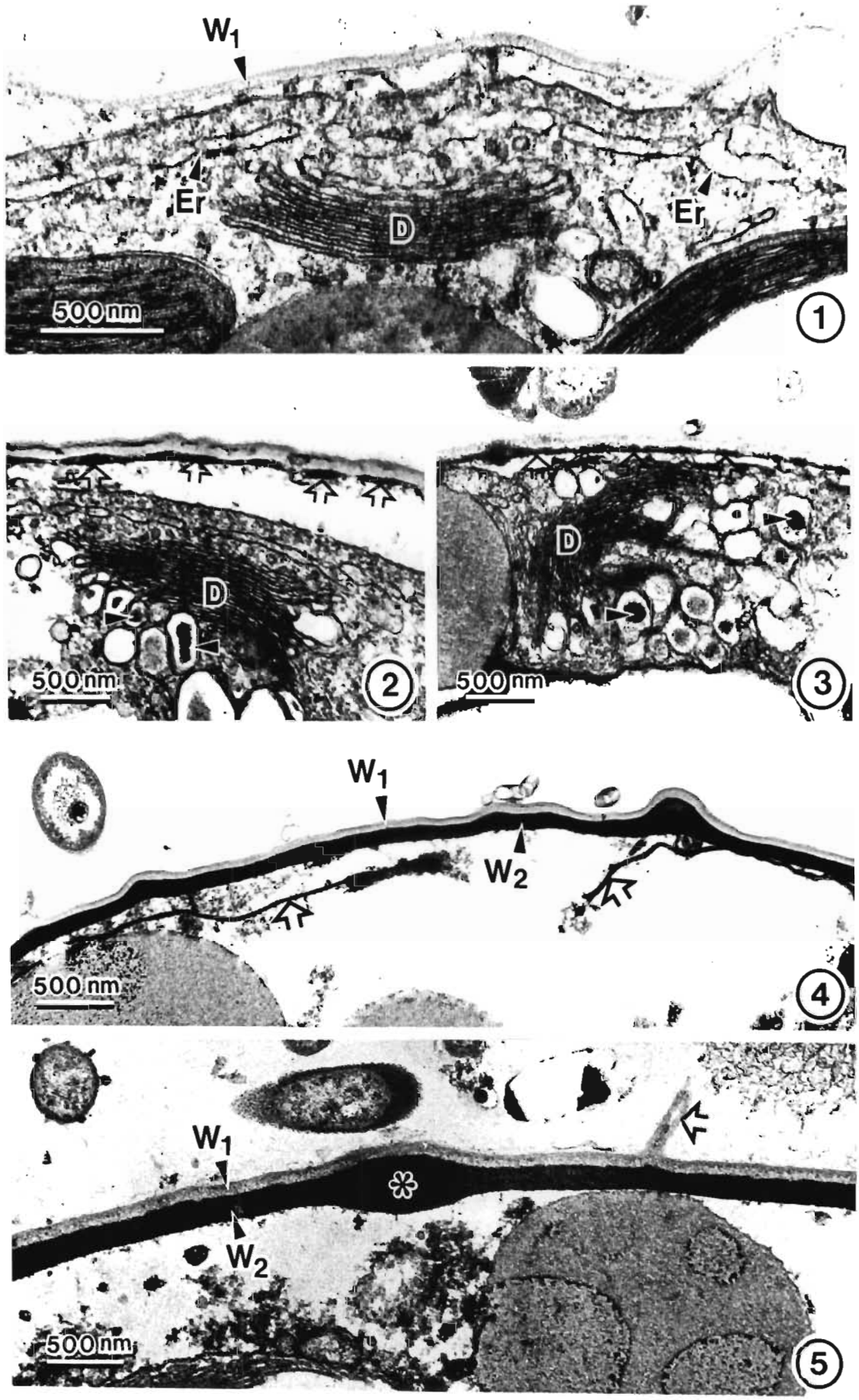
W1
Er
D
Er
500 nm
1
D
500 nm
2
D
500 nm
3
W1
W2
500 nm
4
W1
W2
500 nm
5

PLATE 7.13

The mature cyst.

Fig. 1 A section of a mature cyst showing the thick cell wall (W). The cell has much lipid (L) and starch (S) storage material. A single nucleus (N) is present in the cytoplasm and is associated with the rhizoplast/microbody (arrow).

Fig. 2 A detailed view of the nucleus (N), microbody (Mb) and rhizoplast (arrow) complex present in the cell shown in Fig. 1.

Fig. 3 The flagellar basal bodies (Fb) and rhizoplast (Rh) persist in the non-motile cyst.

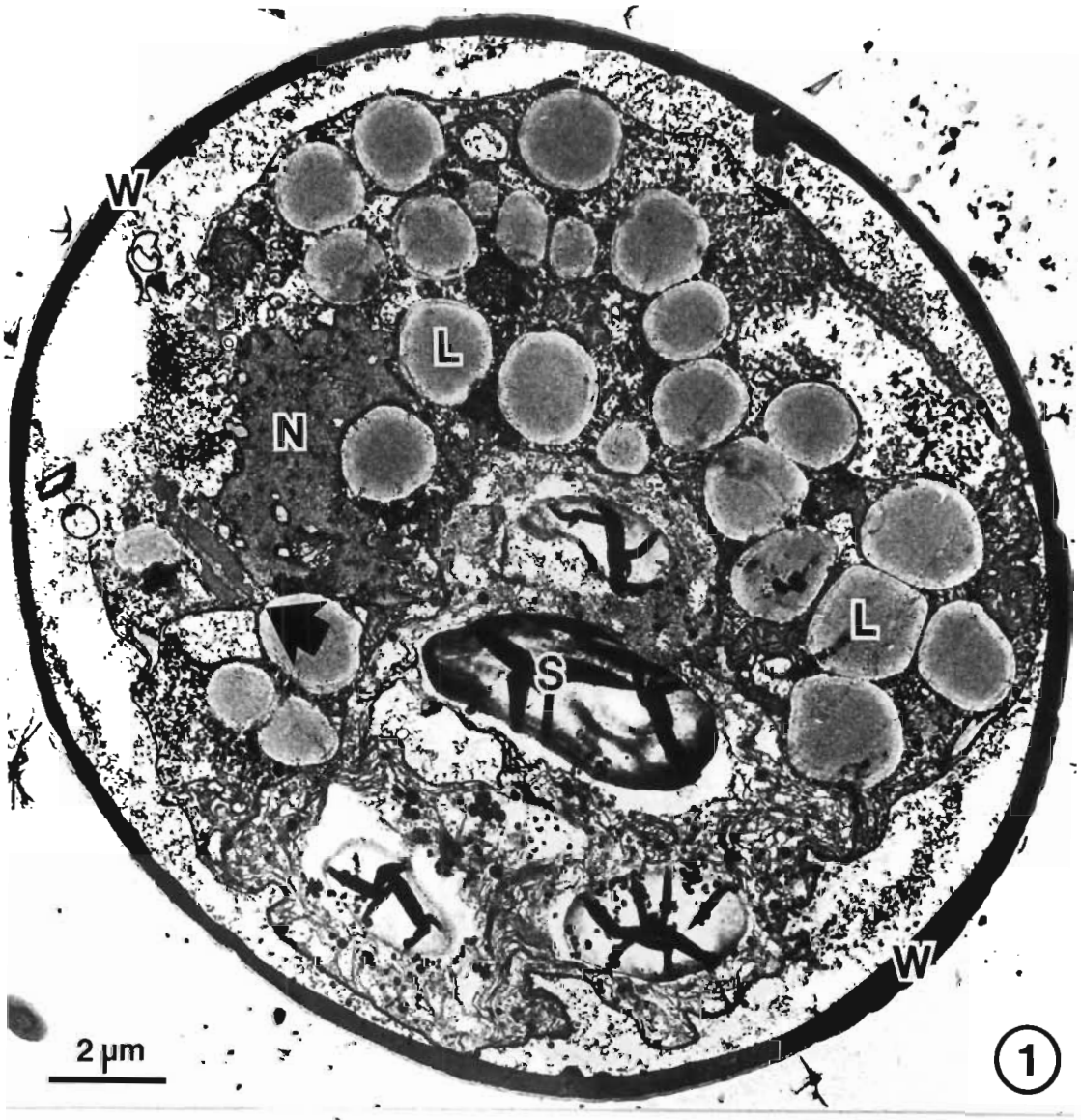
W
L
N
L
S
W
2 µm
1

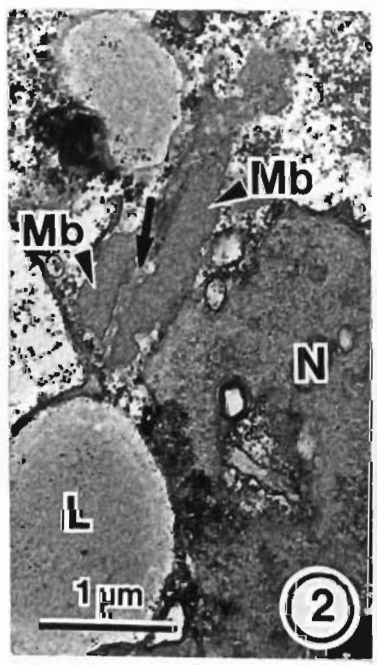
Mb
Mb
N
L
1 µm
2

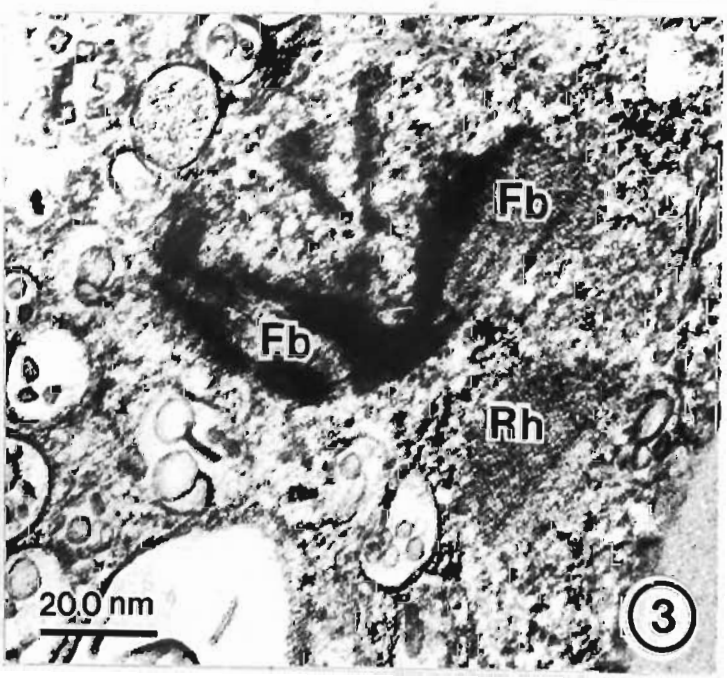
Fb
Fb
Rh
20,0 nm
3

PLATE 7 .14

Structure of buoyant cysts

Fig. 1 A section through a germinating cyst. The thylakoids within the chloroplast (C) of this cell were unusual in that they were dilated. This cell was buoyant and had settled at the air/medium interface on the side of a culture vessel. The chloroplast of this germinating cyst had recently divided (arrowheads).

Figs. 2 and 3. Sections through the peripheral regions of an immature (Fig. 2) and mature (Fig. 3) cyst, showing the dilated thylakoids within the chloroplast (C).

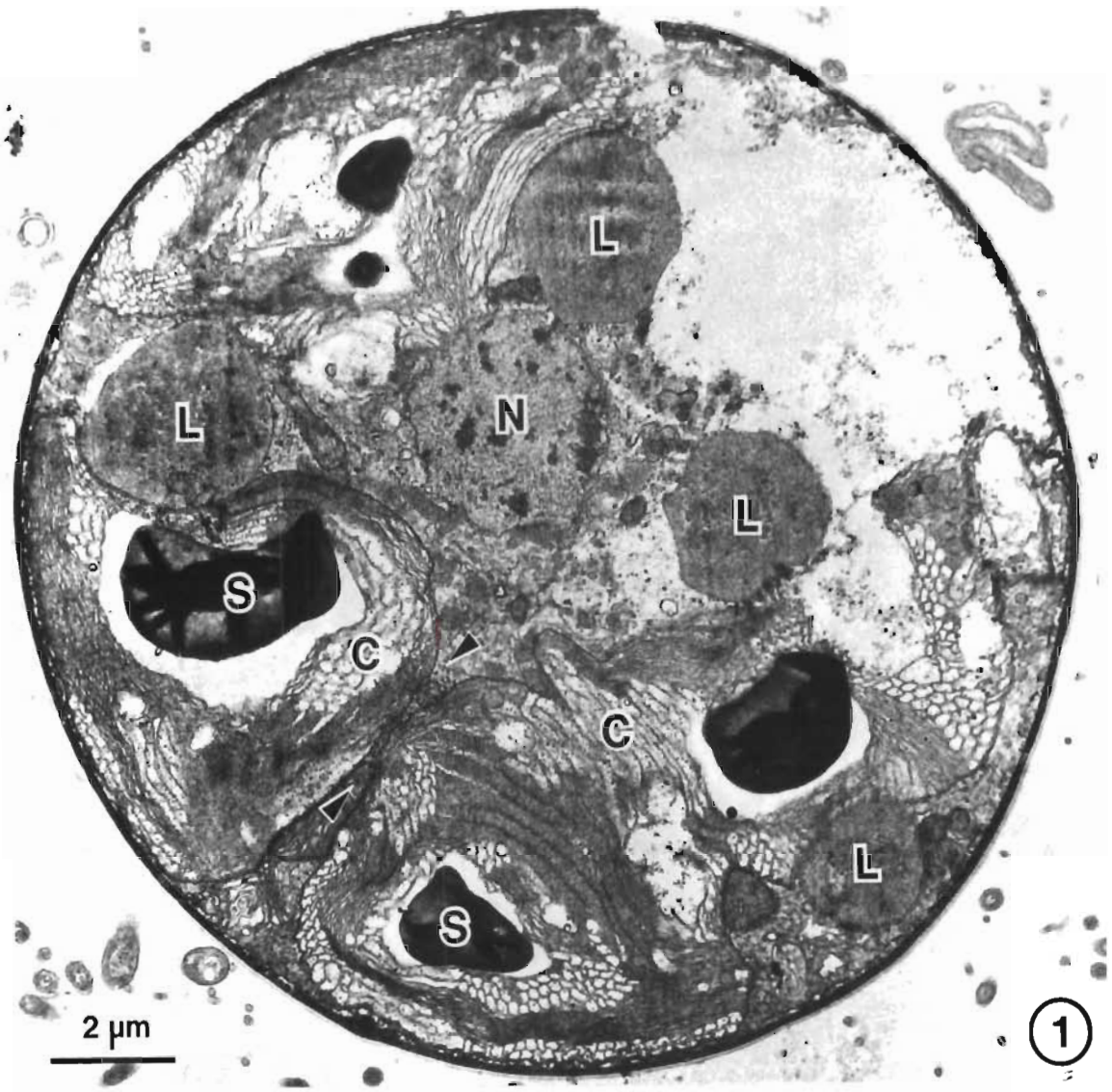
L
L
N
L
S
C
C
L
S
2 µm
1

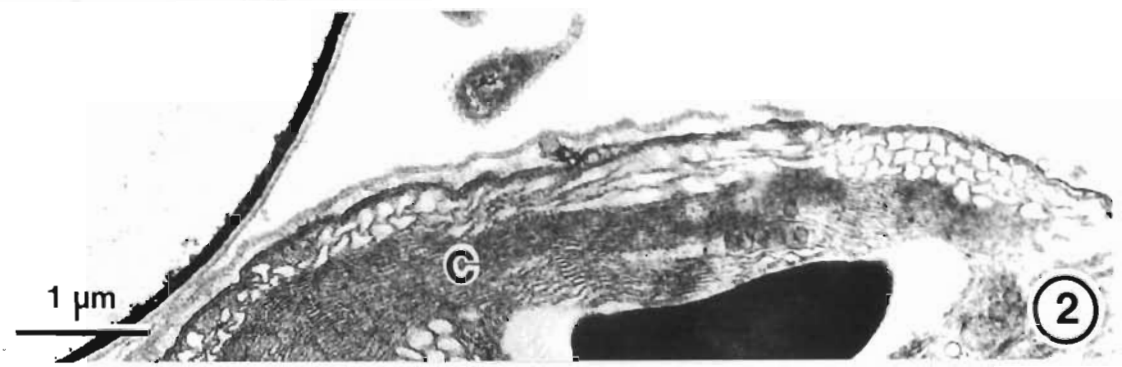
C
1 µm
2

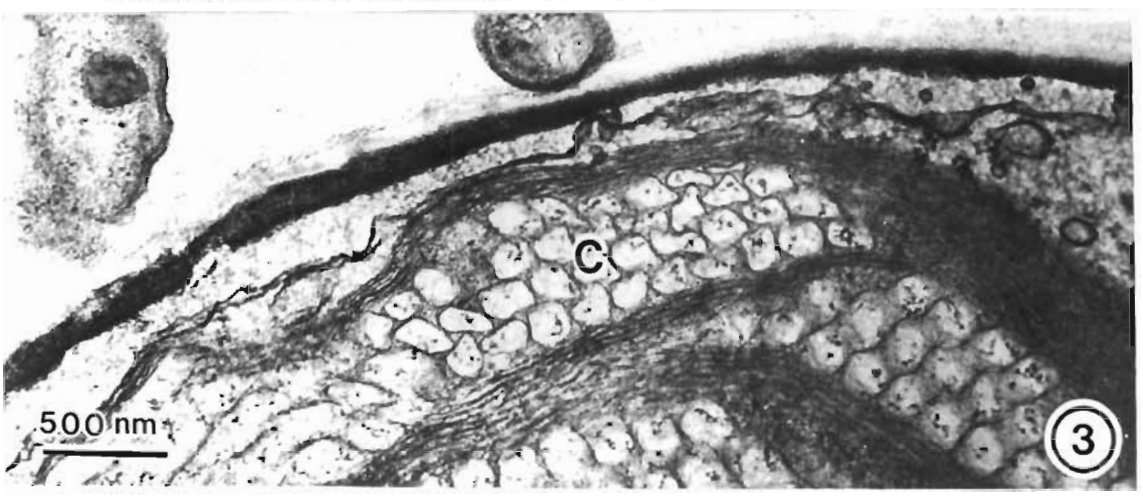
C
500 nm
3

PLATE 7.15

Cyst germination

Fig. 1 A section through a germinating cyst. The chloroplast (C) has begun to cleave (arrows). The cyst wall (W) is intact and the cell still contains much starch (S) and lipid (L) reserve material.

Fig. 2 A detailed view of the dividing chloroplast of the cell shown in Fig. 1. The chloroplast envelope develops an "anterior" and "posterior" invagination (arrowheads) in the region of the pyrenoid (P). A massive microbody (Mb) is associated with the "anterior" invagination of the chloroplast envelope.

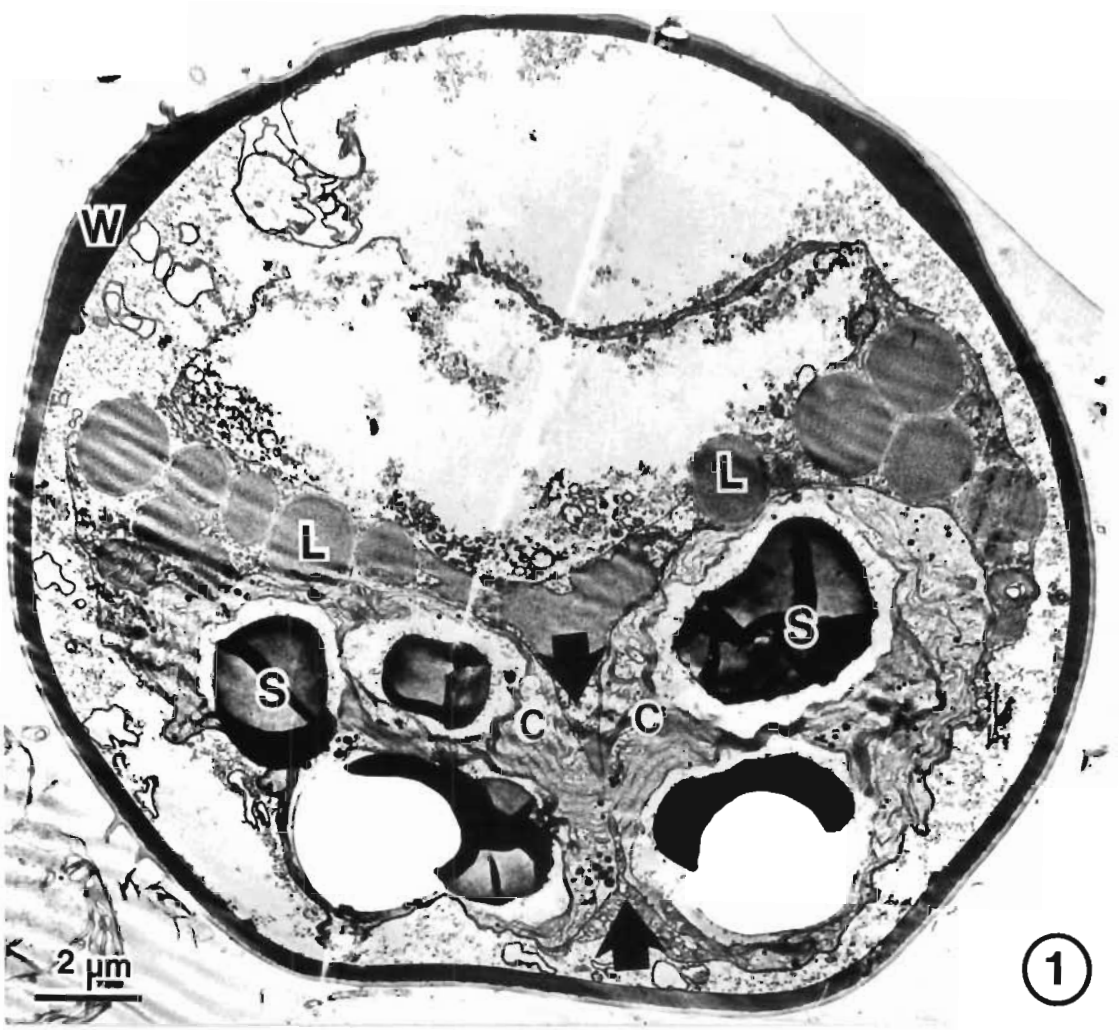

1

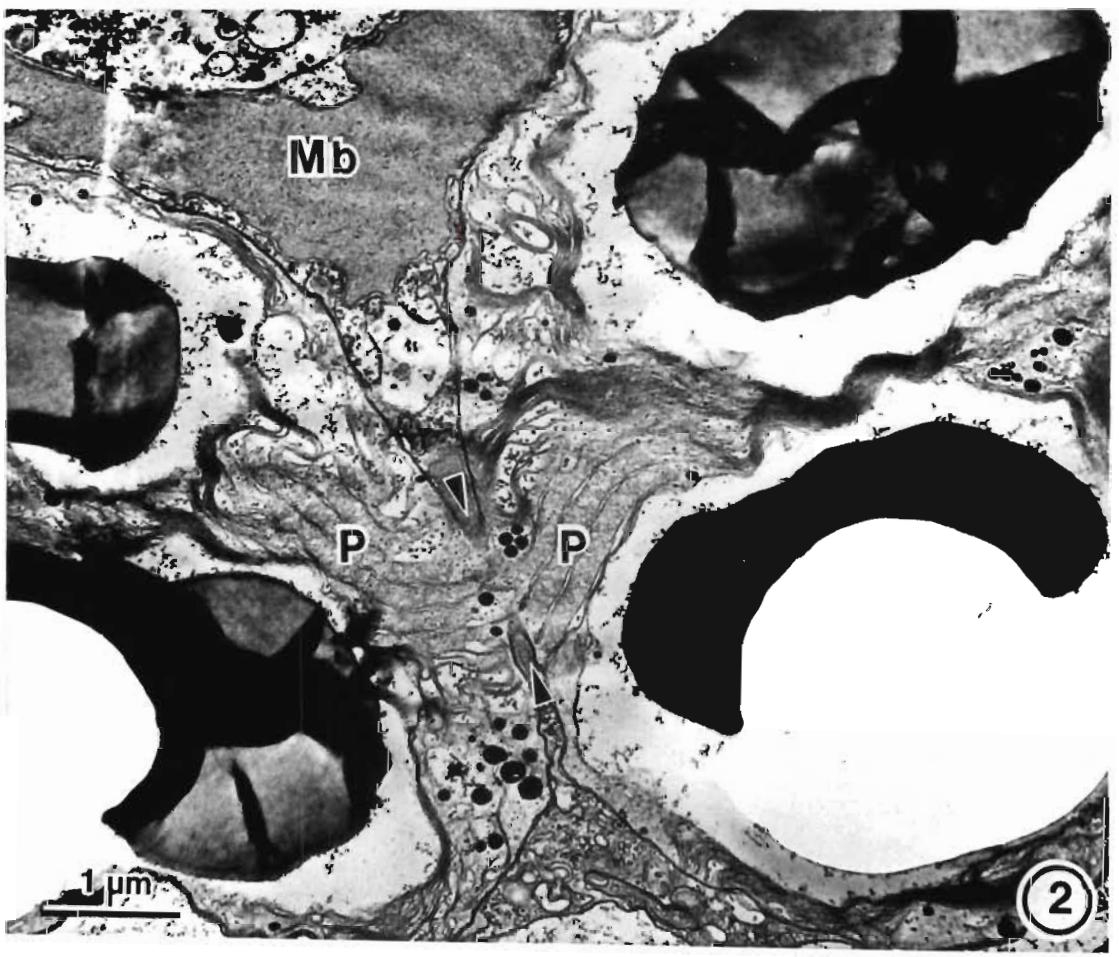

2

PLATE 7.16

Pleomorphic cells

Fig. 1 A longitudinal section through a pleomorphic cell. The chloroplast (C) has divided in the region of the pyrenoid (P). The nucleus has also divided so that two daughter nuclei (N) lie close to one another in the cytoplasm. The cell has not undergone cytokinesis and only a single flagellar pit (Fp) is seen at the anterior end of the cell.

Fig. 2 A longitudinal section through a "V" shaped pleomorphic cell. The nucleus (N) has divided and the flagellar pits (Fp) have become separated. Cytokinesis has been initiated and an anterior cleavage furrow (open arrow) is clearly visible. In dividing t-cells and l-cells telophase nuclei would only be seen when cytokinesis was almost completed. Cytokinesis has been arrested in the cell shown in this micrograph.

Fig. 3 A detailed view of the daughter nuclei (N) of the cell shown in Fig. 2. The spindle microtubules have collapsed and are not visible.

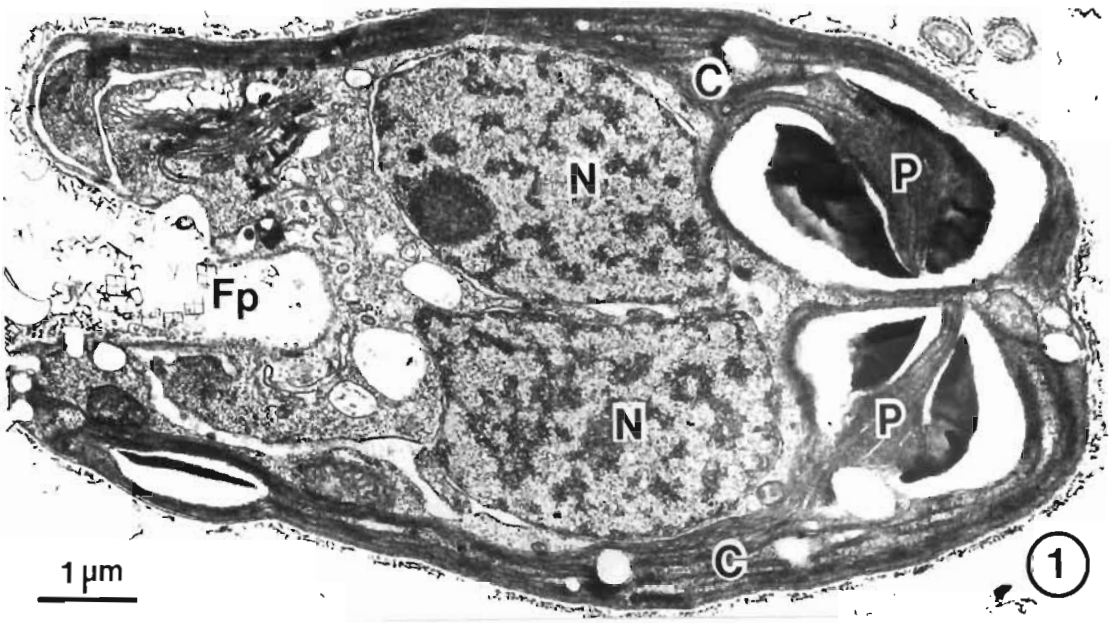
C
N
P
Fp
N
P
C
1 µm
1


Fp
Fp
N
N
2 µm
2

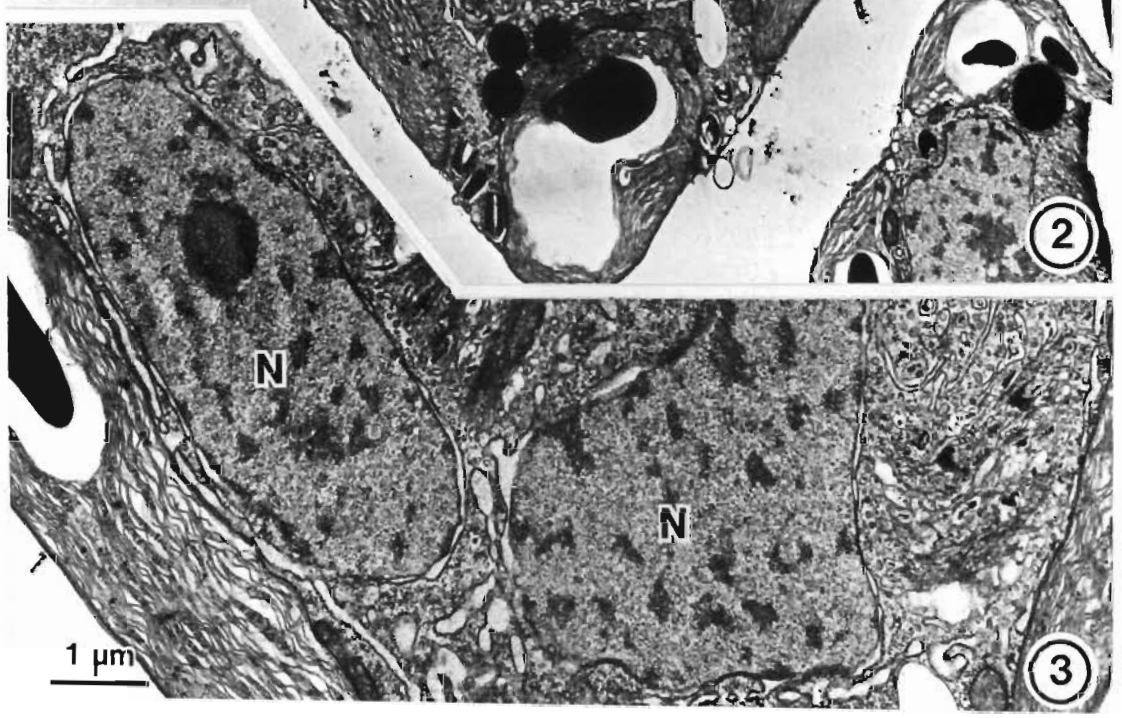
N
N
1 µm
3

PLATE 7.17

Pleomorphic cells

Fig. 1 A longitudinal section through a large bilobed pleomorphic cell. The cell has two nuclei (N), one in each lobe. Though the nucleus had divided and cytokinesis had progressed to give a "back-to-back" stage, the chloroplast had not divided and only a single pyrenoid (P) is present. The left lobe of the cell is markedly larger than that on the right.

Fig. 2 A section through a pleomorphic cell showing two widely separated flagellar pits (Fp). One flagellar pit contains eight flagella indicating that this lobe of the cell is undergoing a further division.

Fig. 3 A section through an irregularly shaped pleomorphic cell. This cell has four flagella in each of three separate flagellar pits (Fp). Two nuclei (N) are seen in this section. One nucleus is usually present in each lobe of the pleomorphic cell.

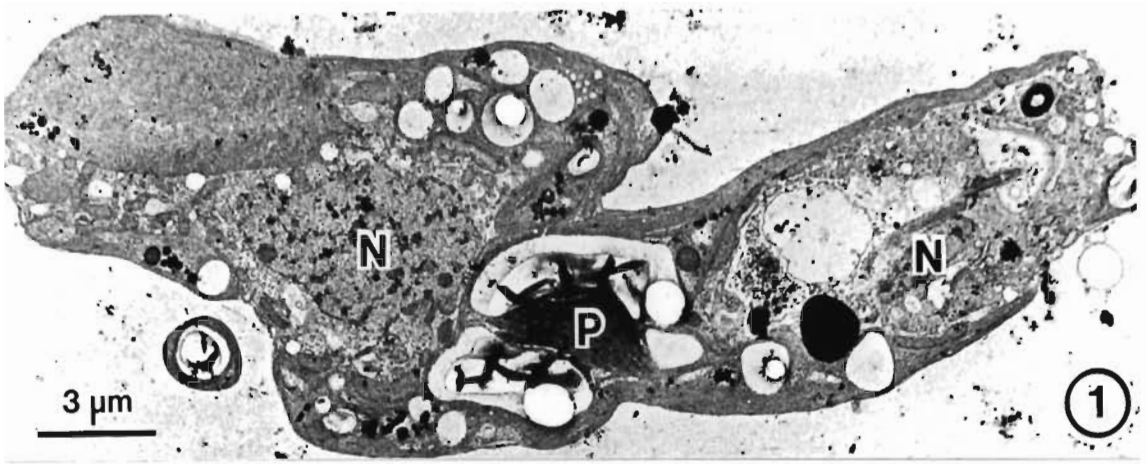
N
P
N
3 µm
1

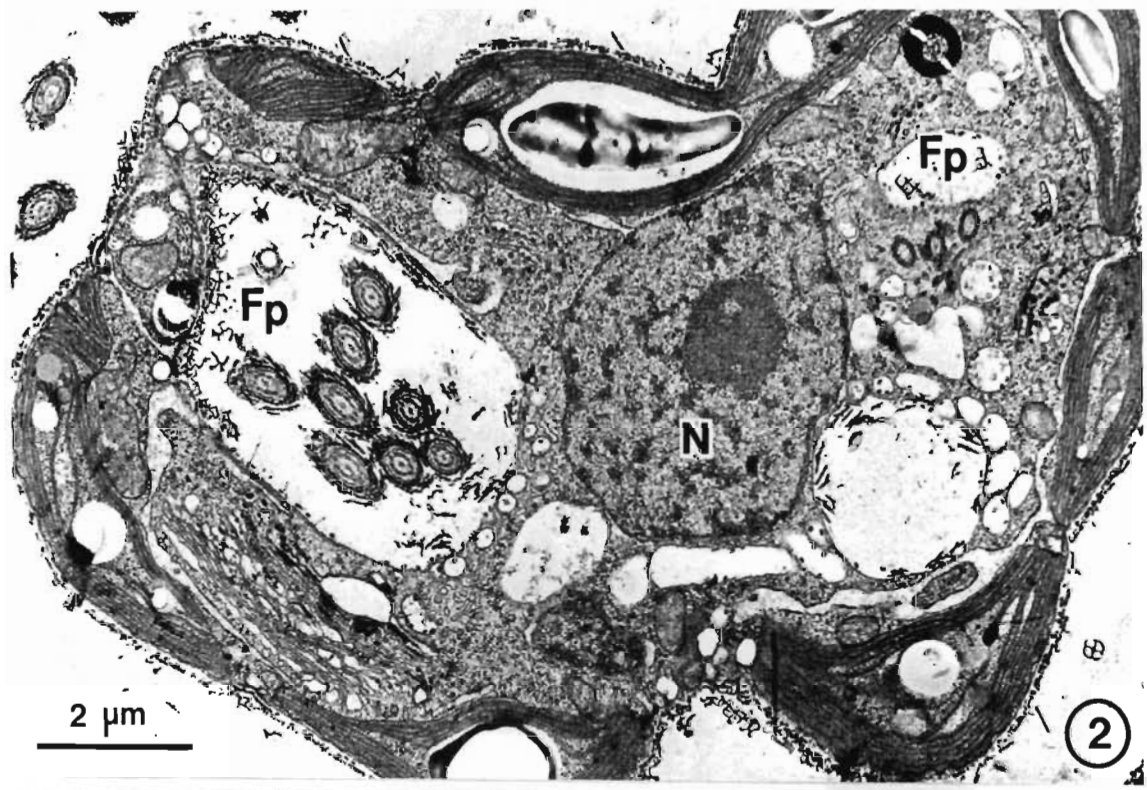
Fp
Fp
N
2 µm
2

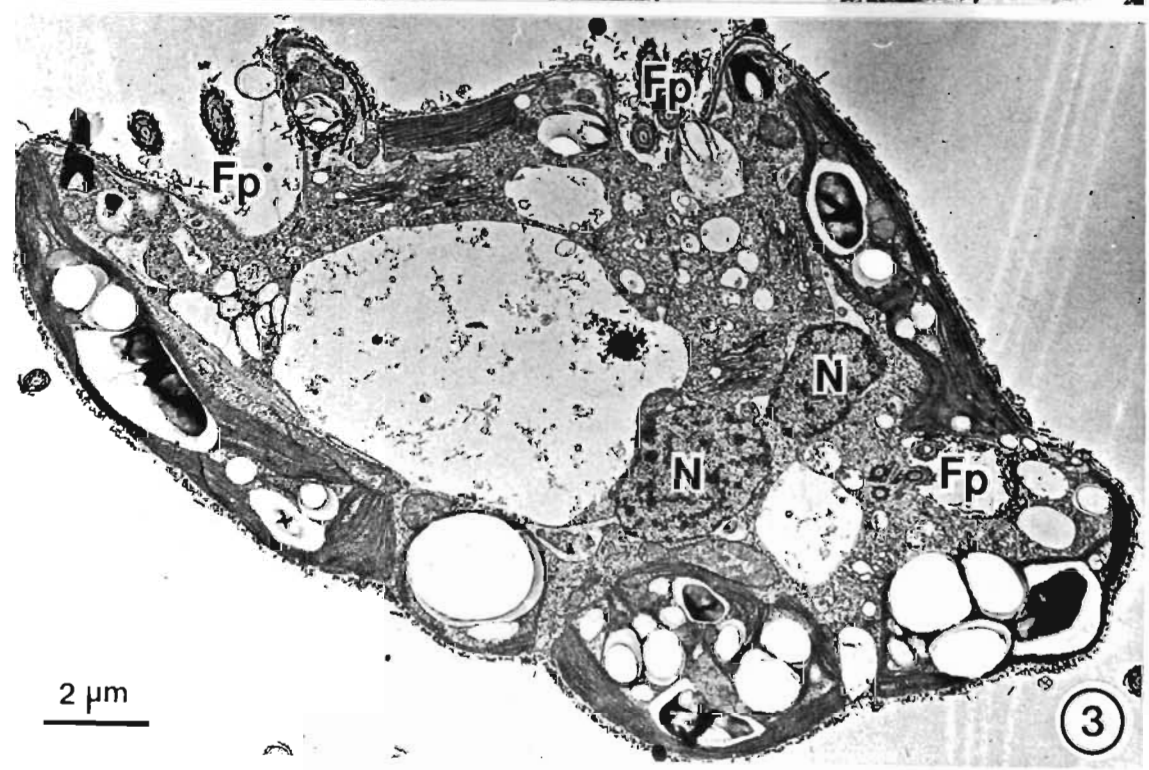
Fp
Fp
N
N
Fp
2 µm
3

PLATE 7.18

A pleomorphic cell with an unusual microbody

Fig. 1 A longitudinal section through a pleomorphic l-cell. The cell contains much starch (S) and lipid (L) reserve material. An unusual microbody is seen beneath the flagellar pit (arrow).

Fig. 2 A detailed view of the unusual microbody (Mb) of the cell shown in Fig. l. The microbody has stained densely and appears to coil around the rhizoplast (Rh) and flagellar basal body apparatus (Fba).

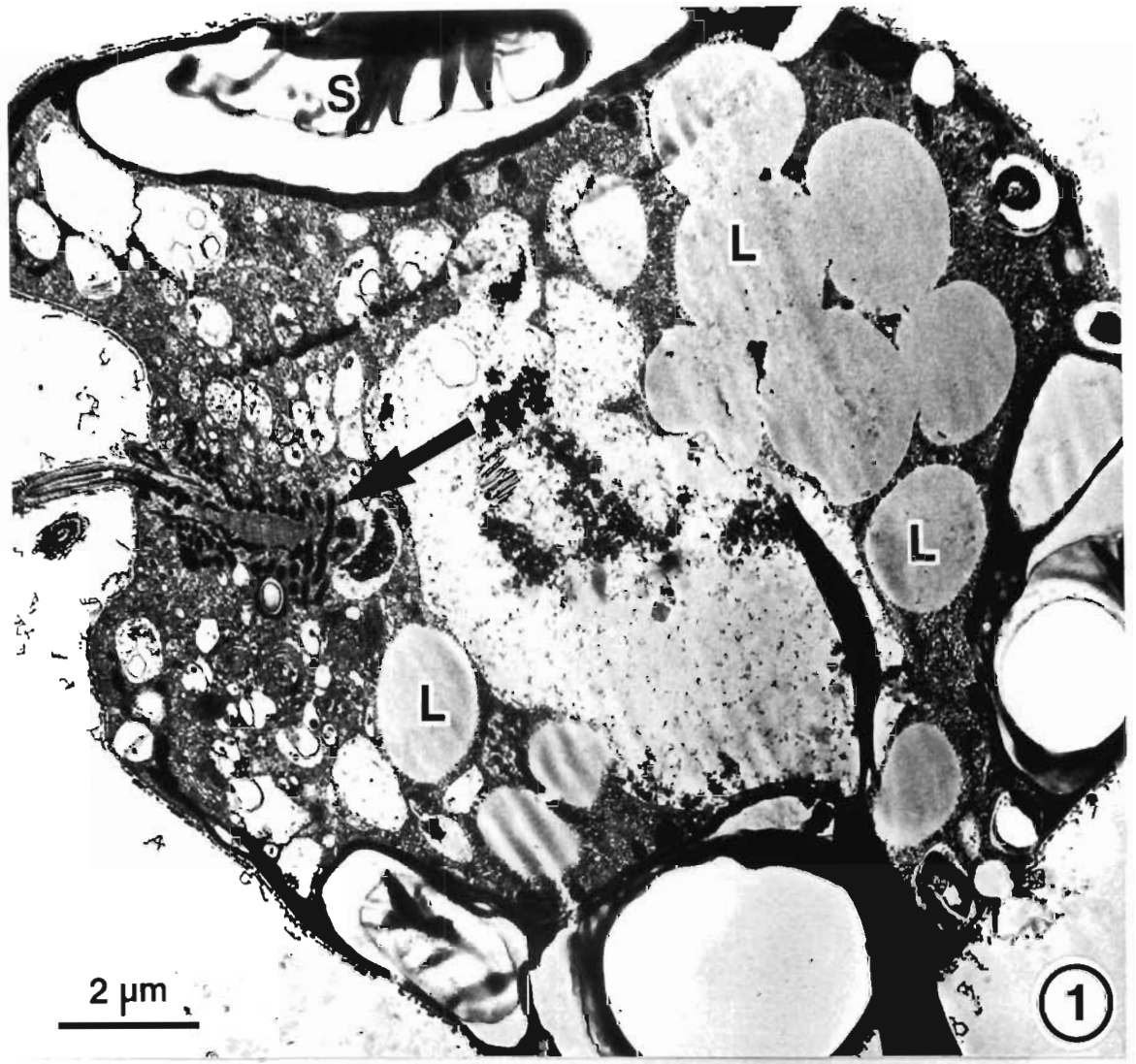
S
L
L
L
2 µm
1

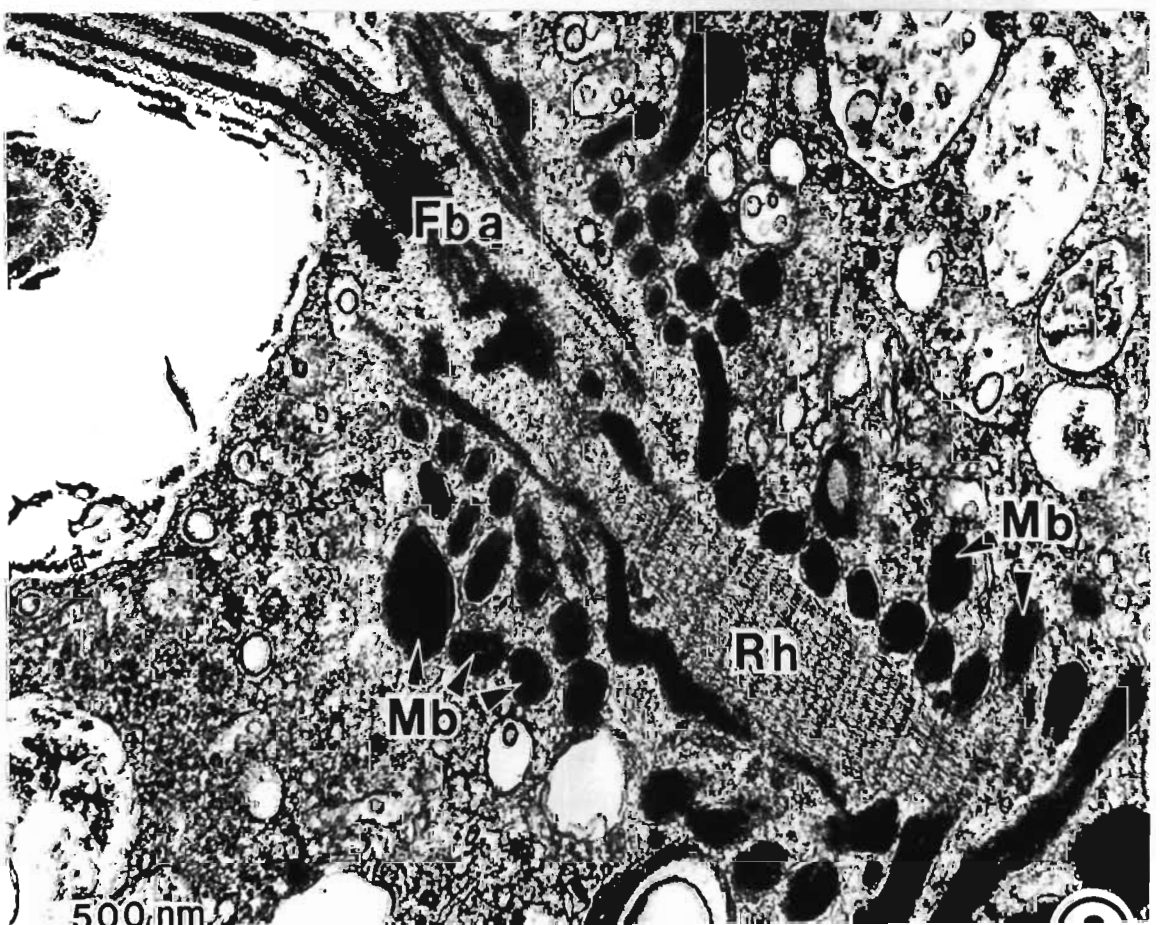
Fba
Mb
Rh
Mb
500 nm

PLATE 7.19

Chromosomes in t-cells and
l-cells

Scale bars on all micrographs = 2,5 µm.

(phase contrast microscopy)

Figs. 1-3 The chromosomes of t-cells. The light micrographs in Figs. 1 and 2 show the chromosomes of a t-cell taken from an actively growing culture. The chromosomes of this cell are illustrated in Fig. 3. It is estimated that the t-cell has 13 (± 1) chromosomes.

Figs. 4-7 The chromosomes of l-cells.
Two l-cells are shown in Fig. 4. The l-cell (LC) on the right contains starch (S) and lipid (L) storage material which obscures the nucleus. The l-cell on the left has well defined chromosomes within the nucleus (N) and it is this spread that was used to determine the chromosome number in l-cells. The nucleus in Figs. 5 and 6 shows the chromosomes as seen at two different focussing levels. The chromosomes of the l-cell are illustrated in Fig. 7. It is estimated that the l-cell has 13 (± 1) chromosomes.

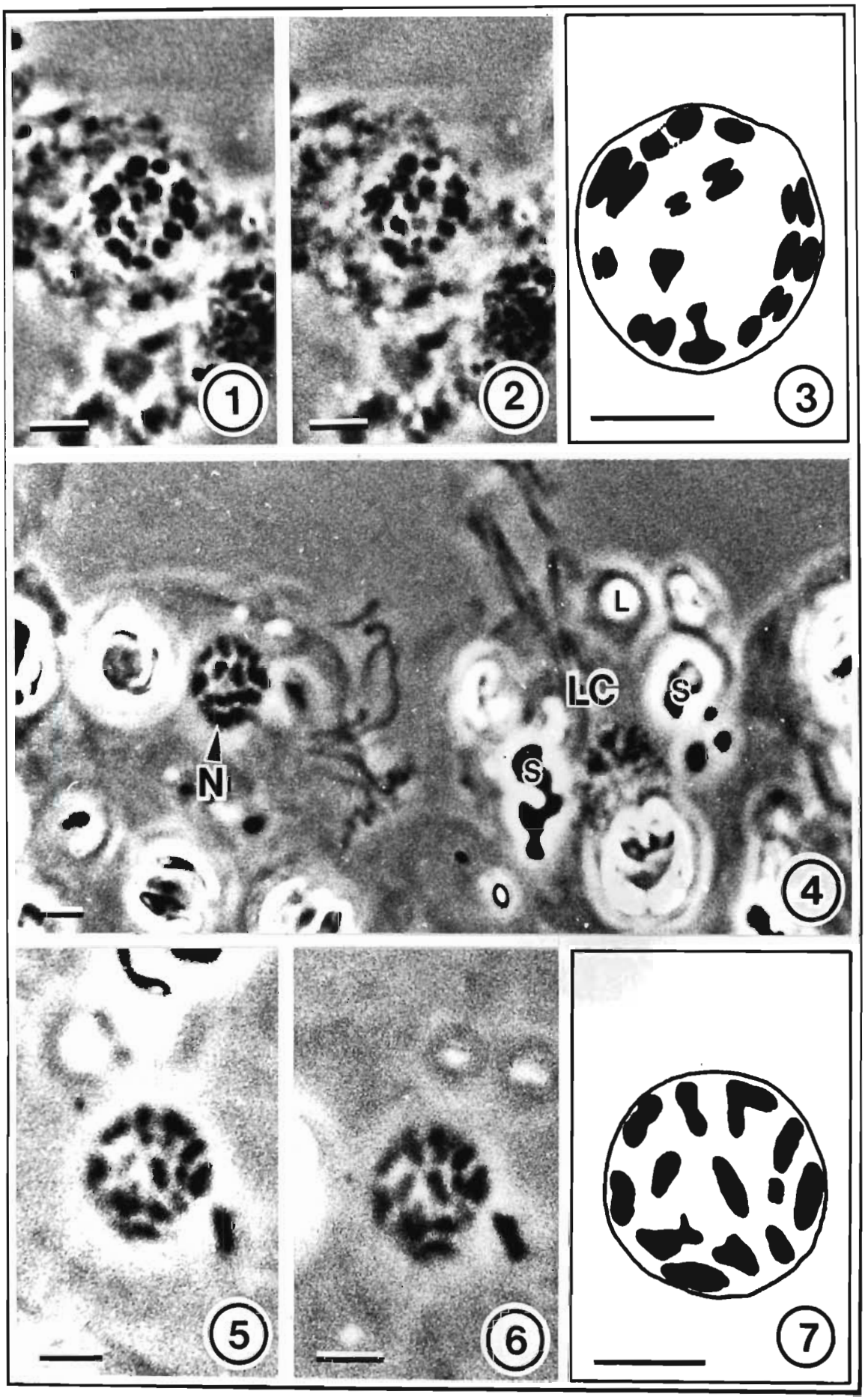
1
2
3
L
LC
S
S
N
O
4
5
6
7

PLATE 7.20

Histochemistry

Scale bars on all light micrographs = 10 µm.

(Figs. 1-3, 12-phase contrast; Figs. 4-8, 11 - bright field)

Figs. 1-3 Cells stained with Gram's iodine.
Fig. 1 shows an l-cell (LC) and t-cell (TC) stained with iodine. The l-cell is much more densely stained than the t-cell because it has large reserves of starch. L-cells usually have four large starch grains (S) in each of the chloroplast lobes (Figs. 2 and 3)

Fig. 4 An empty cyst casing which has stained positively with ruthenium red. This stain is used to localize pectic substances.

Figs. 5 and 6 The cyst wall of *P. pseudoparkeae* stains positively with alcian blue at pH 2,5 (Fig. 5) and pH 0,5 (Fig. 6). The fortuitous delamination of the two layers of the cyst wall (Figs 5 and 6) shows that only the inner wall layer reacts with the stain. A positive staining reaction with alcian blue at pH 0,5 indicates that the inner layer of the cyst wall is composed of a sulphate acidic polysaccharide.

Fig. 7 Cysts and cyst casings stained with Gram's iodine.
The starch grains within the cysts stained dark blue/purple while the cyst wall stained a pale straw colour.

Fig. 8 Encysted cells stained with sudan black B. The lipid material within the cells took up the stain. The cell wall stained a pale grey colour with sudan black B.

Figs. 9 and 10 *En bloc* staining of the cyst wall with ruthenium red. Where cysts were stained with ruthenium red (Fig. 10) the inner layer of the wall (W_2) appeared electron dense. In a control preparation (Fig. 9) the inner layer of the cyst was not as densely stained.

Fig. 11 The cyst wall did not stain after the cells were subjected to the Periodic acid/Schiff reaction. The starch grains within the cells were bright pink in colour thus indicating that the test had been successful.

Fig. 12 The remains of the cyst wall after acetolysis treatment.
The outer layer of the cyst wall, which remains after acetolysis, is thought to be composed of sporopollenin. The inner layer of the cyst wall was digested because no positive staining reaction was obtained with ruthenium red or alcian blue after acetolysis.

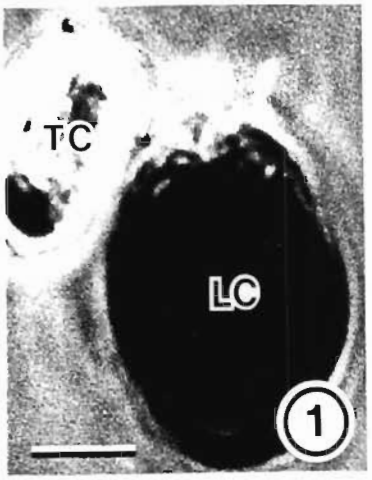
TC
LC
1

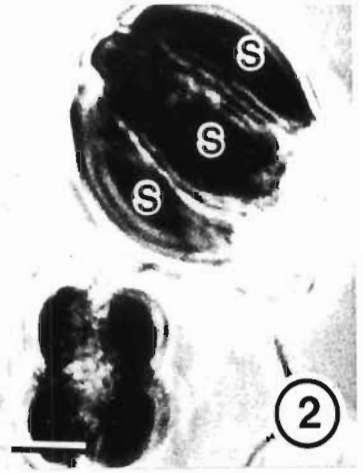
S
S
S
2

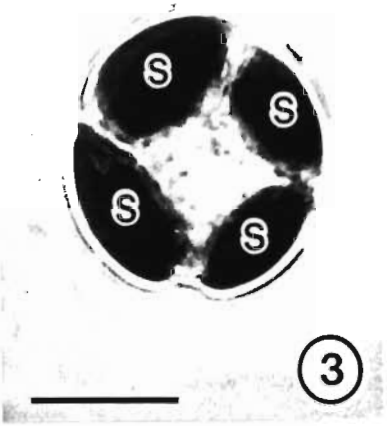
S
S
S
S
3


4

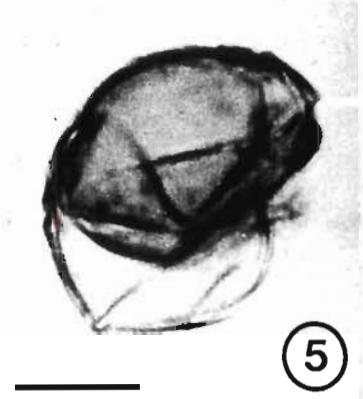
5


6

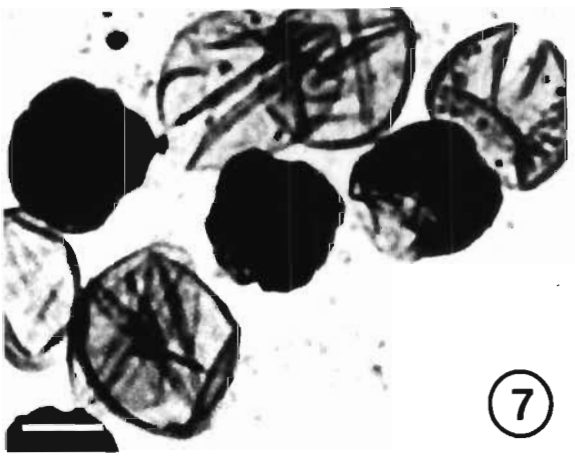
7

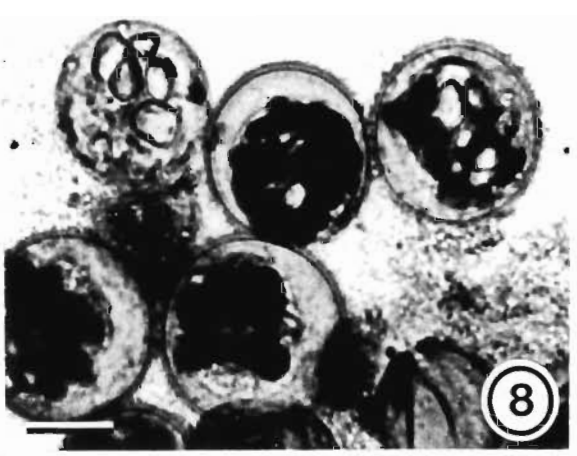
8

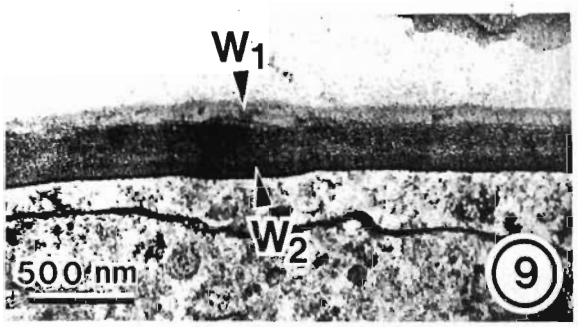
W1
W2
500 nm
9

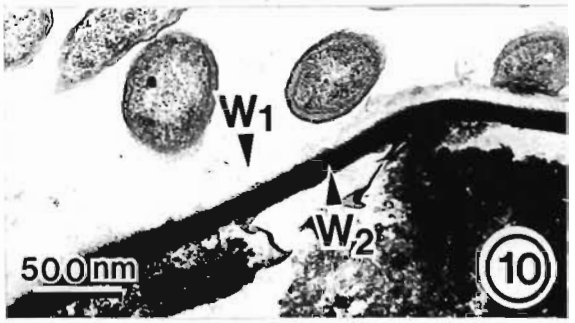
W1
W2
500 nm
10


11

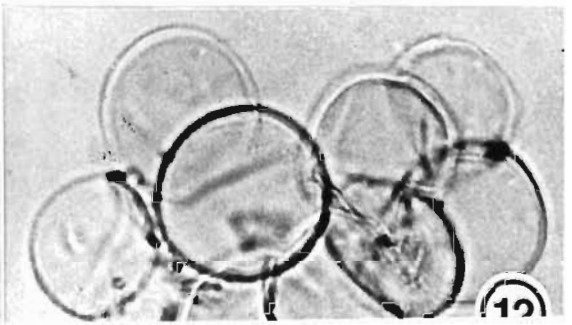
12

PLATE 7.21

The Gomori test for acid phosphatase activity in t-cells

Fig. 1 A transverse section through a t-cell subjected to the Gomori test. A positive Gomori reaction was obvious in the dictyosome (D) cisternae.

Fig. 2 A detailed view of a dictyosome (D) from the cell shown in Fig. 1. Dense deposits of lead phosphate in the cisternae, especially near the forming face, indicate that acid phosphatases are present in the dictyosome.

Fig. 3 A positive Gomori reaction was also seen in the outer regions of the chloroplast (C) and mitochondrion (M).

Fig. 4 A section of the chloroplast (C) of a t-cell showing the deposits of lead phosphate (arrowheads) in the outer regions of the chloroplast.

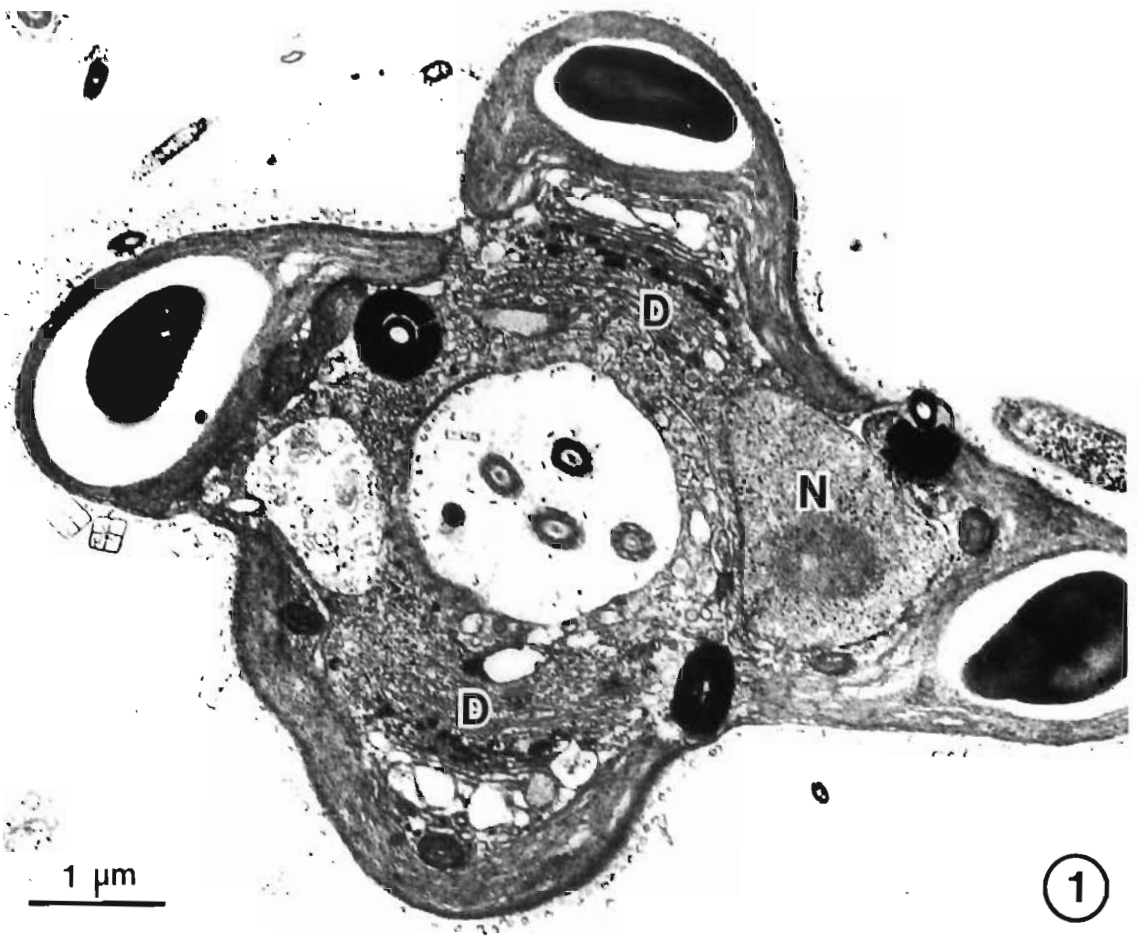
D
N
D
1 µm
1

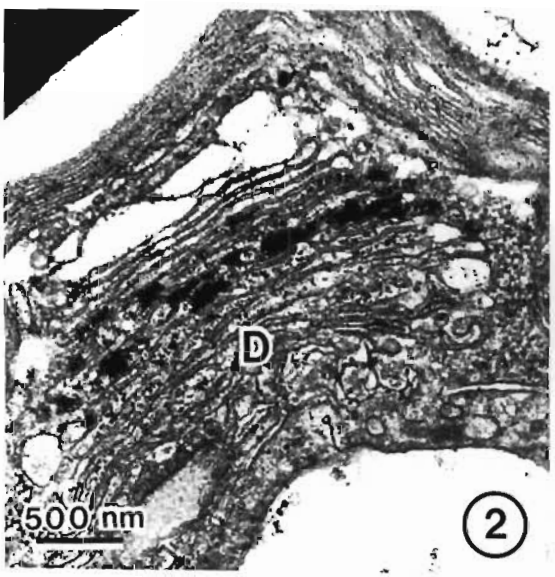
D
500 nm
2

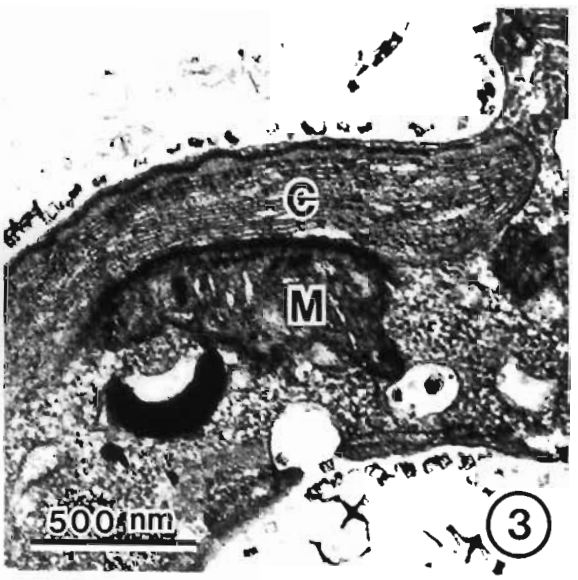
C
M
500 nm
3

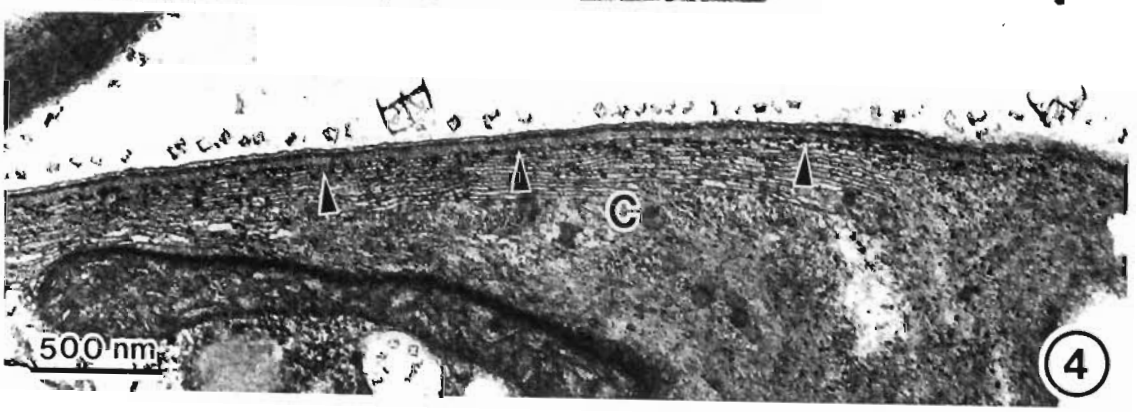
C
500 nm
4

PLATE 7.22

The Gomori test for acid phosphatases in l-cells

Figs. 1 and 2. Sections through l-cells showing a positive Gomori reaction in the dictyosomes (D) and in lysosomal vesicles (LV).

Fig. 3 A positive Gomori reaction was seen in the scale reservoir (Sr) of an l-cell. Lead phosphate deposits were seen to lie over the scales. The region to the left of the scale reservoir is the vacuole. This organelle also contained scales and lead phosphate deposits.

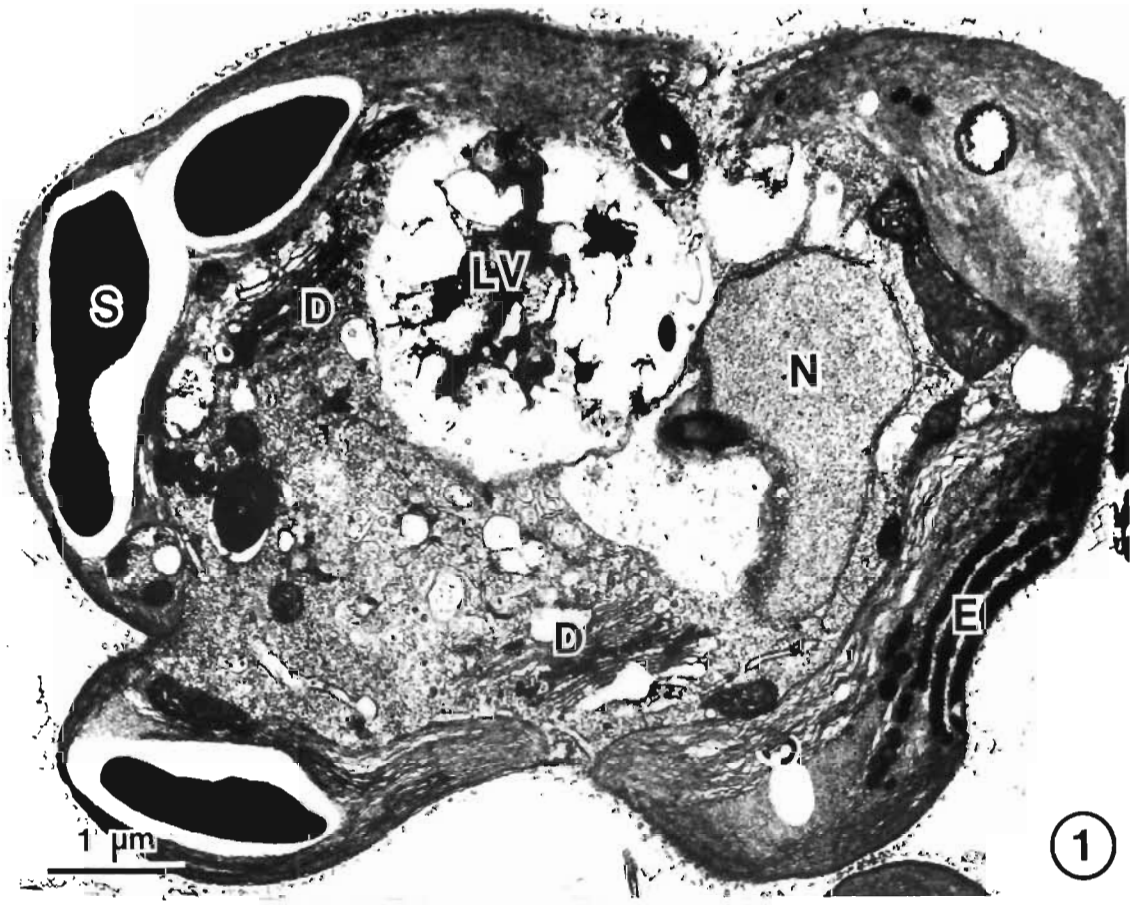
S
D
LV
N
D
E
1 µm
1

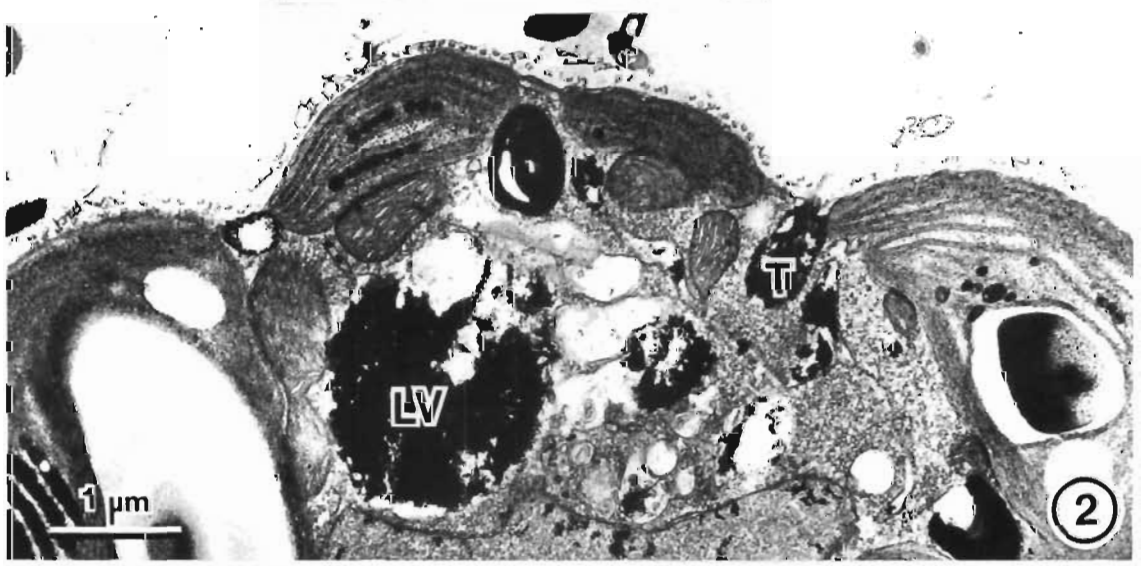
T
LV
1 µm
2

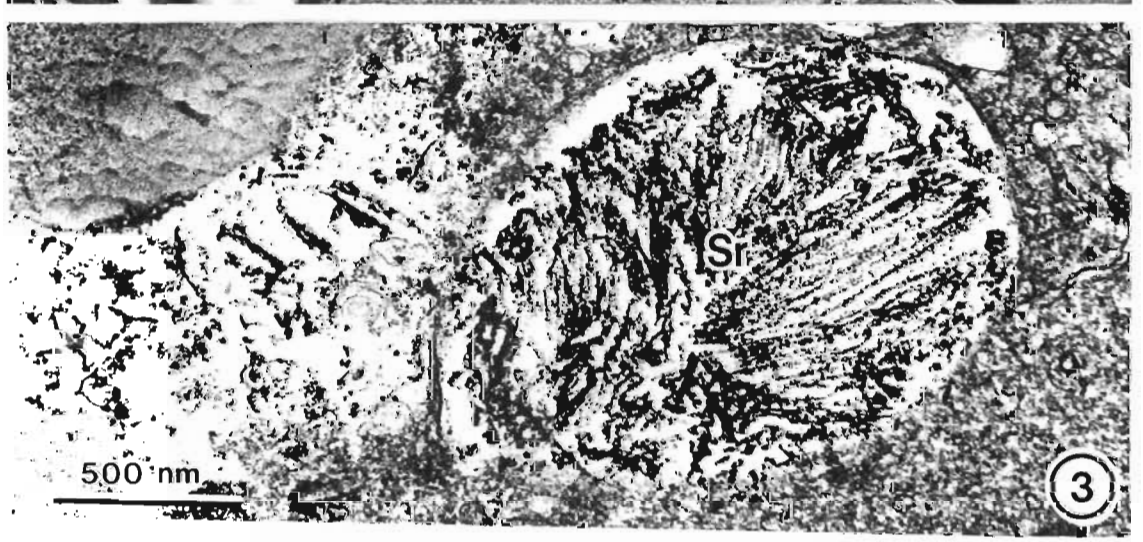
Sr
500 nm
3

PLATE 7.23

The Gomori test

Fig. 1 A positive Gomori reaction was seen in the scale reservoir of an 1-cell. The scale reservoir contained many body scales.

Fig. 2 A lysosomal vesicle (LV) containing dense deposits of lead phosphate. The presence of scales in this vesicle indicates that the scale reservoir may become a lysosomal vesicle.

Fig. 3 A section through a control cell in which the Na-β-glycero-phosphate substrate was omitted from the Gomori reaction medium. A Gomori reaction product is seen in the chloroplast (C), dictyosome (D) and over the scales in the scale reservoir (Sr). A positive Gomori reaction at these sites indicates that acid phosphatase enzyme and substrate must have been present within the cell.

Fig. 4 A section through a control cell which was treated with the metabolic inhibitor NaFl. No enzyme activity was detected in either the scale reservoir (Sr), chloroplast or dictyosome (D).

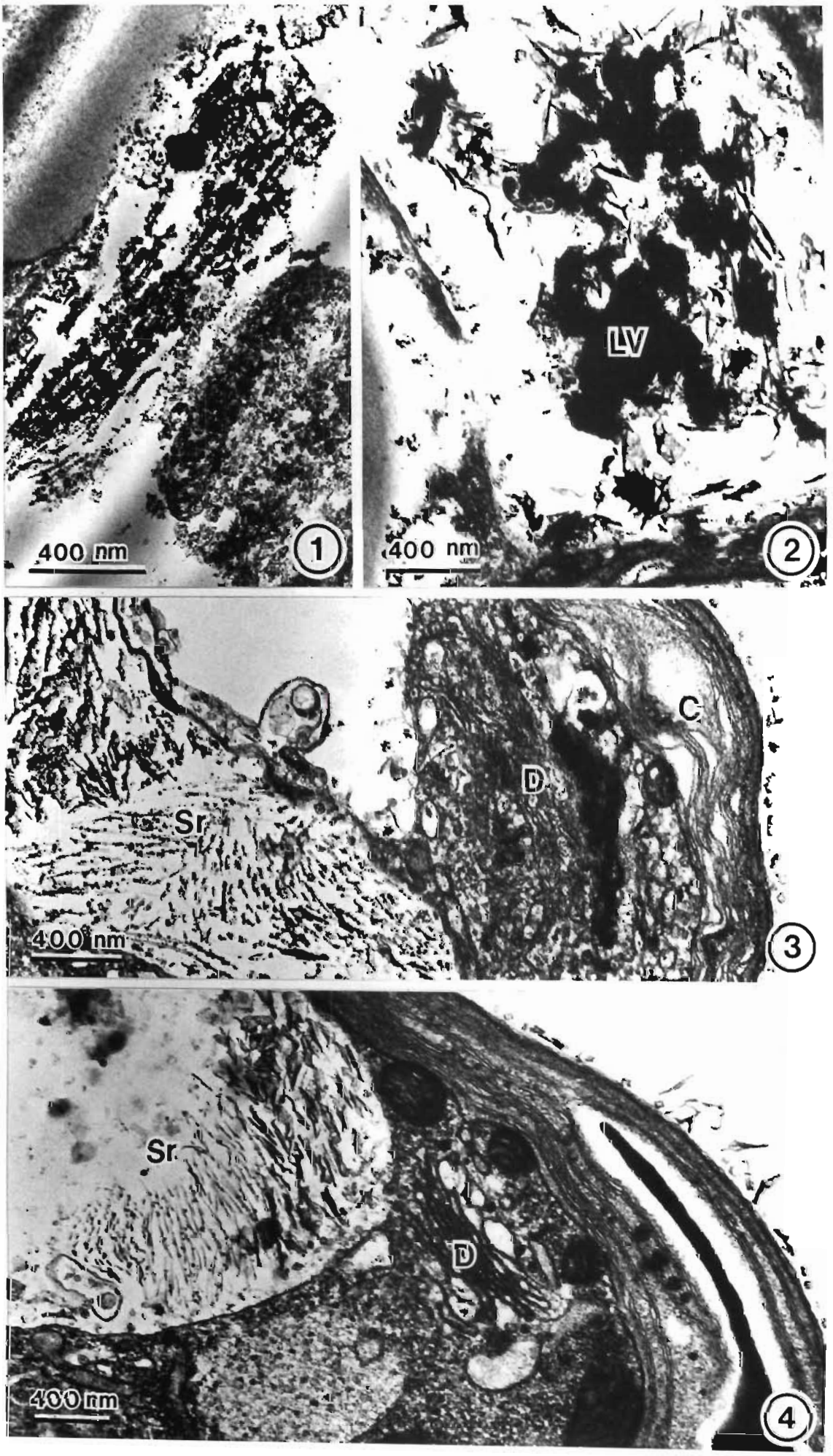
400 nm
1
LV
400 nm
2
C
D
Sr
400 nm
3
Sr
D
400 nm
4

PLATE 7.24

EDX analysis of the cyst wall

Figs. 1 and 2 — Two line scans made across a cyst in the sulphur window (Fig. 1). and calcium window (Fig. 2). These scans show that sulphur and calcium are concentrated in the cyst wall.

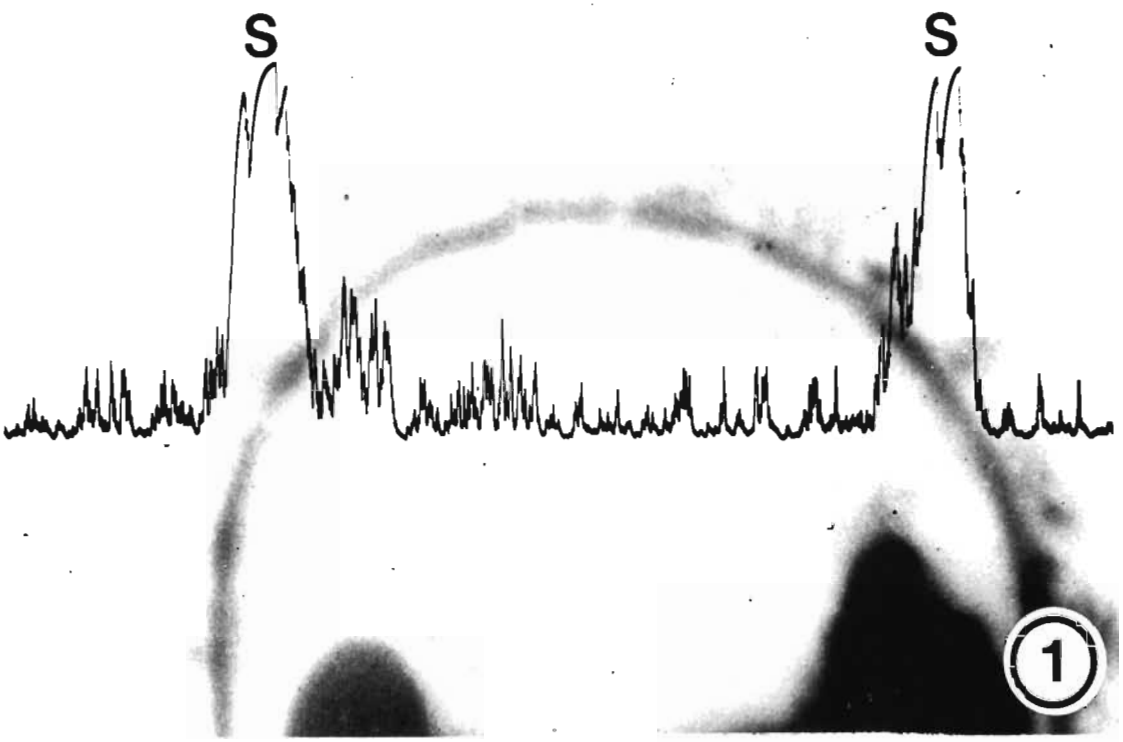
S
S
1

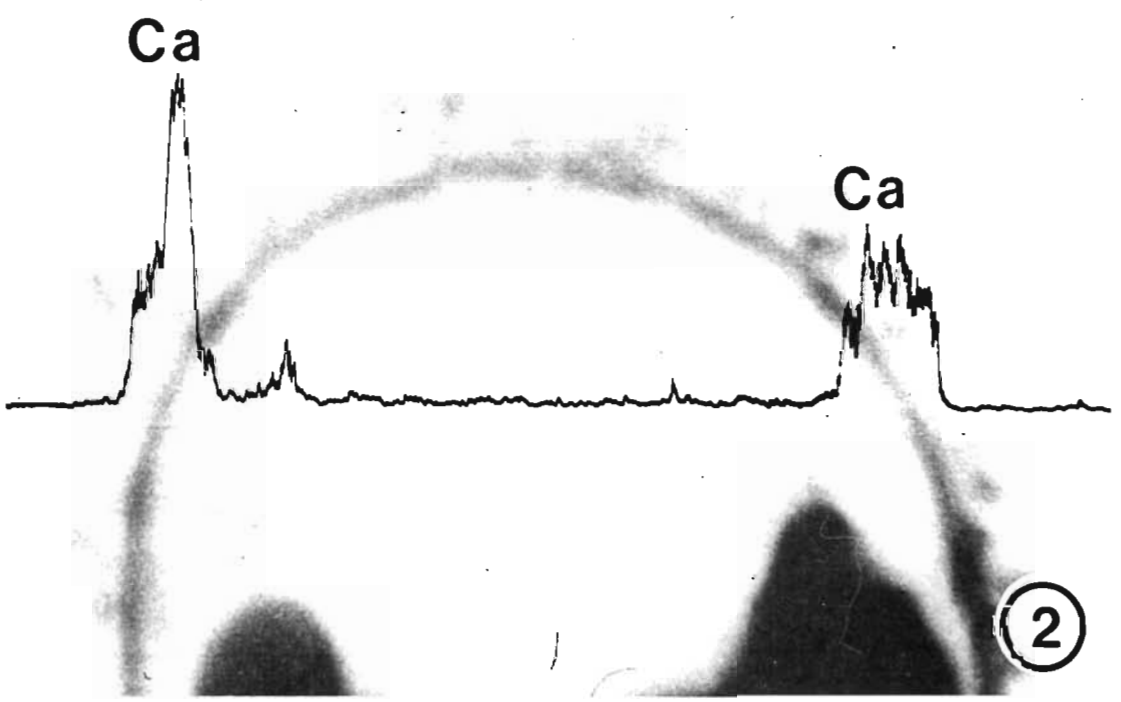
Ca
Ca
2

PLATE 7.25

Variations in scale structure

Scale bar on all micrographs = 200 nm

Figs. 1-6 Variations in the structure of the B_3 scale. This scale type is the most variable. Unusual protrusions (arrowheads) are seen on a B_3 scale in Fig. 1. Often the B_3 scale loses its characteristic cruciate structure and gains additional "spokes" which radiate from the centre of the scale to the rim (Figs. 2 and 3). The B_3 scale may become aberrant as additional scale material is added to the base of the scale to give it a plate-like appearance (Figs. 4-6).

Figs. 7-9 Variations in the structure of the F_3 scale. This scale may develop a pointed (arrowhead) rather than a truncated lamina at the end opposite the free spine. This scale also lacks the large aperture characteristic of the F_3 scale. The lamina of the F_3 scale may also develop a "tail" (arrowhead) which extends from the scale parallel to the free spine (Fig. 8). The spine of the F_3 scale may also extend beyond the lamina at the truncated end (arrowhead - Fig. 9).

Fig. 10 Variations in the structure of the B_2 scale. The B_2 scale may lose one of the arms of the cruciate structure characteristic of the B_2 scale (arrowhead). The substructure material of the B_2 scale is variable and may become elaborated to form a loose network on the base of the scale.

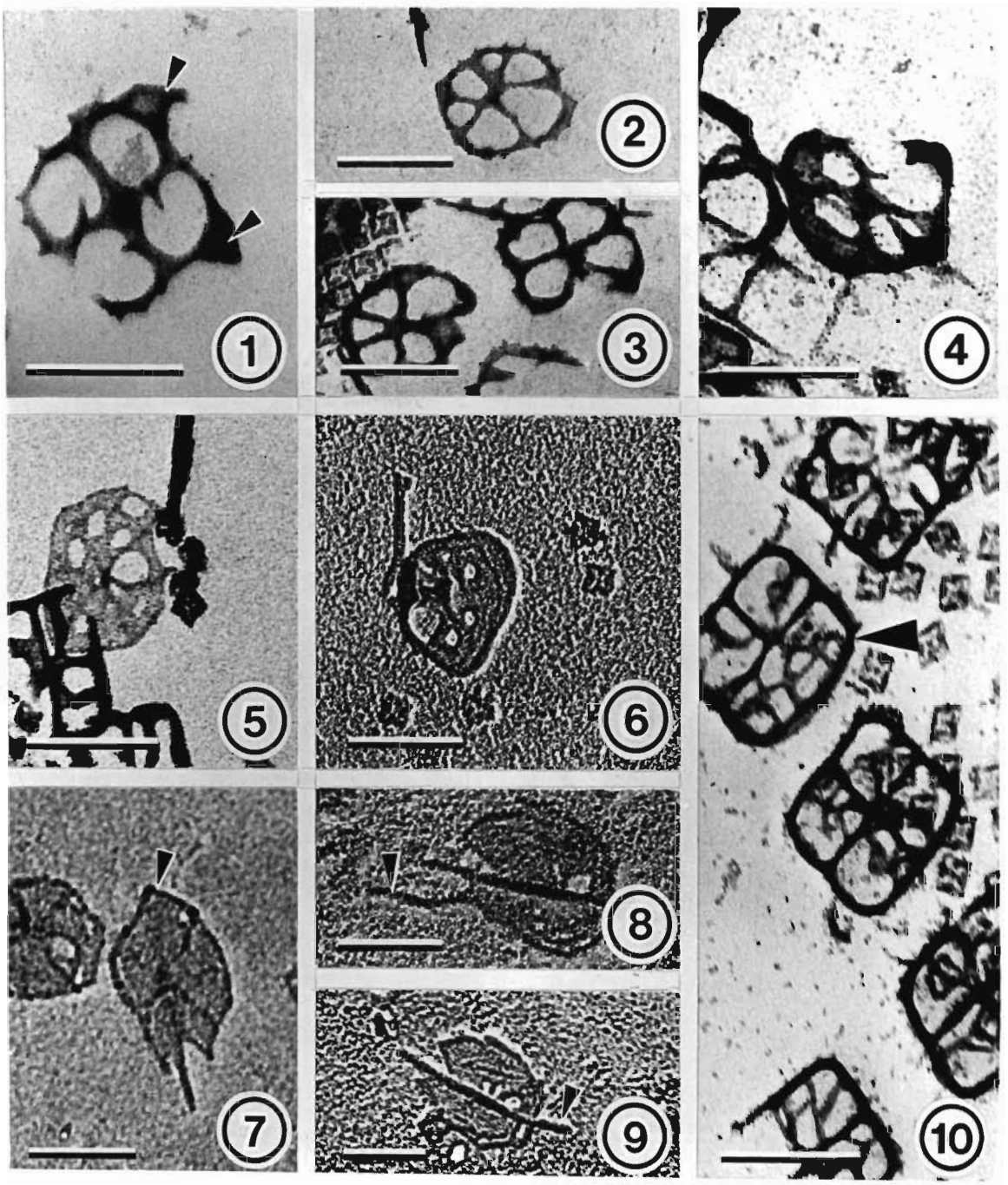
1
2
3
4
5
6
7
8
9
10

PLATE 7.26

Virus infection

Fig. 1 A transverse section through a cell infected with numerous virus particles. The cytoplasm of the cell is generally less dense than that in non-infected cells. The cell has a large scale reservoir (Sr) which contains very few scales. No dictyosomes were seen within the cell. The chloroplast contains two large starch grains (S) in two lobes.

Fig. 2 A detailed view of the flagellar pit and nucleus (N) of the cell shown in Fig. 1. The nucleus is small and appears to be moribund. It is enclosed in a dilated portion of endoplasmic reticulum. One flagellum is malformed and does not have an axoneme.

Fig. 3 The virus (VLP) infecting the cell is hexagonal in outline in all planes of section. Some virus particles were dense while others were lighter and appeared to have released their contents leaving the capsule behind. In some sections the capsule of the lighter virus particles was seen to be ruptured (See Fig. 1).

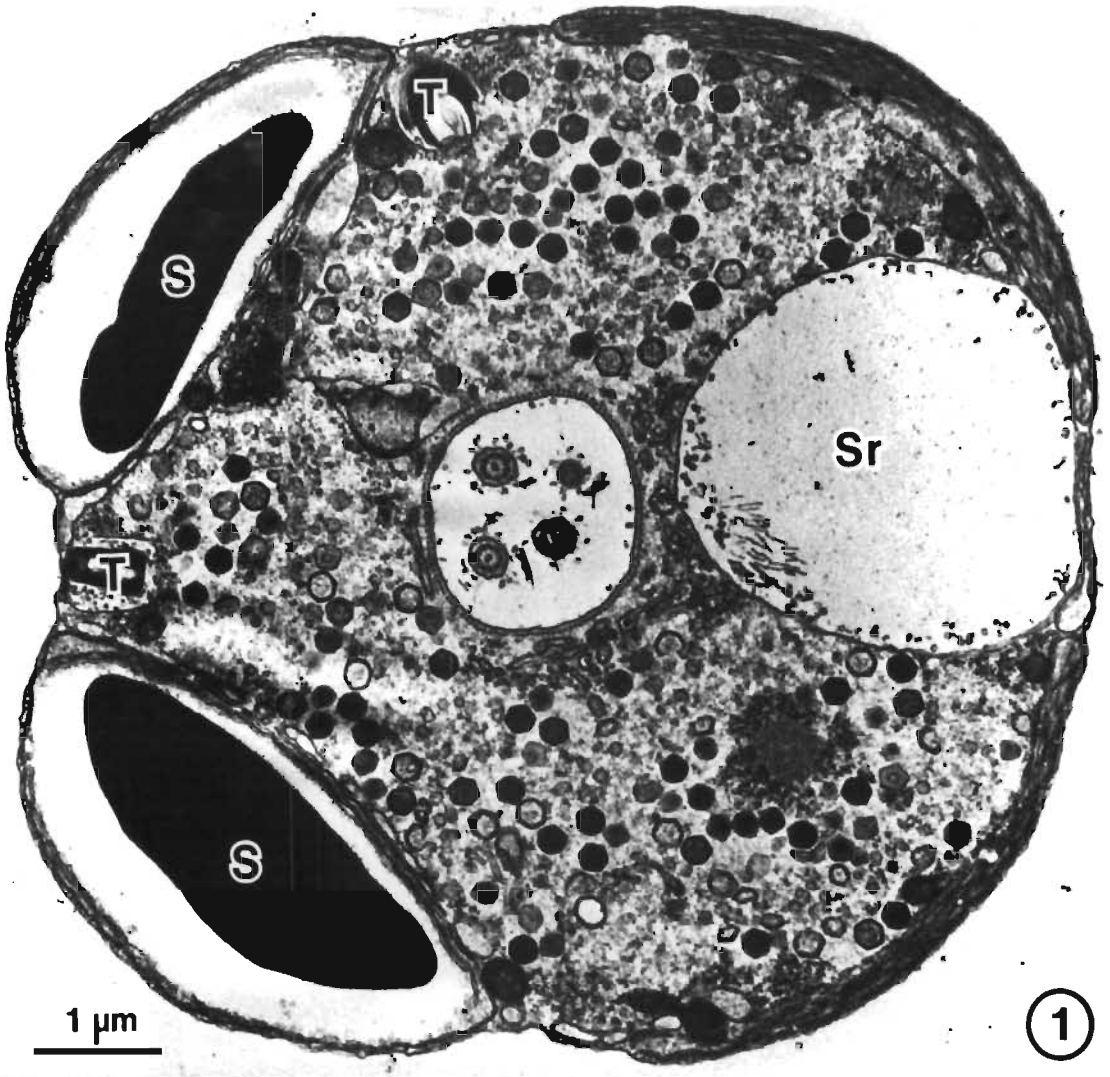
T
S
Sr
T
S
1 µm
1

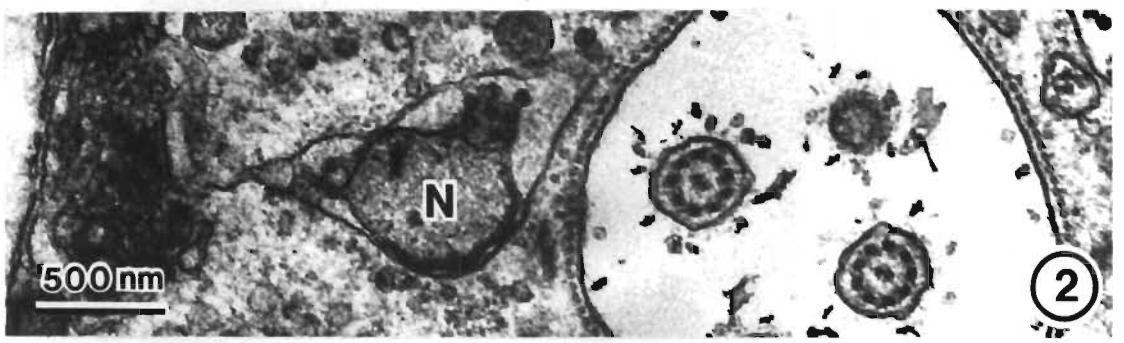
N
500 nm
2

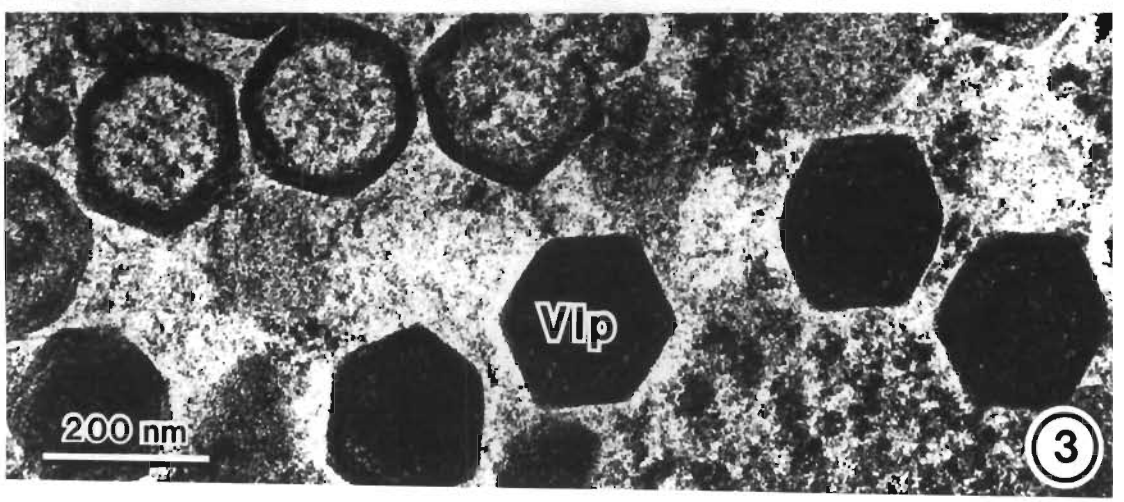
Vlp
200 nm
3

PLATE 7.27

Virus-like particles

Fig. 1 A section through an abnormal cell which was infected with a virus-like particle. The VLP was present both in the nucleus (N) and within vesicles in the cytoplasm. The chloroplast (C) of this cell was unusual in that it contained numerous sinuous thylakoids and scattered carotenoid globules. A pyrenoid (P) was present in one lobe and eyespot (E) was present in the second lobe.

Fig. 2 A detailed view of the moribund nucleus (N) of the cell shown in Fig. 1. The virus-like particles (VLP) were densely stained and were apparently causing the nucleus to disintegrate.

Figs. 3 and 4. A section through the posterior end of an 1-cell showing a cluster of virus-like particles (arrow) near the pyrenoid (P). (Fig. 3). A detailed view of the virus-like particles (VLP) shows them clustered in an almost crystalline array (Fig. 4).

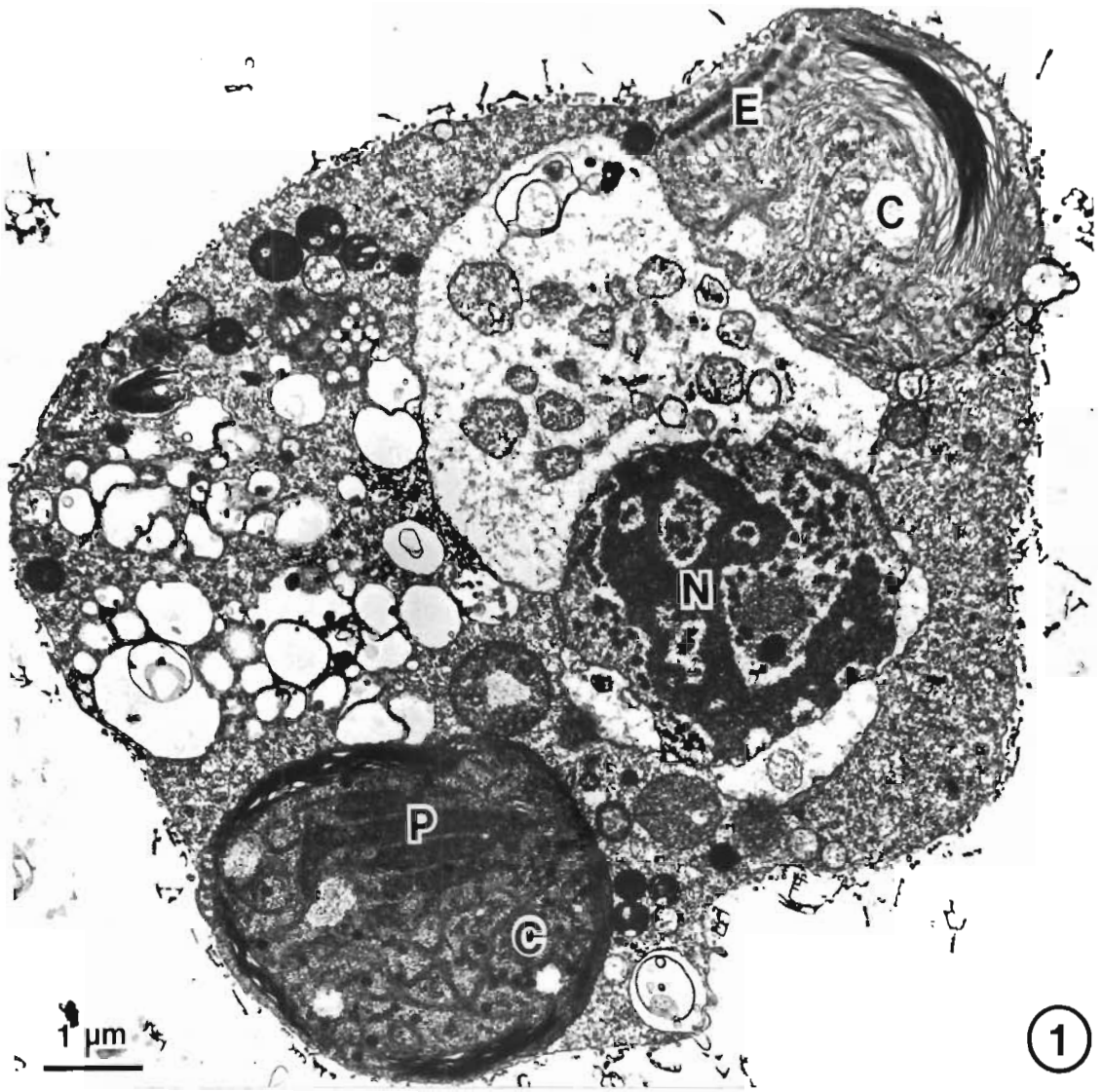
E
C
N
P
C
1 µm
1

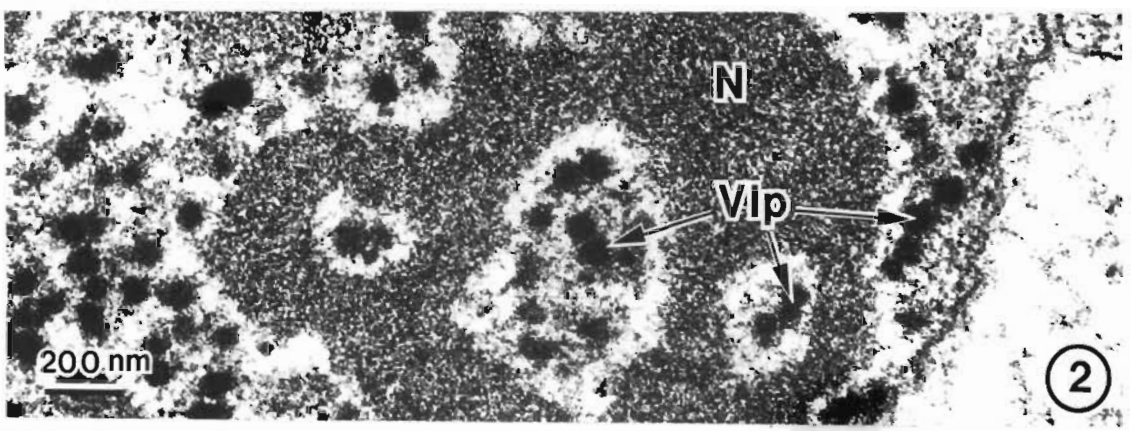
N
Vlp
200 nm
2

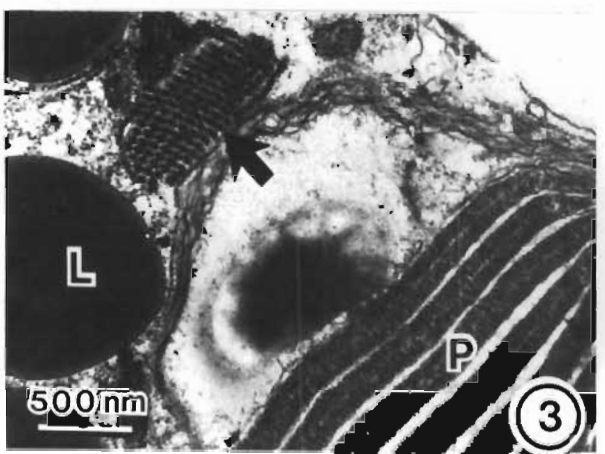
L
P
500 nm
3

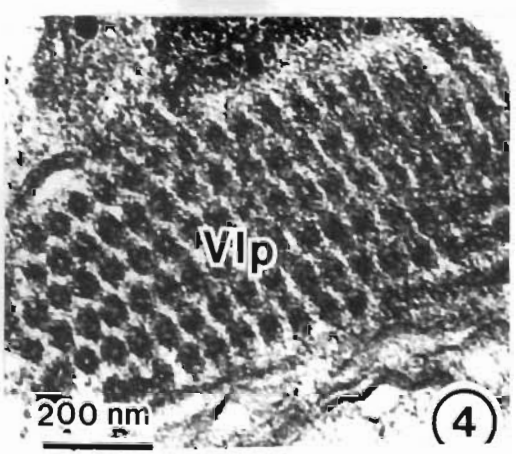
Vlp
200 nm
4